2016

Cargo Shipping Demand Modeling, Infrastructure Mapping, And Emission Impacts Of Selected U.S. Ports

Robert Coffman Richardson
University of Mississippi

CARGO SHIPPING DEMAND MODELING, INFRASTRUCTURE MAPPING, AND EMISSION IMPACTS OF SELECTED U.S. PORTS

A Thesis
presented in partial fulfillment of requirements
for the degree of Master of Science
in the Department of Civil Engineering
The University of Mississippi

By

ROBERT C. RICHARDSON, JR.

December 2016

ABSTRACT

This research included shipping demand modeling, infrastructure asset mapping, and impacts of Carbon Dioxide (CO_2) emission. The current volume of imports and exports was reviewed for U.S. ports in the East Coast, Gulf Coast, and West Coast regions. The import and export of goods is a major part of the U.S. economy, and the volume of cargo handled by U.S. ports is expected to increase in the future as population increases. The major motivation for this thesis was the need for U.S. ports to make plans now to accommodate this expected growth in volume. Ports distribute commodities throughout the U.S., and every state would be adversely affected if improvements are not made to the capacity and infrastructure of U.S. ports. The goals were to: identify an efficient tool for assisting with the analysis of a port's current infrastructure to help with planning for future needs, use a tool to assist with developing alternative shipping routes as needed, and to analyze intermodal integration scenarios to reduce the amount of CO_2 emissions resulting from the rising volume of shipping. The primary objectives were to: (1) review cargo shipping demand for Twenty Foot Equivalent Unit (TEU) data at selected larger ports in the U.S. and distribution to states, develop statistical demand models, and predict the TEU demand data for future 5, 10, 15, and 20 years, (2) create spatial maps of infrastructure and landuse planimetrics of Landsat-8 satellite imagery scenes for selected sites, (3) evaluate the accuracy and efficiency of the calibrated Built-Up Area and Natural Surfaces (BANS) classification of infrastructure features and landuse, (4) estimate cargo shipping volumes using Automatic Identification System (AIS) for selected shipping routes and calculate related CO_2 emissions and their impacts. Case studies involving spatial mapping of selected sites and a

comparison of the planimetrics and calibrated BANS classification were used to determine an efficient method for mapping the assets of a port's existing infrastructure and landuse. The AIS data for selected shipping routes were used through ship counts over a 24-hour period to analyze this data for mapping shipping routes. Geospatial analysis was also performed using a sample shipping route to calculate the amount of CO_2 emitted by a cargo vessel and to make recommendations for the reduction of these emissions. The spatial mapping case studies conducted for the selected areas of the ports of Los Angeles and Long Beach, the Port of Gulfport, and Oxford, MS showed that the calibrated surface classification using multispectral satellite imagery would be more efficient than the manual planimetrics for mapping current infrastructure features and landuse. Global shipping is a major contributor to CO_2 emissions. This is illustrated by a case study for calculating 5,174 tons of CO_2 emissions for a cargo vessel traveling from New York to France. Bigger vessels help to reduce the global CO_2 concentration.

DEDICATION

This thesis is dedicated to parents, Bob and Virginia Richardson, and

to my late grandfather, Van Richardson.

LIST OF ABBREVIATIONS AND SYMBOLS

AAPA	American Association of Port Authorities
ACF	Autocorrelation Function
AIS	Automatic Identification System
ANOVA	Analysis of Variance
AR	AutoRegression
ARIMA	AutoRegressive Integrated Moving Average
AOI	Area of Interest
BANS	Built-Up Area and Natural Surfaces
CAIT	Center for Advanced Infrastructure Technology
CO_2	Carbon Dioxide
EPA	Environmental Protection Agency
ER	Economic Recession
GIS	Geographical Information Systems
GDP	Gross Domestic Product
MA	Moving Average
MARE	Mean Absolute Relative Error
MPG	Miles per Gallon
NCITEC	National Center for Intermodal Transportation for Economic Competitiveness
OLI	Operational Land Imager
O_3	Ozone

PACF	Partial Autocorrelation Function
(p,d,q)	(autoregressive, difference, moving average)
RMSE	Root Mean Square Error
SNR	Signal-to-Noise Radiometric
TEU	Twenty Foot Equivalent Unit
TIRS	Thermal Infrared Sensor
USGS	United States Geological Survey

ACKNOWLEDGEMENTS

Initially, I would like to thank Dr. Waheed Uddin for encouraging me to continue my studies and to pursue a post-graduate degree. I am very grateful for his faith in me, and his advice and guidance will have a lasting impact on me as I begin my career. I will always be thankful for his teaching me to become a better student and preparing me to be a better professional.

I would also like to thank the Center for Advanced Infrastructure Technology (CAIT) and the Department of Civil Engineering of the University of Mississippi for the financial support. I would like to thank my advisory committee members, Dr. Yacoub Najjar and Dr. Tyrus McCarty, for serving in my committee. I would also like to thank Dr. Uddin's other current and former graduate students, Seth Cobb, Alper Dumas, Zul Fahmi Mohamed Jaafar, and Quang Nguyen, for their help and guidance throughout my graduate years.

Finally, I would like to thank my parents, Bob and Virginia Richardson, for their encouragement, faith, and support as I progressed through my academic career, and my late grandfather, Van Richardson, who inspired me from a young age to pursue a career in the field of engineering.

TABLE OF CONTENTS

LIST OF TABLES

LIST OF FIGURES

CHAPTER I

INTRODUCTION

1.1 Background and Motivation

According to the American Association of Port Authorities (AAPA), public ports create many jobs and enhance local and regional economic growth [1]. The annual impact of the U.S. port industry according to the AAPA includes [1]:

- "13.3 million jobs, accounting for $649 billion in personal income and more than $3.15 trillion in marine cargo-related spending [2];
- Some $3.95 trillion in international trade for an all-encompassing range of goods and services, with nearly 1.4 billion tons, valued at $1.4 trillion, in waterborne imports and exports alone [3];
- More than 1 billion tons of domestic goods moved via water in the U.S. [4];
- More than $23.2 billion in U.S. Customs duty revenues in fiscal 2007, representing 70 percent of all Customs duties collected [5]."

As this data indicates, port infrastructure is obviously an important issue. According to the AAPA, U.S. ports have invested more than $34 billion since 1945, including nearly $9 billion in the last five years alone, to improve U.S. port facilities nationwide [1]. These numbers are expected to increase in the coming years [1].

Although large amounts have been spent on port infrastructure over the years, ports must continue to be maintained and improved. According to the AAPA, some of the most pressing issues currently facing the U.S. port system are [1]:

- Port security
- Navigation maintenance and new construction
- Freight congestion/intermodal road/rail access
- Marine facility expansion and modernization
- Coastal environmental protection
- The ability to secure funding and financing
- Competitiveness and diversified revenue sources
- Land acquisition and site development

Many steps are already being taken to address these issues, but these matters will not be resolved overnight. According to the AAPA, these issues could take over "50 years" to be solved [1].

Port security has been one of the main issues facing the U.S. port system since the 2001 terrorist attacks [1]. To prevent attacks on U.S. ports, hundreds of millions of dollars have been invested into facility security enhancements, while the federal government has invested approximately $1.5 billion to enhance security [1].

Emissions are another significant factor facing the U.S. and the world. Figure 1 shows emission rates for different modes of freight shipping [6]. According to this figure, ships emit only 10 grams of carbon dioxide (CO_2)to carry 1 ton of cargo 1 kilometer, which is much lower than the 21 grams by trains, 59 grams by trucks, and 470 grams by aircraft. This indicates that the choice of mode of transportation plays an important role in reducing the amount of CO_2 and other greenhouse gases.

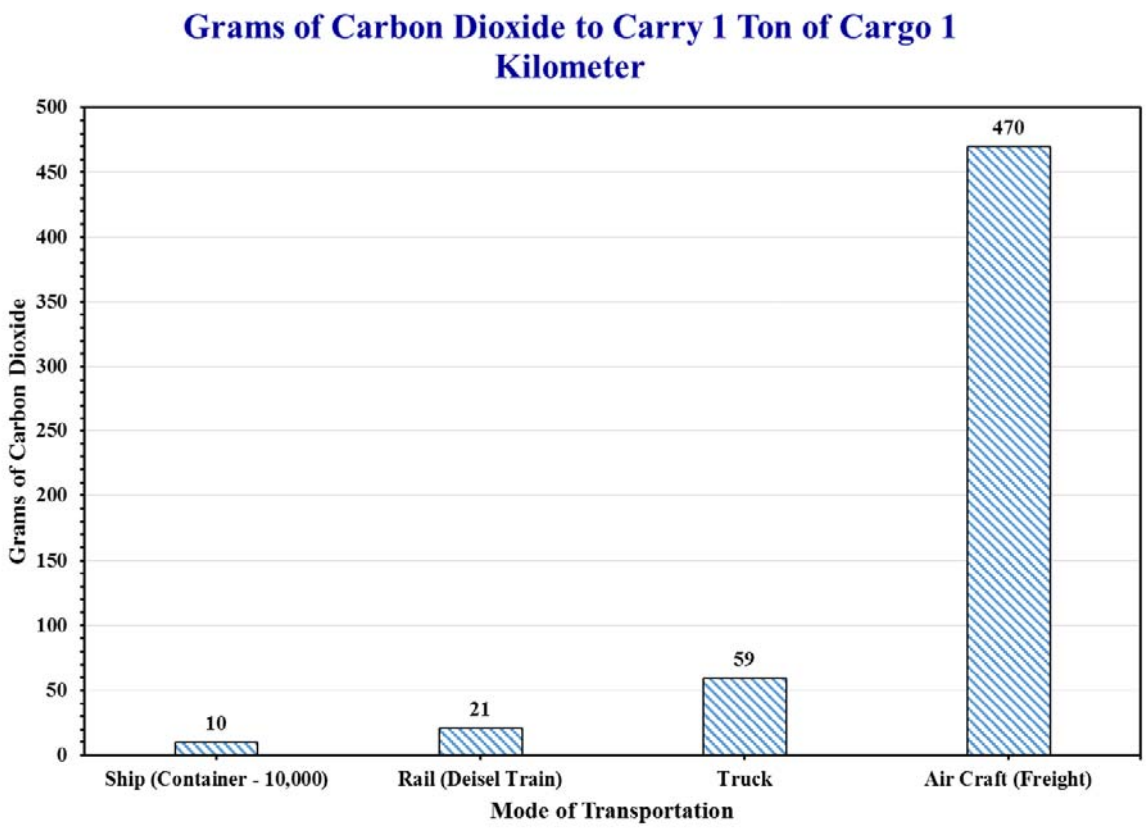

Figure 1. Grams of carbon dioxide for various modes of transportation

According to a report by the AAPA [1], "Ports handle a variety of cargoes, including bulk, or loose, cargo; breakbulk cargo in packages such as bundles, crates, barrels and pallets; liquid bulk cargo like petroleum; dry bulk such as grain; and general cargo in steel boxes called containers, which are measured in 20-foot equivalent units, or TEUs." The most commonly-shipped commodities for domestic and foreign trade in U.S. ports include [1]:

- Crude petroleum and petroleum products, including oil and gasoline
- Chemicals and related products, such as fertilizer
- Bituminous, metallurgical and steam coal
- Food and farm products, including wheat and wheat flour, corn, soybeans, rice, and cotton

- Forest products, such as lumber and wood chips
- Iron and steel
- Soil, sand, gravel, rock, and stone
- Automobiles, auto parts, and machinery
- Clothing, shoes, electronics, and toys

U.S. ports handle a large volume of imported and exported goods, which are distributed throughout the U.S. and around the world. It is clear that maintaining and improving the infrastructure, emissions, and security with regard to U.S. ports and shipping will be increasingly important in the years to come.

The motivation for this research is primarily the Intermodal Optimization for Economically Viable Integration of Surface and Waterborne Freight Transport project being conducted by the Center for Advanced Infrastructure Technology (CAIT), as a part of the National Center for Intermodal Transportation for Economic Competitiveness (NCITEC) grant at the University of Mississippi [7].

1.2 Objectives and Scope

The primary objectives for this thesis were to:

1. Review cargo shipping demand for TEU data at selected larger ports in the U.S. and distribution to states, develop statistical demand models, and predict the TEU demand data for future 5, 10, 15, and 20 years.
2. Create spatial maps of infrastructure and landuse planimetrics of Landsat-8 satellite imagery scenes for selected sites.
3. Evaluate the accuracy and efficiency of the calibrated Built-Up Area and Natural Surfaces (BANS) classification of infrastructure features and landuse.

4. Estimate cargo shipping volumes using AIS for selected shipping routes and calculate related CO_2 emissions and their impacts.

This thesis evaluates cargo demand at the study area of the ports of Los Angeles and Long Beach. The study includes cargo import and export data for major U.S. ports, including the study area. An optimization analysis is made for freight shipment from the study area to destinations in selected states.

This thesis will also look at container ship TEU prediction modeling for selected ports. Regression and AutoRegressive Integrated Moving Average (ARIMA) analysis are made and compared for TEU demand modeling. Regression equations are used to make prediction for future years.

Spatial mapping is made of selected areas to determine each areas' infrastructure and landuse. A comparison of calibrated BANS classification and planimetrics is made. Surface temperatures and population densities are also evaluated for selected areas. This thesis also examines cargo vessel data through Automatic Identification System (AIS) data and spatial mapping. Shipping emissions data is obtained through the study of a sample cargo vessel trip.

The use of geographical information systems (GIS) for infrastructure inventory and spatial maps has been shown by Uddin [8]. According to Uddin, Hudson, and Haas [9], "GIS and geospatial applications will greatly improve with the availability of remote sensing data from terrestrial, airborne, airborne technologies. It will have a dramatic impact in the coming decade as more user-friendly and generally applicable systems are developed and implemented." If GIS technologies continue to improve in the next decade as is suggested here, U.S. ports could use these GIS technologies to identify present assets and to assist in maintaining and improving infrastructure and landuse. U.S. ports will also be able to use these GIS technologies to help

with port congestion. Port congestion can be helped by these GIS technologies by identifying new routes for vessels to enter and exit congested ports. GIS technologies will also help with routes to other ports. Finding faster and more efficient routes can help reduce CO_2 emissions throughout a trip.

1.3 Research Methodology

The research methodology for this thesis is broken into several parts. The research methodology for the U.S. ports data and for the ports of Los Angeles and Long Beach distribution data is as follows:

- Collect the most current tonnage data of imports and exports for all container liner service ports in the U.S.
- Create maps and graphs of the data obtained.
- Collect distribution data for the ports of Los Angeles and Long Beach to each U.S. state.
- Create spatial maps and plots of the distribution data obtained.

The research methodology for the ports of Los Angeles and Long Beach ARIMA modeling is as follows:

- Collect TEU data from 1995-2013 of the ports of Los Angeles and Long Beach.
- Collect Gross Domestic Product (GDP) data from 2005-2014 for Los Angeles, CA.
- Develop a regression equation using time as the independent variable.
- Develop an ARIMA model using time as the independent variable.
- Develop a regression equation using GDP as the independent variable.
- Compare the models made.

- Make plots of the data found from the ARIMA (1,2,1), regression equation with time as the independent variable, and regression equation with California GDP as the independent variable and compare results.
- Predict TEU values for 5, 10, 15 and 20 years in the future.

The research methodology for spatial mapping of selected areas and identifying current infrastructure and landuse of the ports of Los Angeles and Long Beach, the Port of Gulfport, and Oxford, MS, are as follows:

- Create pan-sharpened images of the selected ports and locations.
- Develop the planimetrics and calibrated BANS classification for each location.
- Compare the results obtained from the planimetrics and calibrated BANS classification.
- Compare the findings for each location to each other.

The research methodology for the AIS data, vessel shipping emissions, and ports environmental impacts are as follows:

- Collect cargo vessel count data for selected areas.
- Create plots of cargo vessel data for all study areas analyzed.
- Examine the environmental impacts of shipping by calculating shipping-related CO_2 emissions data using a sample cargo vessel trip.

CHAPTER II

CARGO DEMAND AT THE PORTS OF LOS ANGELES AND LONG BEACH AND DISTRIBUTION BY STATE

The ports of Los Angeles and Long Beach are areas of focus in this thesis. These ports handle a significant amount of the total U.S. container liner service freight and have a large impact on the U.S. The motivation behind choosing these two ports was to perform a study on larger U.S. ports with little known research already done.

2.1 Cargo Import and Export Demands at Major Ports in the U.S.

Container liner service ports in the U.S. are a main focus of this thesis. These ports handle most of the goods that are imported to and exported from the U.S. by way of waterway shipping. Figure 2 shows all the U.S. container liner service ports [10].

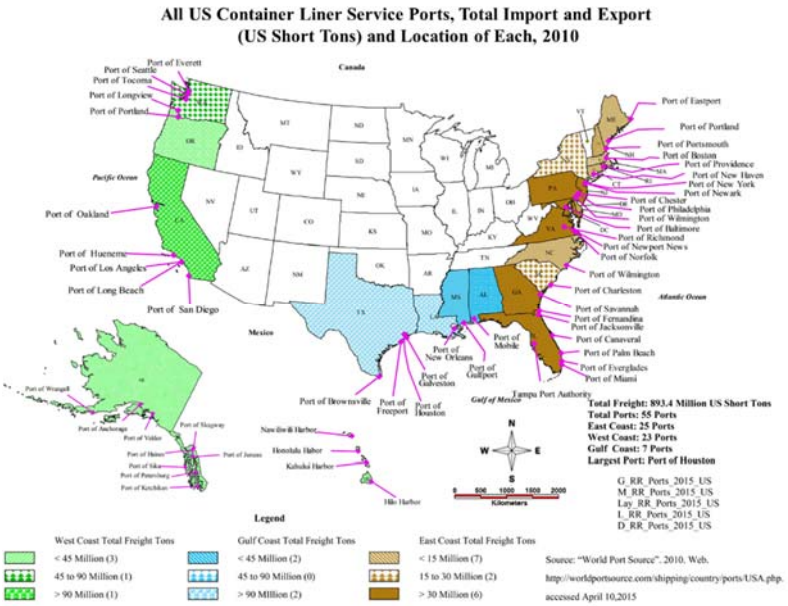

Figure 2. All U.S. container liner service ports

As shown in Figure 2, container liner service ports in the U.S. may be divided into three different regional locations: the West Coast, the East Coast, and the Gulf Coast. Based on 2010 data, California handled the most total freight in the West Coast region at over 90 million short tons. On the Gulf Coast, Texas and Louisiana both handled over 90 million total short tons of freight. On the East Coast, six states each handled over 30 million short tons of total freight [10]. Although the East Coast does not have a port as large as the West Coast or the Gulf Coast, this region has the most container liner service ports with 25. The West Coast has 23 container liner service ports, and the Gulf Coast has only 7 container liner service ports. The imports and exports tonnage for each region will be discussed in this thesis.

2.1.1 U.S. West Coast States Container Liner Service Port Freight Data

Data for the U.S. West Coast container liner service ports was obtained and broken down for each state on the U.S. West Coast that had a container liner service port. Figure 3 shows the percentage of imported freight that each of the West Coast states accounted for in 2010. The imports accounted for 49% of the total U.S. West Coast freight. As can be seen from Figure 3, California accounted for 74.50% of the entire West Coast imports.

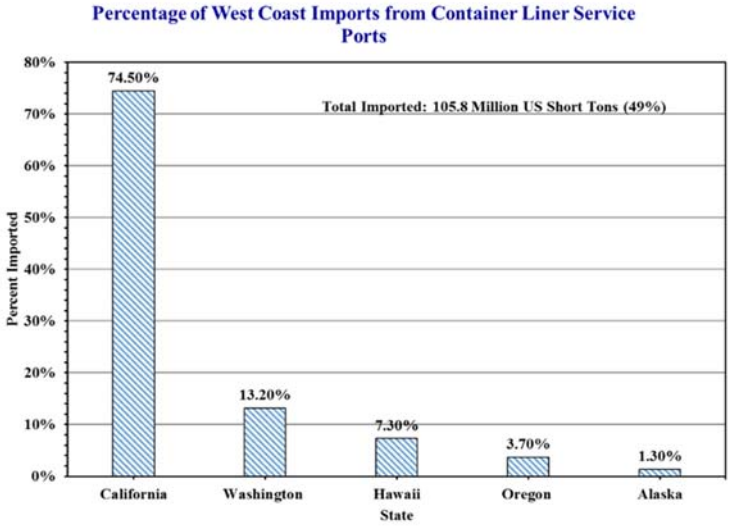

Figure 3. Imports for the U.S. West Coast container liner service ports

Figure 4 shows the percentage of exported freight that each of the West Coast states accounted for in 2010. The exports accounted for 51% of the total U.S. West Coast freight. California again led the way in the West Coast region with 53.13% of the total exports.

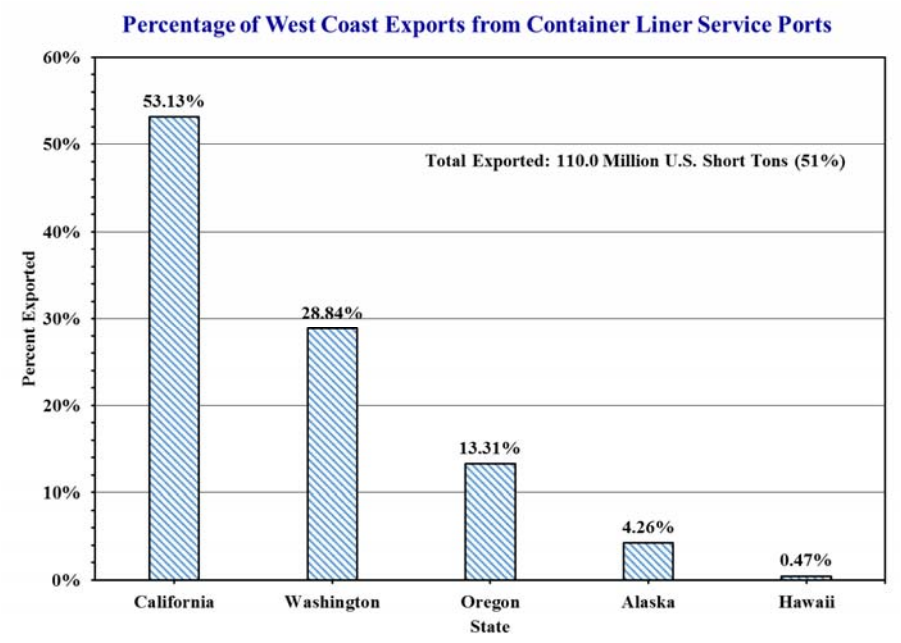

Figure 4. Exports for the U.S. West Coast container liner service ports

Figure 5 shows the total freight from container liner service ports in each West Coast state and the percentage of the total freight each state accounted for in 2010. As shown in Figure 5, California had the most total freight with 137.3 million short tons, or 63.13% of the total U.S. West Coast freight. Washington accounted for 21.1%, Oregon 8.6%, Hawaii 3.8%, and Alaska 2.8%. California and Washington accounted for the majority of the U.S. West Coast total freight. Figure 6 shows the total freight for the U.S. West Coast container liner service ports and shows the number of ports in each state. Alaska has 9 ports, California 5, Washington 4, Hawaii 4, and Oregon 1. The ports of Los Angeles and Long Beach accounted for 119 million short tons or 55% of the total West Coast freight. These ports will be discussed in more depth throughout this thesis.

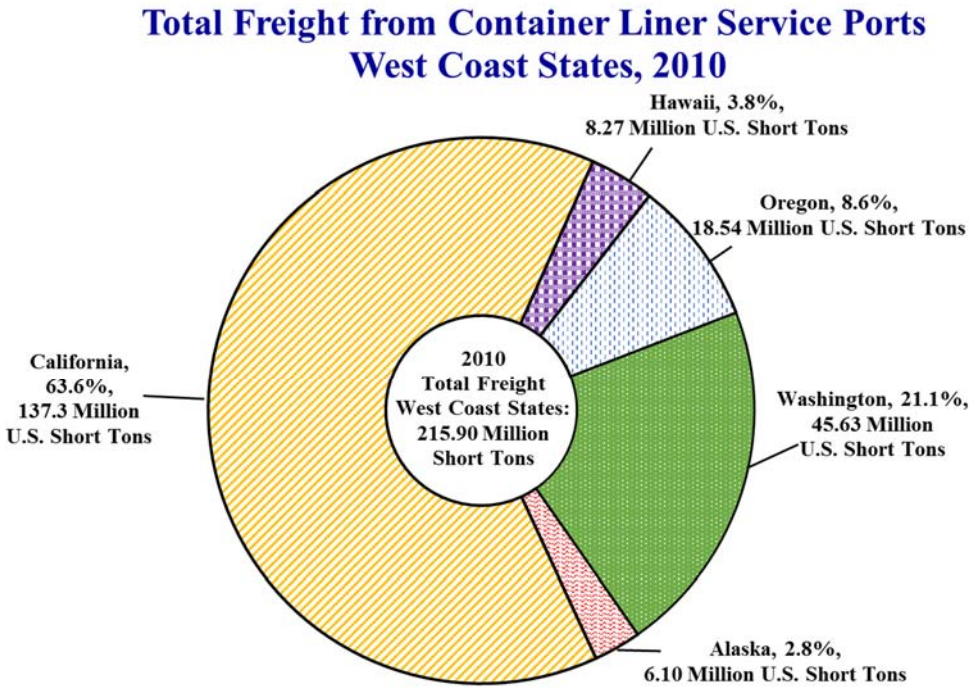

Figure 5. Total freight from U.S. West Coast container liner service ports

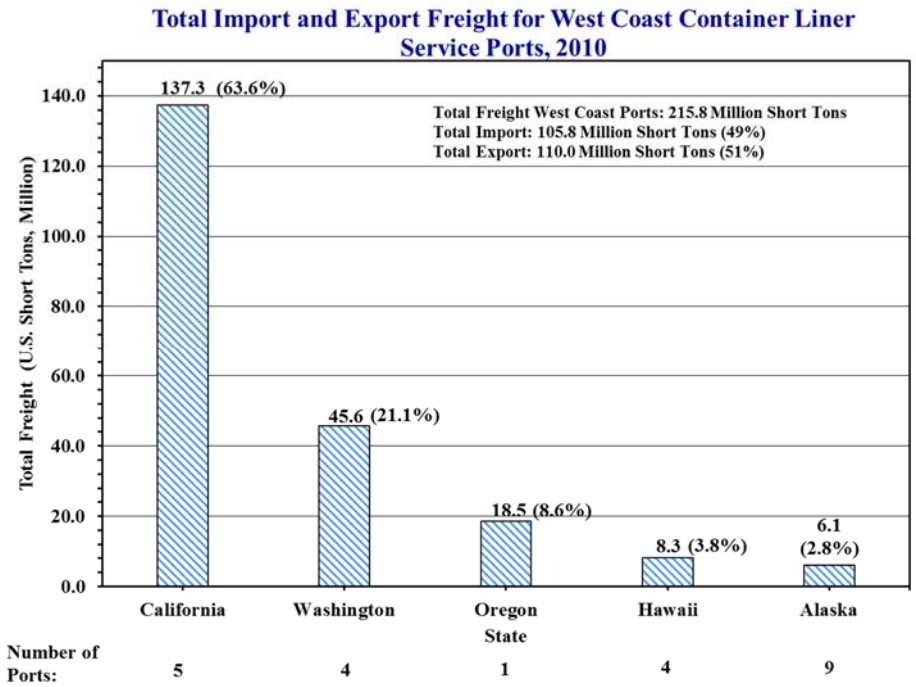

Figure 6. Total freight from U.S. West Coast container liner service ports with number of container liner service ports in each state

2.1.2 U.S. Gulf Coast States Container Liner Service Port Freight Data

Data for the U.S. Gulf Coast container liner service ports was obtained and broken down for every state on the U.S. Gulf Coast that had a container liner service port. Figure 7 shows the percentage of imported freight that each of the Gulf Coast states accounted for in 2010. The imports accounted for 49% of the total U.S. Gulf Coast freight. As can be seen from Figure 7, Texas accounted for 71.47% of the entire Gulf Coast imports.

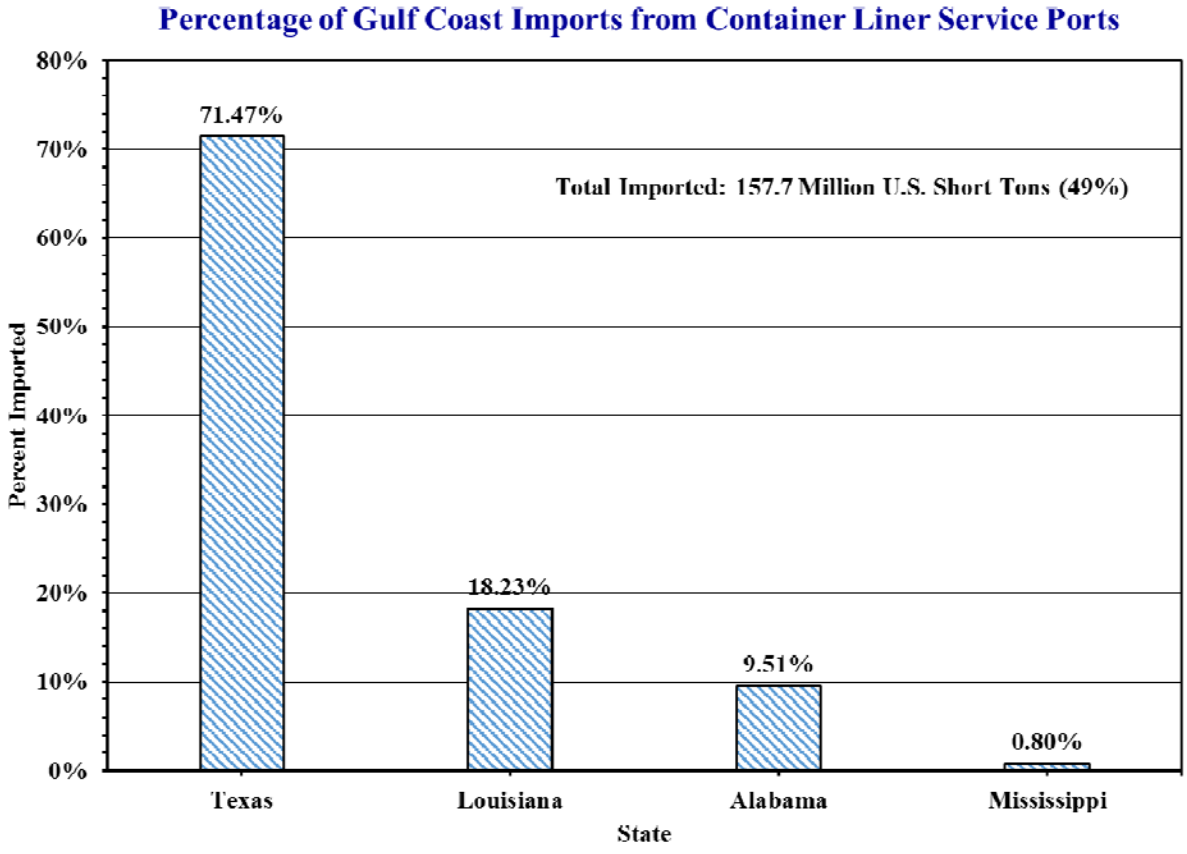

Figure 7. Imports for the U.S. Gulf Coast container liner service ports

Figure 8 shows the percentage of exported freight that each of the Gulf Coast states accounted for in 2010. The exports accounted for 51% of the total U.S. Gulf Coast freight. Texas again led the way with 49.13% of the total Gulf Coast exports.

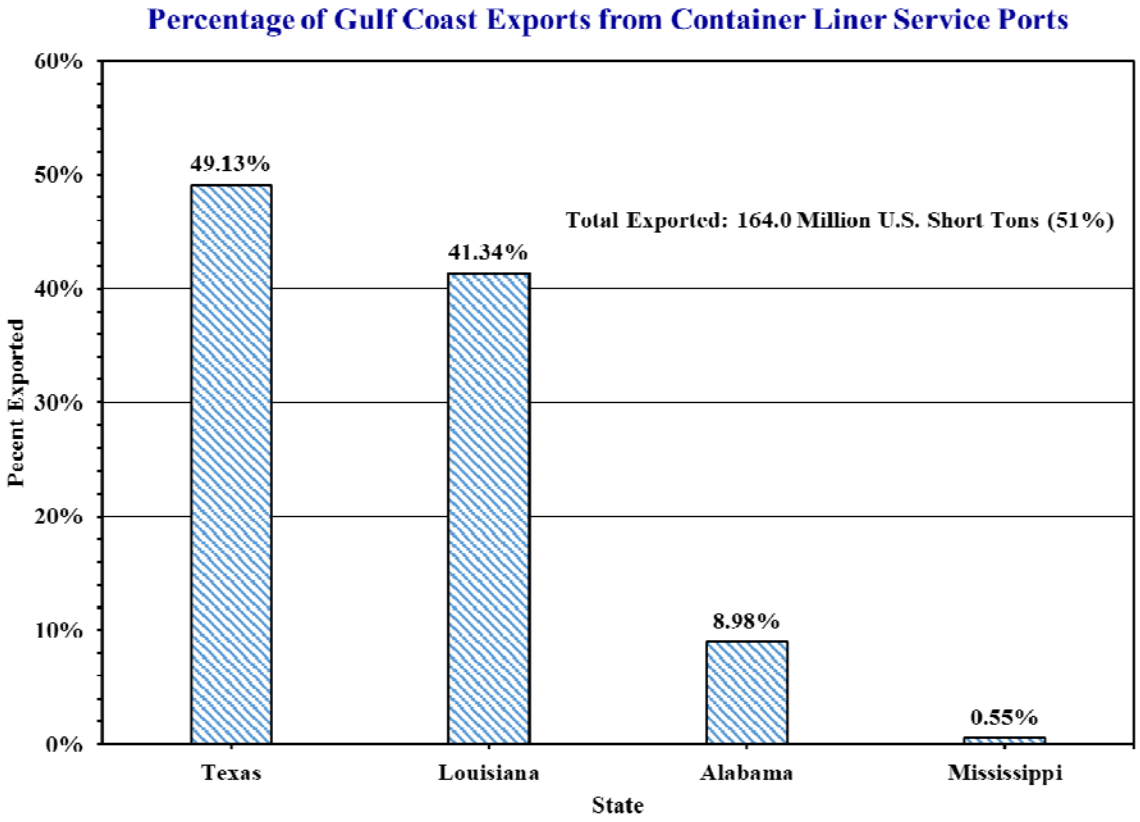

Figure 8. Exports for the U.S. Gulf Coast container liner service ports

Figure 9 shows the total freight from container liner service ports in each Gulf Coast state and the percentage of the total freight each state accounted for in 2010. As shown in Figure 9, Texas had the most total freight with 193.3 million short tons or 63.13% of the total U.S. Gulf Coast freight. Louisiana accounted for 30.01%, Alabama 9.24%, and Mississippi 0.67%. Texas and Louisiana accounted for the majority of the U.S. Gulf Coast total freight. Figure 10 shows the total freight for the U.S. Gulf Coast container liner service ports and the number of ports in each state. Texas had 4 ports, Louisiana 1, Alabama 1, and Mississippi 1.

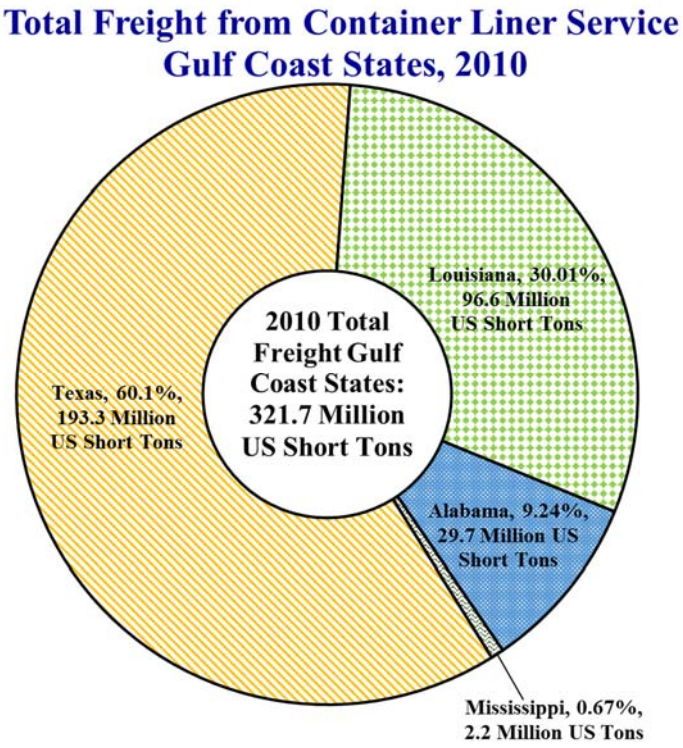

Figure 9. Total freight from U.S. Gulf Coast container liner service ports

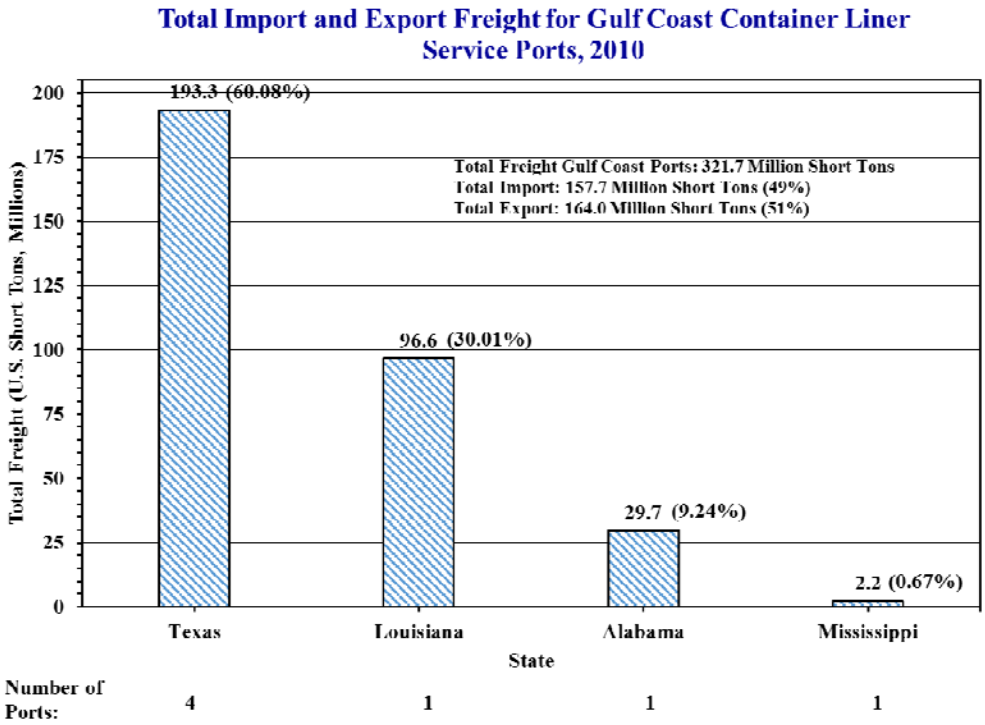

Figure 10. Total freight from U.S. Gulf Coast container liner service ports with number of container liner service ports in each state

2.1.3 U.S. East Coast States Container Liner Service Port Freight Data

Data for the U.S. East Coast container liner service ports was obtained and broken down for every state on the U.S. East Coast that had a container liner service port. Figure 11 shows the percentage of imported freight that each of the East Coast states accounted for in 2010. The imports accounted for 64% of the total U.S. East Coast freight. As can be seen from Figure 11, the East Coast had two states that handled almost half of its imports, with New Jersey at 22.86% and Pennsylvania at 22.72%.

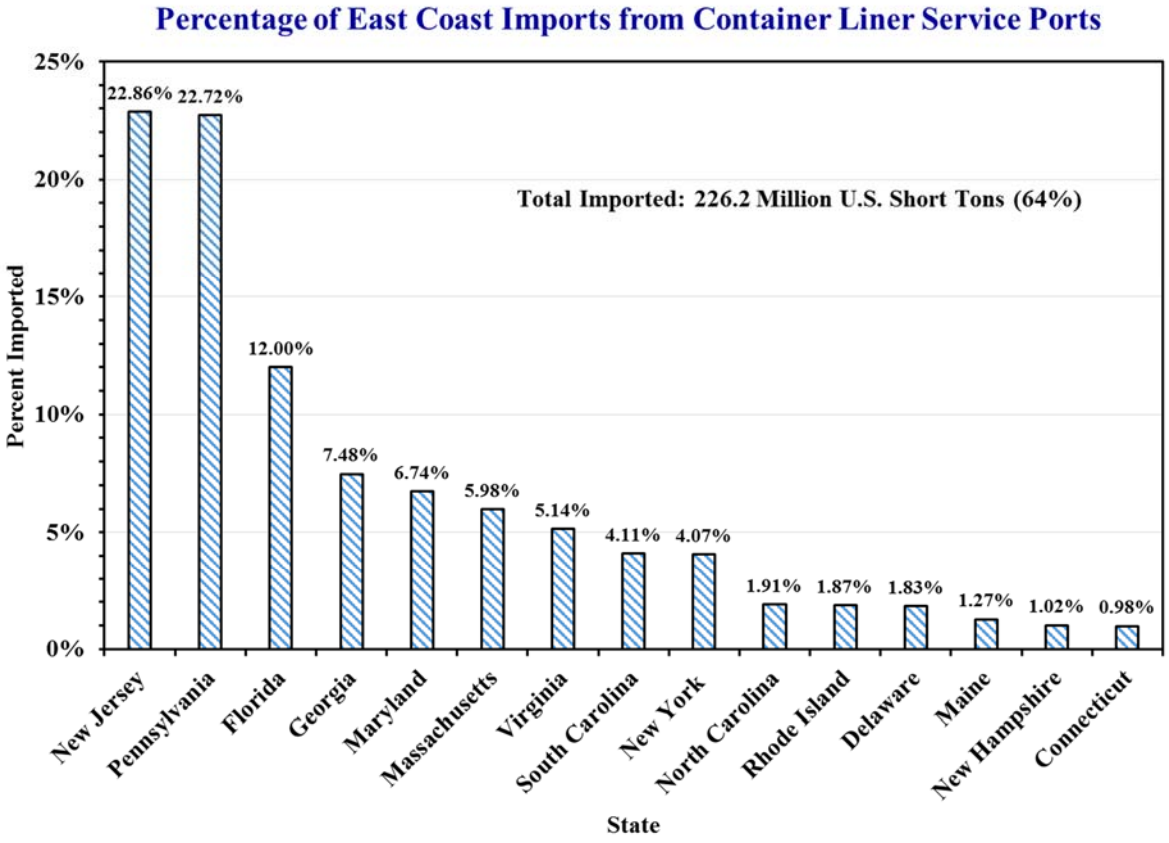

Figure 11. Imports for the U.S. East Coast container liner service ports

Figure 12 shows the percentages of exported freight that each of the East Coast states accounted for in 2010. The exports accounted for 36% of the total U.S. East Coast freight. For the U.S. East Coast, Virginia led the way with 32.86% of the total exports.

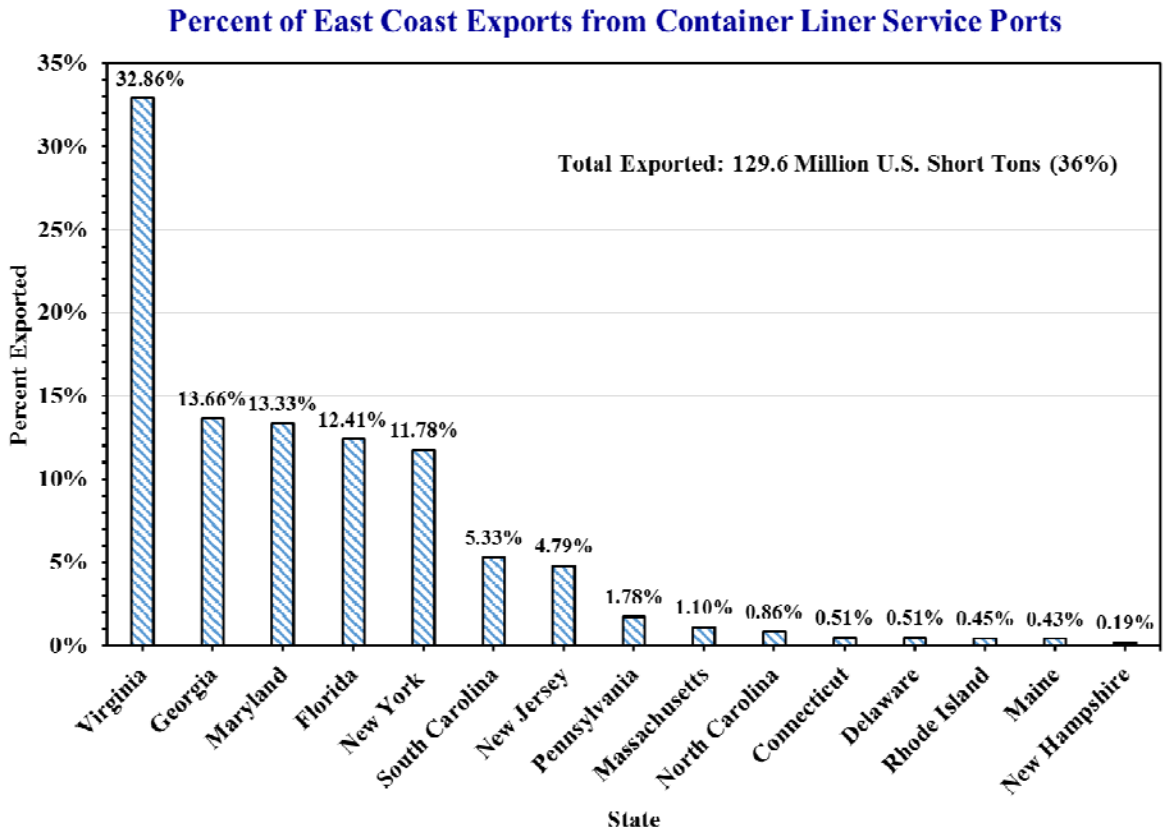

Figure 12. Exports for the U.S. East Coast container liner service ports

Figure 13 shows the total freight from container liner service ports in each East Coast state and the percentage of the total freight each state accounted for in 2010. As shown in Figure 13, New Jersey had the most total freight with 57.92 million short tons or 16.3% of the total U.S. East Coast freight. Of the 15 U.S. East Coast states that had container liner service ports, 6 of these states accounted for 9% or more of the U.S. East Coast total freight. Figure 14 shows the total freight for the U.S. East Coast container liner service ports and the number of ports in each state. Florida had 7 ports, Virginia 3, Pennsylvania 2, Maine 2, and the remaining states contain 1 port each.

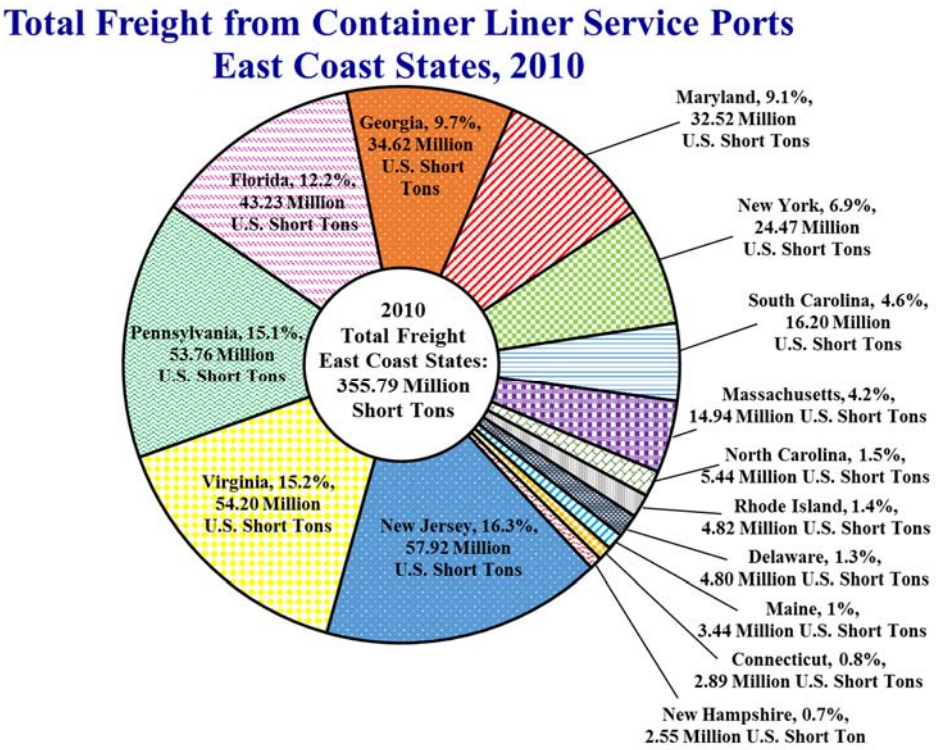

Figure 13. Total freight from U.S. East Coast container liner service ports

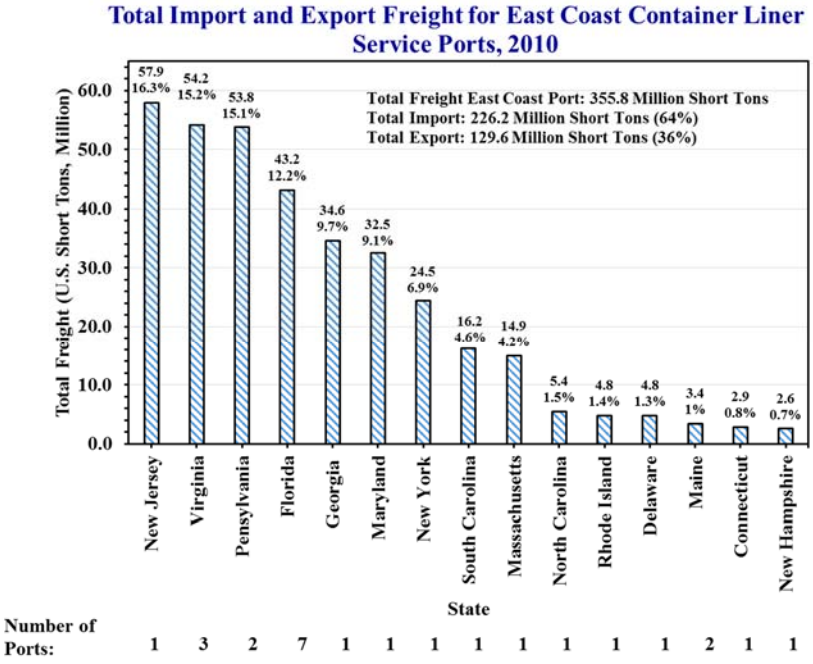

Figure 14. Total freight from U.S. East Coast container liner service ports with number of container liner service ports in each state

2.1.4 Comparison of U.S. West, Gulf, and East Coast States Total Freight Data

In this section of the thesis, the three coastal regions in the U.S. with container liner service ports are compared. Figure 15 shows the total freight for container liner service ports in the entire U.S. based on 2010 data, including the totals for the West Coast, Gulf Coast, and East Coast regions. As seen in Figure 15, the East Coast had the largest amount of freight at 355.8 million short tons or 39.83% of the total U.S. freight. The Gulf Coast accounted for 321.7 million short tons or 36.01% of the total U.S. freight, and the West Coast accounted for 215.9 million short tons or 24.17% [10].

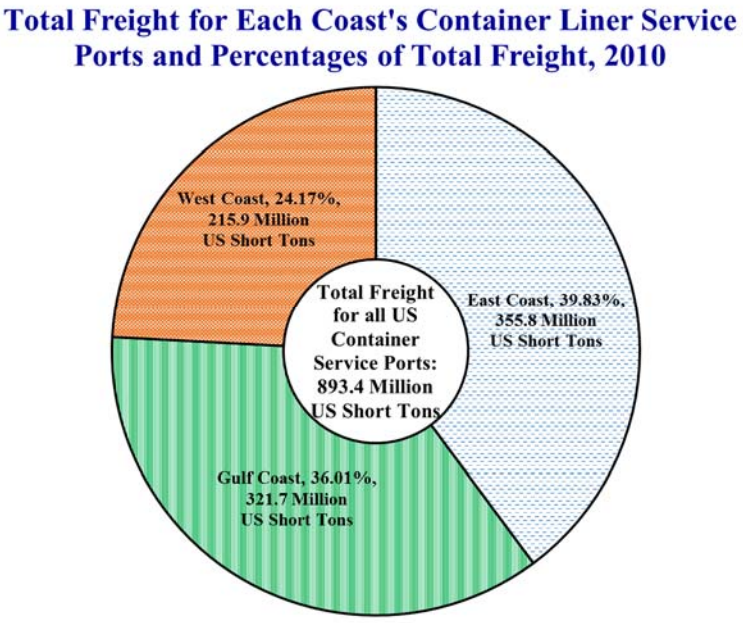

Figure 15. Total U.S. container liner service port freight

2.2 Preliminary Cargo Spatial Mapping of Infrastructure Features of the Ports of Los Angeles and Long Beach

This section shows preliminary mapping of the infrastructure features for the ports of Los Angeles and Long Beach. Chapter 4 of this thesis will provide a more in-depth view of the ports' infrastructures and landuse.

Figure 16 shows the water and port locations of the ports of Los Angeles and Long Beach. It is important to note that the ports of Los Angeles and Long Beach are within just a few feet of one another. The infrastructure and landuse of the ports of Los Angeles and Long Beach will be further discussed later in this thesis.

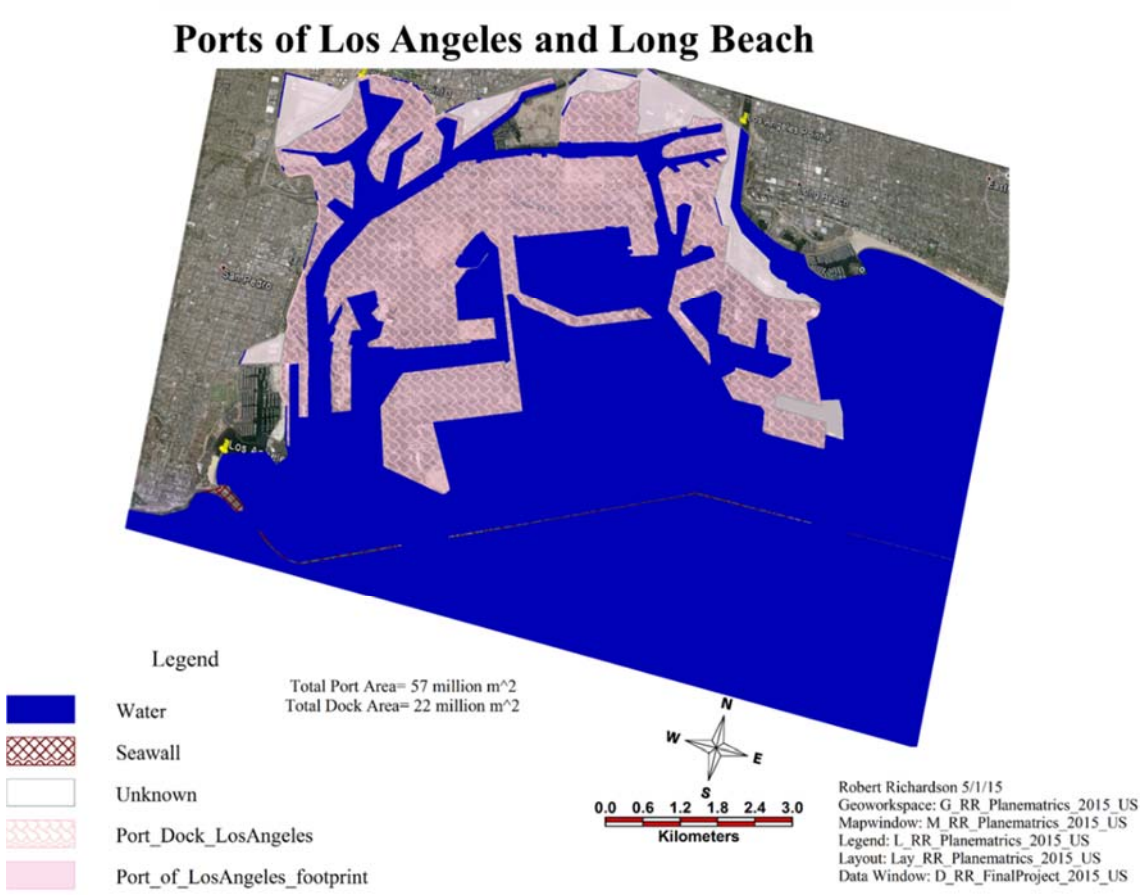

Figure 16. Preliminary mapping of the ports of Los Angeles and Long Beach infrastructure

2.3 Import Distribution from the Ports of Los Angeles and Long Beach to U.S. States

This section covers the distribution of imports from the ports of Los Angeles and Long Beach throughout the U.S. Figure 17 is a map of the West Coast states, showing how many imports California handled [10]. As can be seen from Figure 17, California handled over 90 million total short tons in 2010. The actual number for California was 137,304,074 short tons.

Of this 137,304,074, the ports of Los Angeles and Long Beach accounted for 119 million short tons. Of this 119 million, 70,434,335 short tons were imported and 48,565,665 short tons were exported [10].

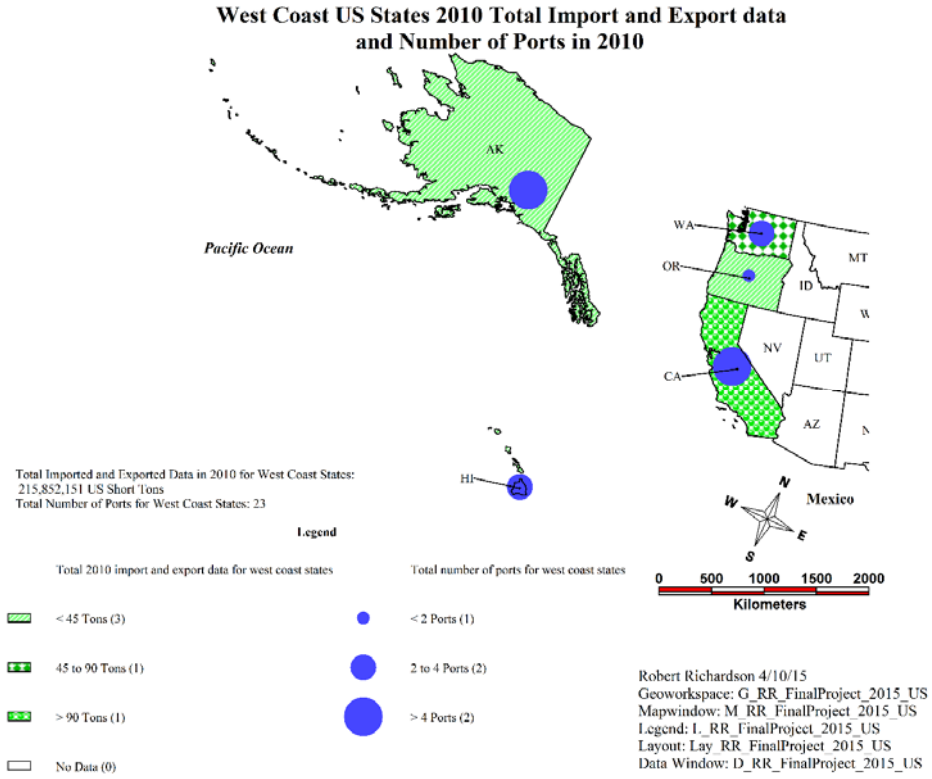

Figure 17. Imported and exported tons of the U.S. West Coast states

The ports of Los Angeles and Long Beach are the two largest ports in terms of import tonnage on the U.S. West Coast. Commodity flow survey data was obtained to determine where these ports' imports are sent [11]. This data shows domestic freight shipments by American establishments in mining, manufacturing, wholesale, auxiliaries, and selected retail and services trade industries. The total number of import tons at the ports of Los Angeles and Long Beach to top five states was 66.76 million tons. To find the ports' distribution data, the following percentages of the total freight shipped to the states were assumed: CA (93.63%), AZ (2.15%), NV (2.14%), TX (1.24%), and WA (0.84%). After this percentage was found, the percentage

was taken from each state to which Los Angeles and Long Beach distribute to. The data initially obtained for this topic included import totals that were much larger than expected. It was found that the imported vessel freight was 19% of the total freight shipped from the Los Angeles and Long Beach area [10, 11]. After finding 19% of each U.S. state's imported totals, the total imported cargo vessel counts were calculated. After these numbers were determined, the total tonnage distributed per capita for each U.S. state was found [12]. After obtaining this data, Figures 18, 19, and 20 were created.

Figure 18 shows the top five states to which the ports of Los Angeles and Long Beach distribute their imports. California retained most of the total imported freight from the ports of Los Angeles and Long Beach at 62,651,460 tons or 93.63%.

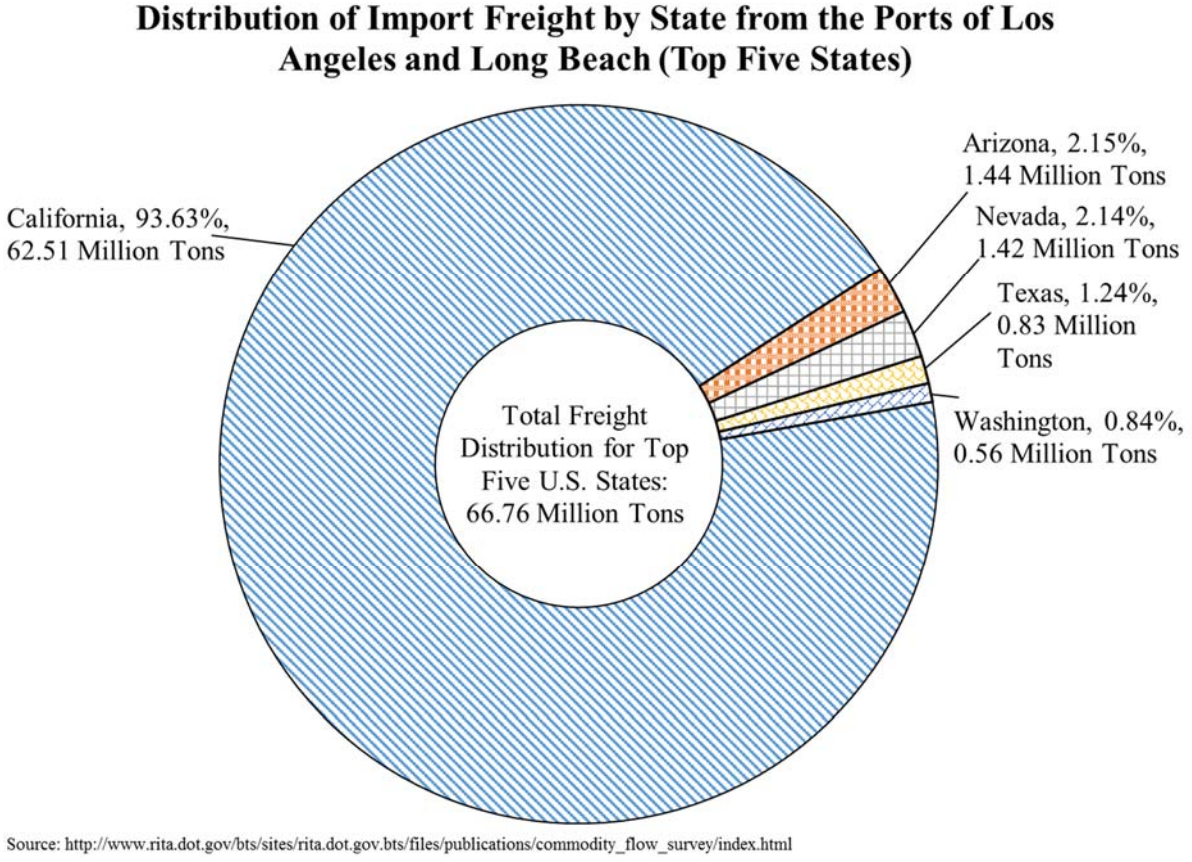

Figure 18. Top five states to which the Ports of Los Angeles and Long Beach sent their imports

Figure 19 shows the top five tonnage per capita states to which distributions were made from the ports of Los Angeles and Long Beach. California was the highest with 1.68 tons per capita and was the only state to be over 1 ton per capita. Other states have a larger percentage per capita because California's population is higher. This is why the 61.12% for California is not higher.

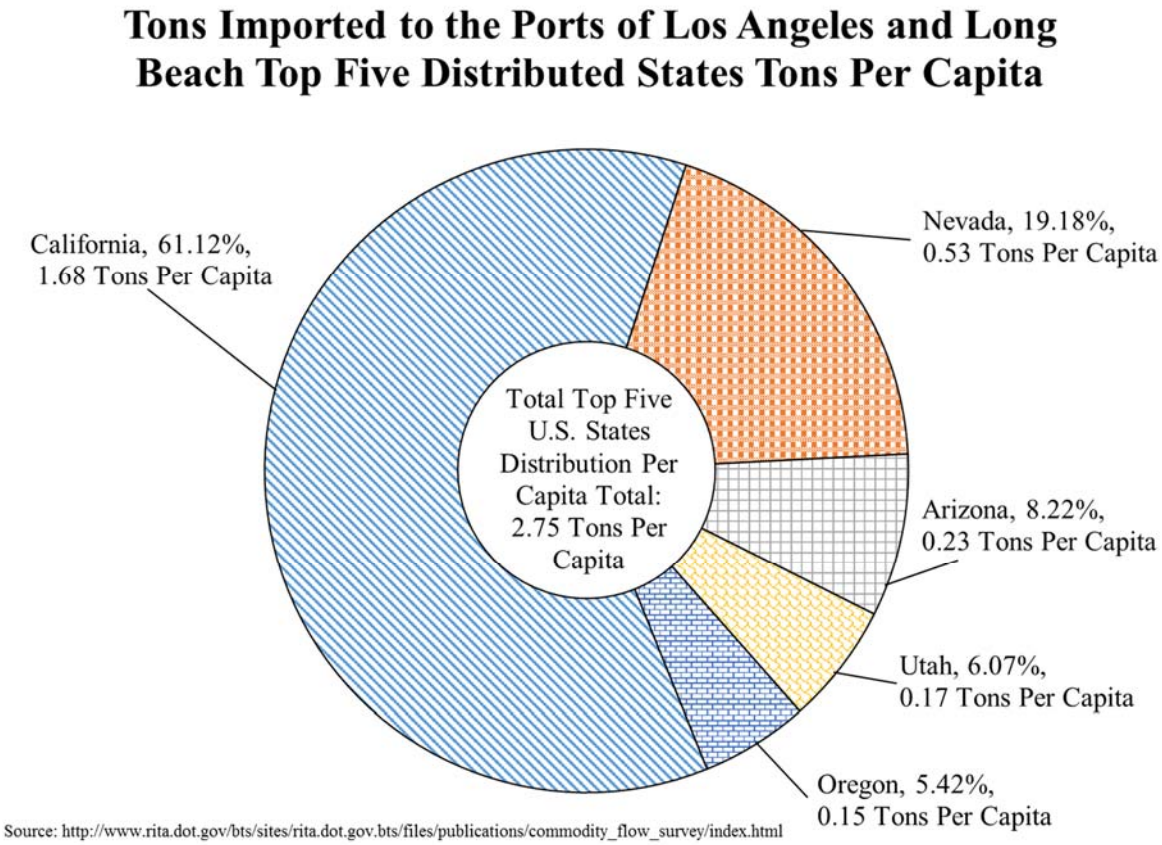

Figure 19. Top five tonnage per capita states to which the ports of Los Angeles and Long Beach made distributions

Figure 20 is a map of per capita distribution by U.S. state from the ports of Los Angeles and Long Beach. As shown on the map, the West Coast states had over .01 freight tons per capita distributed to them, except for Alaska.

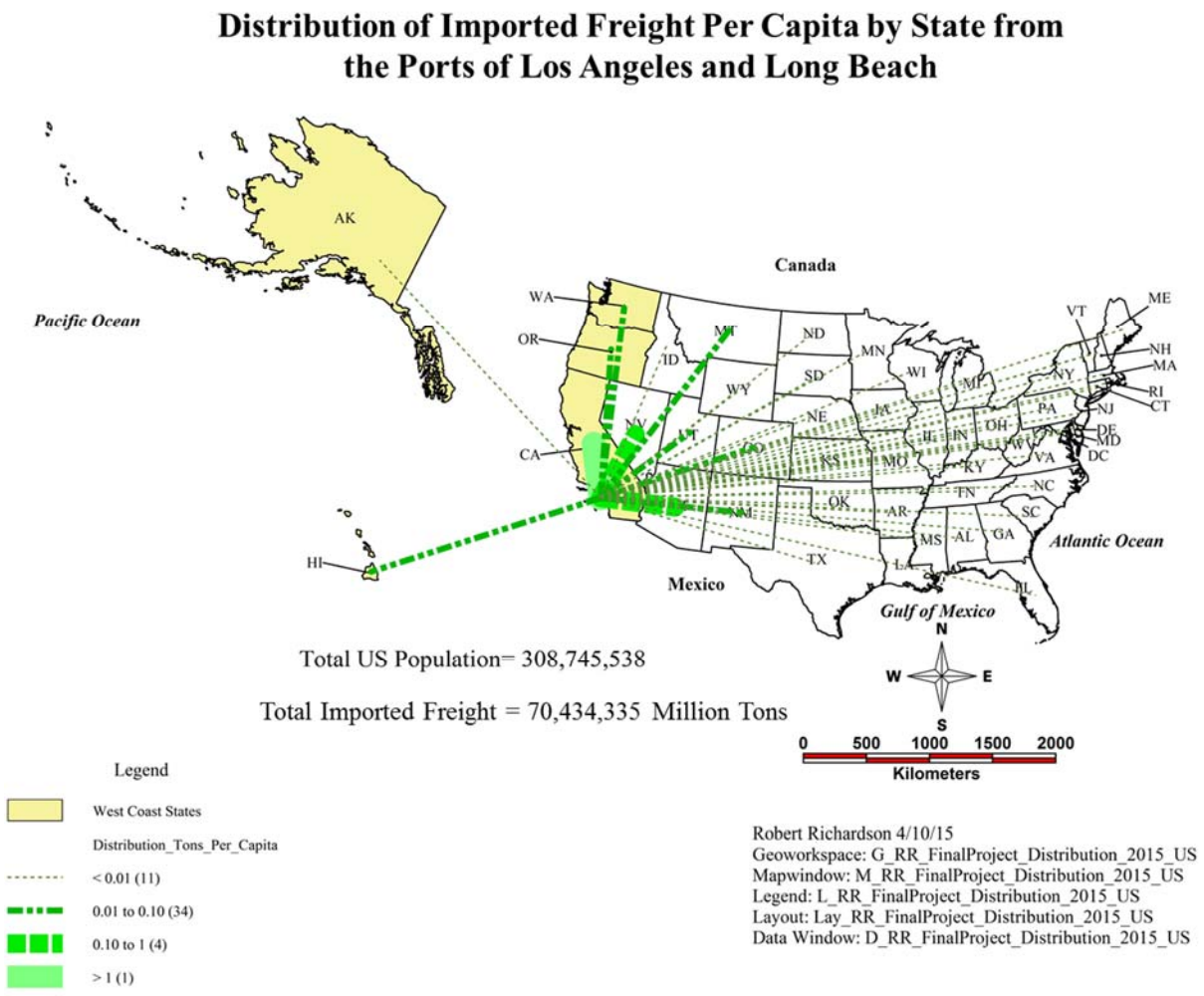

Figure 20. Distribution of imported freight per capita by the ports of Los Angeles and Long Beach by state

2.4 Optimization Analysis for Freight Shipment from the Ports of Los Angeles and Long Beach

In this section, the freight shipment was analyzed using linear optimization. Excel Solver was used to solve a linear optimization problem involving a port that was sending freight tonnage to five separate state markets. An objective function and constraints were created to solve the problem. The first step was to determine the shipping distances from the ports of Los Angeles and Long Beach to the five state markets to which the freight for these ports is

distributed. The linear distances were determined using Google Earth [27]. Figure 21 illustrates the coordinates for the ports and the origin and destination points for the linear distances between the ports and the five selected state market locations.

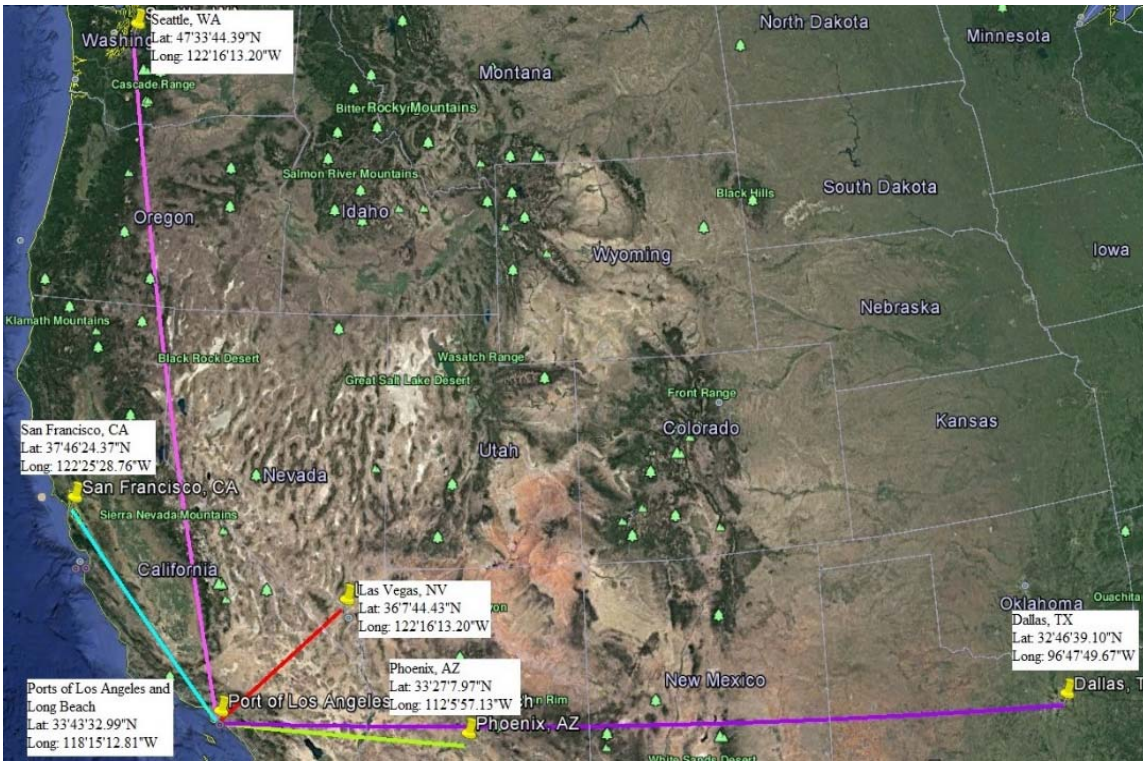

Figure 21. Linear routes between the ports of Los Angeles and Long Beach to the five state markets [27]

Table 1. Estimated linear distance between ports of Los Angeles and Long Beach and five state markets

Ports	State Markets	Distance (Miles)
Ports of Los Angeles and Long Beach	California, CA	364.0
	Arizona, AZ	355.9
	Nevada, NV	243.6
	Texas, TX	1,241.7
	Washington, WA	981.3

Table 1 shows the linear distance from the ports to all five state markets. The maximum distance is from the ports to Texas. The minimum distance is from the ports to Nevada, which is about one-sixth of the distance from the ports to Texas.

The next step was to calculate the total shipping costs based on million tons of freight and miles traveled. The unit cost per ton-mile used for shipping by rail was 3.70 cents per ton-mile and 42.38 cents per ton-mile for shipping by truck [13]. Unit cost in U.S. dollars per ton freight was calculated by dividing cents per ton-mile by 100, and then multiplying this amount by the distance traveled.

A comparison was made between: 1) the total shipping cost of the freight entirely by road, and 2) the total shipping cost of the freight transported 70% by road and 30% by rail. The cents per ton-mile for 70% road and 30% rail was the summation of 0.70 multiplied by 42.38 cents and 0.3 multiplied by 3.70 cents. The result was 30.78 cents per ton-mile or 0.3078 U.S. dollars per ton-mile. Table 2 and Table 3 show the unit costs per ton transported by road, and integration between road and rail, respectively.

Table 2. Unit cost in U.S. dollars per ton (100% road) for base scenario

Linear Distance from the Ports to each State Market and Unit Cost per Ton			
Ports (i)	State Markets (j)	Distance (Miles)	(b_{ij})U.S. Dollars Per Ton Distances x (42.38/100)
Ports of Los Angeles and Long Beach	California, CA	364.0	$154.24
	Arizona, AZ	355.9	$150.81
	Nevada, NV	243.6	$103.22
	Texas, TX	1,241.7	$526.24
	Washington, WA	981.3	$415.87

The right column in Table 2 shows the cost function b_{ij} for base scenario and Table 3 shows b_{ij} for the alternative scenario. The Following Equation 1 was used to calculate b_{ij}.

$$b_{ij} = (\text{Distance from port to state market x (unit cost/100)}) \quad (1)$$

Table 3. Unit cost in U.S. dollars per ton (70% road, 30% rail) for alternative scenario

Linear Distance from the Ports to each State Market and Unit Cost per Ton			
Ports (i)	State Markets (j)	Distance (Miles)	(b_{ij})U.S. Dollars Per Ton Distances x (30.78/100)
Ports of Los Angeles and Long Beach	California, CA	364.0	$112.02
	Arizona, AZ	355.9	$109.53
	Nevada, NV	243.6	$74.97
	Texas, TX	1,241.7	$382.20
	Washington, WA	981.3	$302.04

2.4.1 Objective function and formulation of constraint inequalities

Before the analysis was conducted, certain conditions must be met for the objective function and constraints as shown in Equations 2 through 5 [39]. The formulation of the objective function to minimize total shipping costs from the selected port to each state is shown in Equation 2 for the base scenario and alternative scenario cases.

$$\text{Minimize: } Z = \sum_{i=1}^{I} \sum_{j=1}^{J} (y_{ij} \; x \; b_{ij}) \tag{2}$$

Z= Total cost (U.S.$) to ship from port (i) to each state market (j), where i=1,…I and j=1,2,3,…J

y_{ij}= Quantity of the freight tonnage shipped from port (i) to state market (j)

b_{ij}= Unit cost per ton-mile for freight shipping from port (i) to state market (j) (distance is d_{ij}) (This basic unit cost for freight truck is 42.38 cents per ton-mile and the freight rail unit cost is 3.70 cents per ton-mile.)

The next step was to formulate the constraints for this objective function. All constraints and inequalities must be equal or more than certain values. The first constraint deals with the summing of all commodity freight shipped from the port location to all state markets, which cannot exceed the total commodity freight available at the port (Equation 3).

$$\sum_{j=1}^{J} y_{ij} \geq -T \quad (3)$$

Where, T= Total freight available at port, where i=1,…I and j=1,2,3,…J

The second constraint deals with the total amount sent to a state market, which cannot be less than the amount of the commodity required in that state market as shown in Equation 4.

$$\sum_{i=1}^{I} y_{ij} \geq r_j \quad (4)$$

r_j= Freight required at each port (i) for the state market (j), where i=1,…I and j=1,2,3,…J

Finally, a non-negative constraint was applied to ensure that tonnage values shipped by each mode always remained positive [39]. The amount of freight from port to state market must be a positive value as shown in Equation 5.

$$y_{ij} \geq 0 \quad (5)$$

y_{ij}= Quantity of the freight tonnage shipped from port (i) to state market (j),

where i=1,..I and j=1,2,3,..J

The linear programming optimization was conducted using Excel Solver for the following scenarios:

- Base scenario of freight shipping 100% by road.
- Alternative scenario of freight shipping 70% by road and 30% by rail.

The results can be seen in Table 4 and Table 5.

Table 4. Optimized minimum transportation costs for freight shipping 100% by road (base scenario)

Base Scenario (100% Truck)	Ports of Los Angeles and Long Beach Freight Available: 66.76 million tons					Z
	a	b	c	d	e	(Millions U.S. Dollars)
	CA	AZ	NV	TX	WA	
Unit Cost Per Ton	$154.24	$150.81	$103.22	$526.24	$415.87	
Freight Million Tons (Distributed)	62.51	1.44	1.42	0.83	0.56	$10,675.09

For the base case scenario, the optimized minimum cost is $10,675,090,000. This cost is based on higher unit costs per ton ranging from $103.22 to $526.24 for specific state markets. The highest freight tons (62.51 million) were shipped to a market destination in California. The lowest freight tons were shipped to Washington state, which is approximately less than 1% of the freight tons shipped within California.

Table 5. Optimized minimum transportation costs for freight shipping 70% by road and 30% by rail (alternative scenario)

Alternative Scenario (70 % Truck and 30% Rail)	Ports of Los Angeles and Long Beach Freight Available: 66.76 million tons					Z
	a	b	c	d	e	(Millions U.S. Dollars)
	CA	AZ	NV	TX	WA	
Unit Cost Per Ton	$112.02	$109.53	$74.97	$382.20	$302.04	
Freight Million Tons (Distributed)	62.51	1.44	1.42	0.83	0.56	$7,753.16

For the alternative scenario, the optimized minimal cost is $7,753,160,000. This cost resulted from lower unit costs per ton ranging from $74.97 to $382.20, under the same number of freight tons as in the base scenario.

It was observed that the optimized shipping cost for the alternative scenario was $2,921,939,000 lower compared to the base scenario. The decrease in the shipping cost for the

alternative scenario was 27.4% when 30% of the truck freight was diverted to rail. This linear optimization analysis shows a reduction in shipping costs as more freight is diverted from road transportation options to intermodal rail transportation options for the following freight distributions to the top five selected state markets (Table 6). A detailed step-by-step procedure conducted for linear optimization analysis is described in Appendix A.

Table 6. Freight distribution (million tons) to state market

Ports Distribution to Each State Market		
State Market	Freight Distribution (Million Tons)	% Freight Distributed
California, CA	62.51	93.63%
Arizona, AZ	1.44	2.15%
Nevada, NV	1.42	2.14%
Texas, TX	0.83	1.24%
Washington, WA	0.56	0.84%
Total	66.76	100%

2.5 Concluding Remarks

Sea ports in the U.S. play a very important role in the daily lives of every American. Millions of tons of freight are handled by U.S. ports annually, helping Americans to acquire their basic needs and other goods. The West Coast is home to two of the top five largest ports in the U.S. [10]. The two ports, the ports of Los Angeles and Long Beach, are further discussed in this thesis, including the ports' tonnage, TEUs, infrastructure, and landuse.

CHAPTER III

CONTAINER SHIP TEU PREDICTION MODELING FOR SELECTED PORTS

3.1 TEU Data Visualization and ARIMA Modeling for the Ports of Los Angeles and Long Beach

The ports of Los Angeles and Long Beach in the State of California are located directly next to each other. Based on demand, vessels can go to the port in Los Angeles or to the port in Long Beach when they arrive in this area. Knowing this, TEU data for these ports from 1995-2014 was combined [14]. Figure 22 shows the raw TEU time series data at these ports [14]. The time series plot shows a significant difference in TEU value in year 2008, which is the year of the most recent economic recession (ER) in the U.S. Therefore, the two data sets (before and after 2008) were analyzed for statistically significant difference.

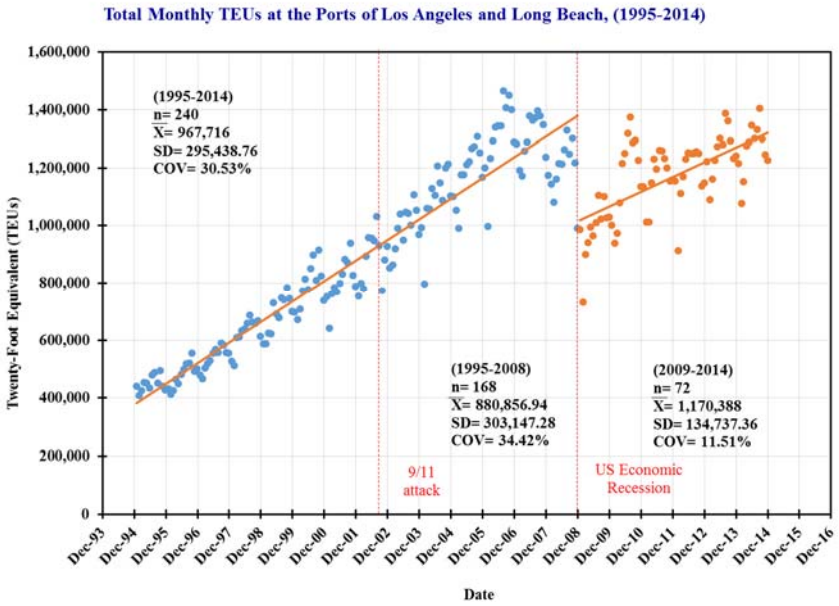

Figure 22. TEU time series data of the ports of Los Angeles and Long Beach

3.1.1 Setting up a One-Way Analysis of Variance (ANOVA) Hypothesis Test

The following assumptions are made for ANOVA test [15]:

1) Random sampling
2) Normality
3) Equal variances

Step 1 is to conduct an ANOVA hypothesis test of significance; a null and an alternative hypothesis are made [16].

- H_0: $\mu_1 = \mu_2$
- H_A: $\mu_1 \neq \mu_2$
- μ_1 = Population mean of annual TEUs before 2008 economic recession
- μ_2 = Population mean of annual TEUs after 2008 economic recession

Step 2 is to select an alpha value for statistical significance test.

- $\alpha = .05$

Step 3 is to define the critical F and the $\alpha/2$ level.

- df = 227
- df between = 1
- df within = 226
- $\alpha/2 = 0.025$
- $F_{Critical} = 5.02$ (Found from F-table [8]).

Step 4 is to establish the Decision Rule.

- Reject H_0 if $F_{test} \geq F_{Critical}$
- $44.663 \geq 5.02$

Step 5 is to calculate the Grand Mean.

- $\overline{X}_{GM} = \sum X / N$
- $\overline{X}_{GM}$ = Grand Mean = 952,258.22
- N = total sample size
- X = total of all data values

Step 6 is to find the total sample variation.

- SS (T) = $\sum (x - \overline{X}_{GM})^2$
- SS (T) = Total Variation = 1.965×10^{13}

Step 7 is to solve the between-group variation.

- SS (B) = $\sum n (\overline{x} - \overline{X}_{GM})^2$
- SS (B) = sum of squares between groups = 3.242×10^{12}

Step 8 is to find the within-group variation.

- SS (W) = $\sum df * s^2$
- SS (W) = sum of squares within group = 1.640×10^{13}
- df = N-k =229-2 = 227
- k = number of samples

Step 9 is to calculate the F test statistic.

- F_{test} = MSBG / MSWG
- F_{test} = 44.663

Step 10 is to report the final results.

- F_{test} (44.663) > $F_{critical}$ (5.02)
- Therefore, H_0 cannot be accepted.

To see the effect of the U.S. economic recession in 2008, a comparison of data before and after was made using the one-way ANOVA analysis using SPSS [17]. Table 7 shows the SPSS

output for the ANOVA test. There was a statistically significant difference between the two data sets and TEU data because Sig. is 0.000 (less than α/2, or 0.025) as shown in the right column of Table 7.

Table 7. One-Way ANOVA Results

	Sum of Squares	df	Mean Square	F	Sig.
Between Groups	3241717809987.834	1	3241717809987.834	44.663	.000
Within Groups	16403392230991.781	226	72581381553.061		
Total	19645110040979.613	227			

3.1.2 Developing Regression Equations for TEUs

Because of the statistically significant difference in post-2008 and prior years TEU data, a dummy variable for post-economic recession was used to develop a regression equation. Every month in 2008 and in prior years, the ER_Dummy was assigned 0.00, and every month after the ER_Dummy was assigned a 1.00 in the dummy variable column. This was done to model the difference in the TEU data from 1995-2008 and 2009-2014 [17]. Equation 5 was developed from combined ports of Los Angeles and Long Beach data. The R value for the 1995-2013 ports of Los Angeles and Long Beach data is 0.95. Figure 23 shows measured vs. predicted data using Equation 5 on all the TEU data, from 1995 to 2013. The mean absolute relative error (MARE) and root mean square error (RMSE) were the methods used to compare if each analysis was acceptable [18, 19]. The equations for the MARE and RMSE can be seen in Equations 6 and 7 [18, 19]. According to these sources, "The MARE is a statistical accuracy measure that is used to filter out the most promising optimal networks or models. If the value of MARE is small, close to zero, it means that the model's performance is good" [18]. The RMSE is generally used

as a measure of the difference between values predicted by the model and measured values. RMSE is an indicator of model accuracy or precision. "RMSE should be as low, or as close to zero, as possible" [19]. Figure 23 shows that the MARE is 7.10% and the RMSE was 92,131.72 for the regression equation 1995-2013 TEU data. Figure 24 shows validation of Equation 5 using 2014 TEU data. The MARE for the measured and predicted 2014 TEU data is 8.78%, which is reasonable. The RMSE for the data is 127,342.46. Figure 25 shows further validation of Equation 5 using 1995-2014 TEU data. The RMSE for the data is 115,448.67. The MARE is 9.86%, which is reasonable.

TEU = 308,935.109 + (5,917.916 x Month_R) + (-403,857.290 x ER_Dummy) (5)

$$\text{MARE} = \frac{\sum_{i=1}^{N}\left|\left(\frac{\widehat{Q}t_i - Qt_i}{Qt_i}\right)\right|}{N}\ x\ 100 \quad (6)$$

$$\text{RMSE} = \sqrt{\frac{\sum_{i=1}^{n}(y_i - \hat{y}_i)^2}{n}} \quad (7)$$

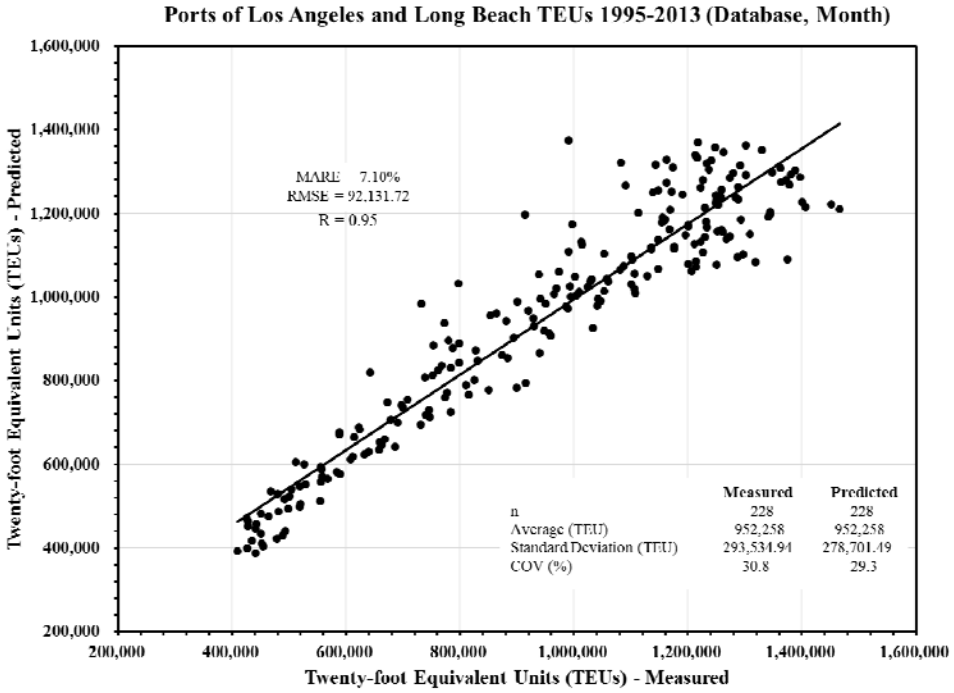

Figure 23. Measured vs. predicted TEUs 1995-2013 (Regression Equation)

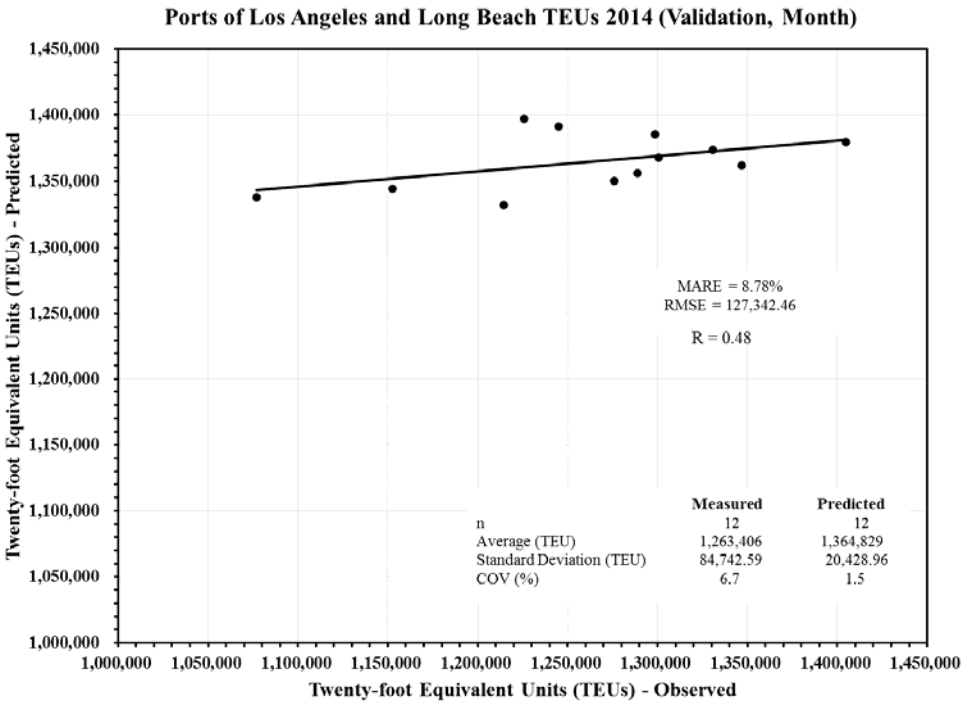

Figure 24. Validation of measured vs. predicted TEUs 2014 (Regression Equation)

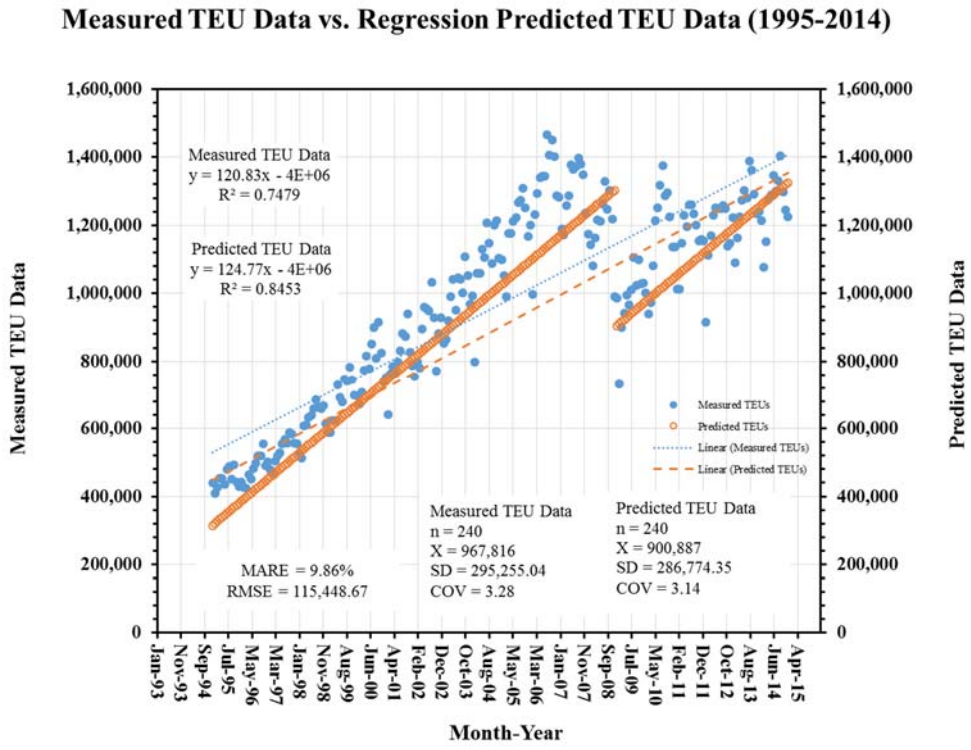

Figure 25. Measured vs. predicted TEU data for the regression equation

ARIMA modeling was performed next due to a high sequential R value of 0.97 for the TEU data set. This high sequential R means that the regression analysis does not meet the criterion for no sequential correlation. Therefore, ARIMA modeling was pursued.

3.1.3 ARIMA Modeling of TEU time series

First, several ARIMA models were developed using the procedure described in the book, *Applied Times Series Analysis for the Social Sciences* by McCleary and Hay, Jr. in SPSS software [17, 20]. McCleary and Hay, Jr. [20] discuss in depth the criteria to select the appropriate (p,d,q) terms in the ARIMA model. In the ARIMA model, p stands for autoregressive term, d is for series differencing term, and q is for moving average term.

For selecting the (p,d,q) terms to model this TEU data, the Pearson's correlation table from Nguyen's dissertation [21] was created. In this table sequential R, AutoRegression (AR) lag 1 vs. month, AR lag 2 vs. month, month vs. one differencing, month vs. two month moving average (MA), and month vs. three month MA will all be found to determine what (p,d,q) to select. To accomplish this, Excel software was needed. The following steps were used to find the correct (p,d,q):

Step 1 was to obtain all raw data of monthly TEUs for the ports of Los Angeles and Long Beach [14].

- Obtain raw TEU data for the Port of Los Angeles [14].
- Obtain raw TEU data for the Port of Long Beach [14].
- Combine the Port of Los Angeles and Port of Long Beach TEU data to get the final TEU raw monthly data numbers.

Step 2 was to determine which AR or "p" term to use.

- Find AR lag 1 vs. month.

- Find AR lag 2 vs. month.
- Make a correlation equation between month values and TEU values.
- For AR lag 1 TEU values move down one month leaving January 1995 empty.
- For AR lag 2 TEU values move down two months leaving January and February 1995 empty.
- Select the higher of the two AR values.

In this case, both of the lags had a value of 0.86, and either term would have been acceptable to select. For this case, lag 1 was selected for AR or "p". Table 8 shows the AR values.

Step 3 was to select the differencing term or "d" for the ARIMA model.

- Find month vs. differencing term.

To find differencing, a correlation between the month and difference between each month's values was made. For differencing 1 the value was skipped so it was the first value minus the second value. This was repeatedly done until December of 2014. The differencing term was 1. However, a greater or lesser difference may affect the TEU data. A model with 0 and 2 for differencing was also made. Table 8 shows the "d" or differencing value.

Step 4 was to select the moving average term or "q" for the ARIMA model.

- Find month vs. two month MA.
- Find month vs. three month MA.
- For two month MA take two values and take the average of that.
- For three month MA take three values and take the average of that.
- Select the higher of the two MA values.

The MA helps smooth out the curve of the data. In this case, two month MA and three month MA had the same value. For MA or "q", 1 was also selected. The value for MA can be seen in Table 8. Figure 26 also shows the values of AR lag 1, AR lag 2, differencing, two month MA, and three month MA.

Table 8. Pearson's correlation table

A	B	C	D	E	F	G	H
Sequential Correlation (Lag 1)	AR Lag 1 (TEUs) vs. Month	AR Lag 2 (TEUs) vs. Month	Month vs. One Differencing	Month vs. Two Differencing	Month vs. One Month Moving Average	Month vs. Two Months Moving Average	Month vs. Three Months Moving Average
0.97	0.86	0.86	-0.027	-0.043	0.87	0.87	0.87

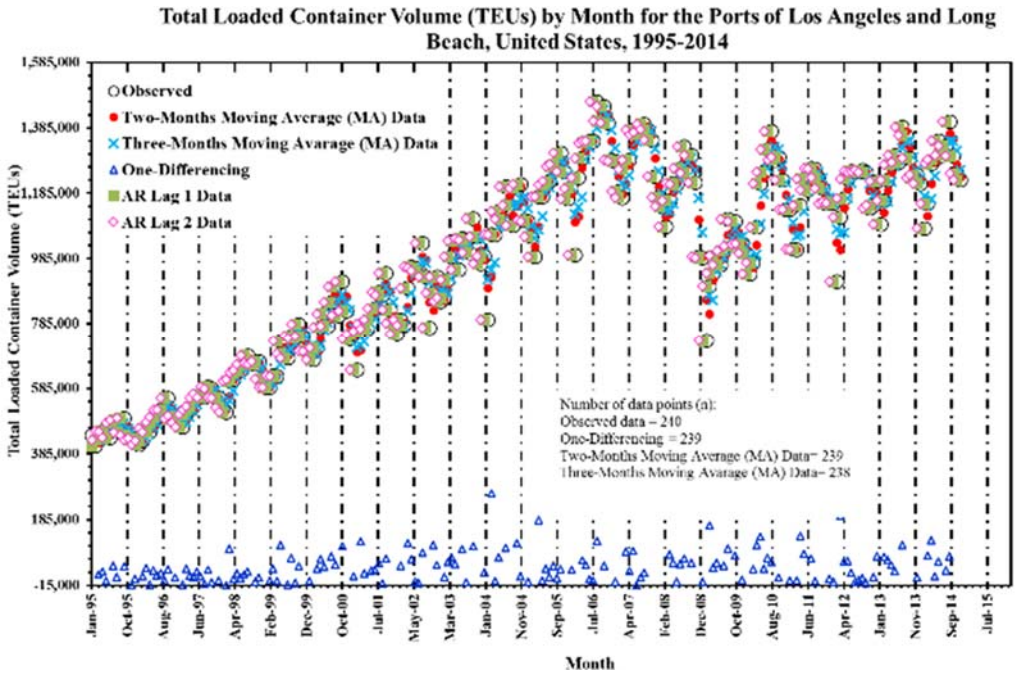

Figure 26. Values of AR lags, differencing, and MA values

Next, run the final ARIMA (1,1,1), (1,0,1), (1,2,1) to get final results and predict which will be the best model. Figure 27 shows the results for the final ARIMA (1,1,1). In Figure 27, it can be seen in the residual autocorrelation function (ACF) and residual partial autocorrelation

function (PACF) plots that some of the residual numbers go outside of the confidence intervals, however, the final three residual numbers are very near 0.0. Figure 28 shows a high R value for 1995-2013 predicted vs. measured data with a R=0.97. Figure 29 is validation of the ARIMA (1,1,1). Figure 29 shows that MARE for the measured and predicted 2014 TEU data for ARIMA (1,1,1) is 4.89%. ARIMA (1,0,1) was then run to determine if better results could be obtained.

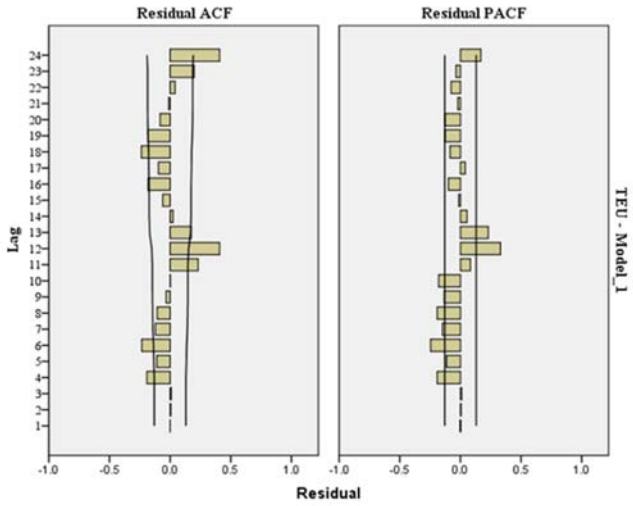

Figure 27. Residual ACF and PACF plot for ARIMA (1,1,1) model equation

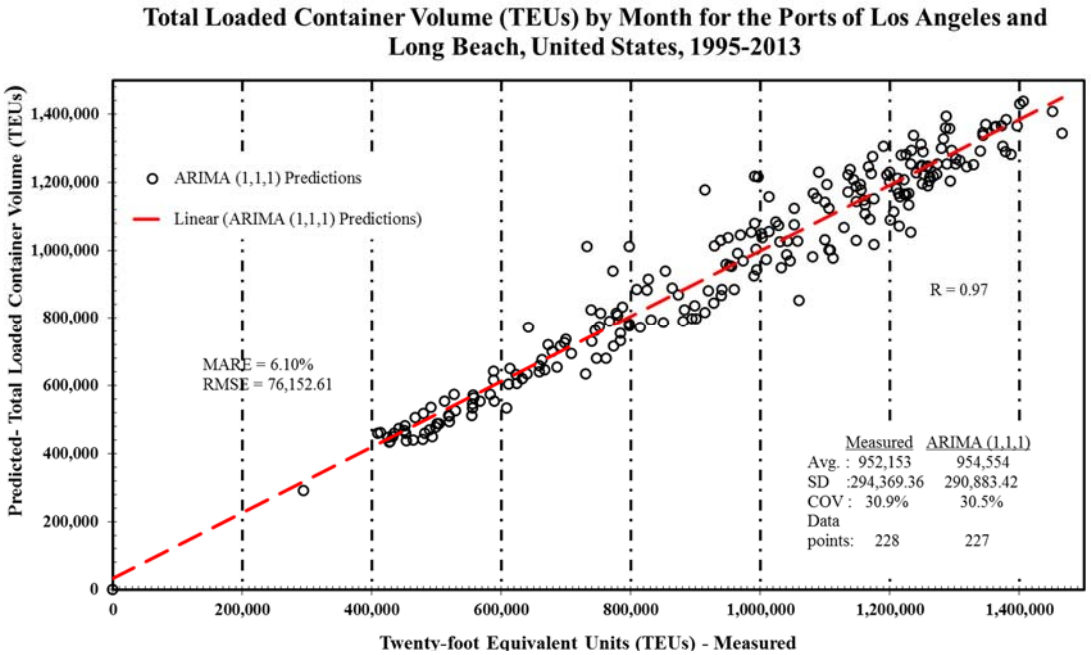

Figure 28. Measured vs. predicted TEUs 1995-2013 ARIMA (1,1,1) model equation

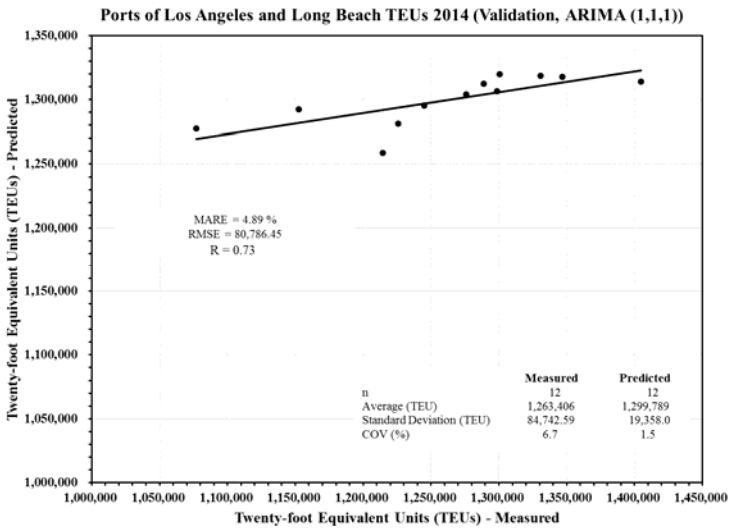

Figure 29. Validation of measured vs. predicted TEUs 2014 ARIMA (1,1,1) model equation

Figure 30 shows the results for the final ARIMA (1,0,1). In Figure 30, it can be seen that only 4 or 5 residual numbers go outside of the confidence intervals of the residual ACF or residual PACF plots. Figure 31 shows a high R value for 1995-2013 predicted vs. measured data with a R=0.97. Figure 32 is validation of the ARIMA (1,0,1). Figure 32 shows that MARE for the measured and predicted 2014 TEU data for ARIMA (1,0,1) is 7.50%. This is a higher MARE value between the measured and predicted difference. Therefore, ARIMA (1,2,1) was then used to determine if better results could be obtained.

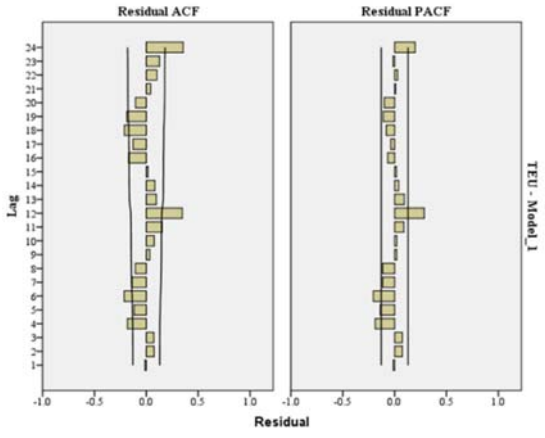

Figure 30. Residual ACF and PACF plot for ARIMA (1,0,1) model equation

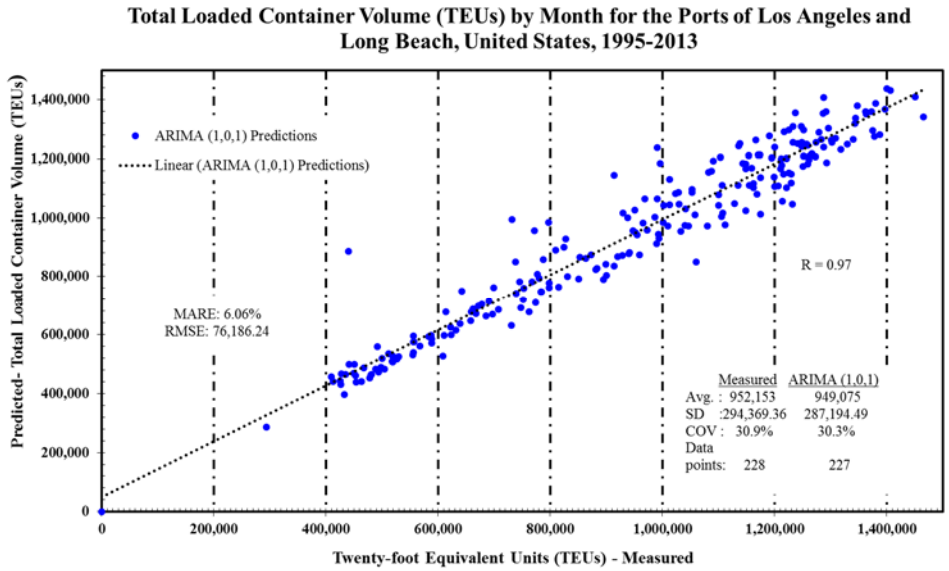

Figure 31. Measured vs. predicted TEUs 1995-2013 ARIMA (1,0,1) model equation

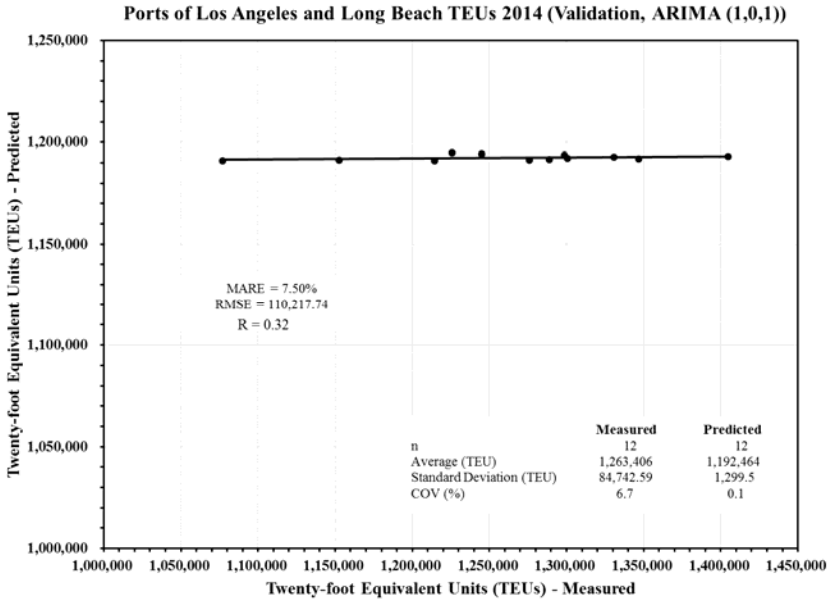

Figure 32. Validation of measured vs. predicted TEUs 2014 ARIMA (1,0,1) model equation

Figure 33 shows the results for the final ARIMA (1,2,1). In Figure 33, it can be seen that only 2 or 3 residual numbers go outside of the confidence intervals of the residual ACF or residual PACF plots. Figure 34 shows a high R value for 1995-2013 predicted vs. measured data with a R=0.97. Figure 35 is validation of the ARIMA (1,2,1). Figure 35 shows that MARE for

the measured and predicted 2014 TEU data for ARIMA (1,2,1) is 3.54%. The ARIMA (1,2,1) validation yielded the best results with the lowest MARE of 3.54%.

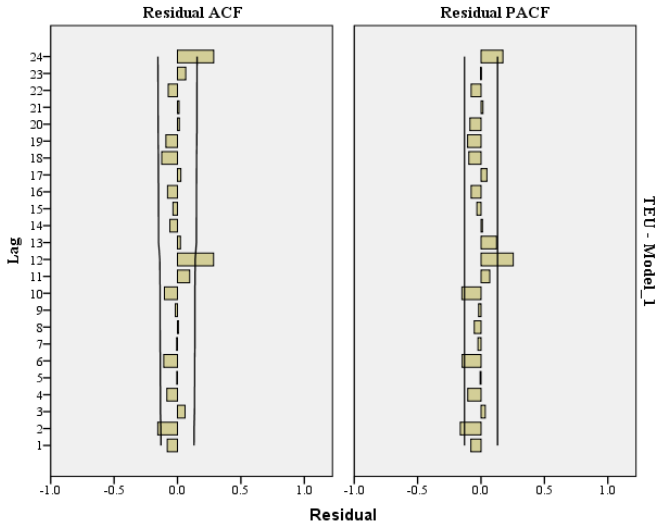

Figure 33. Residual ACF and PACF plot for ARIMA (1,2,1) model equation

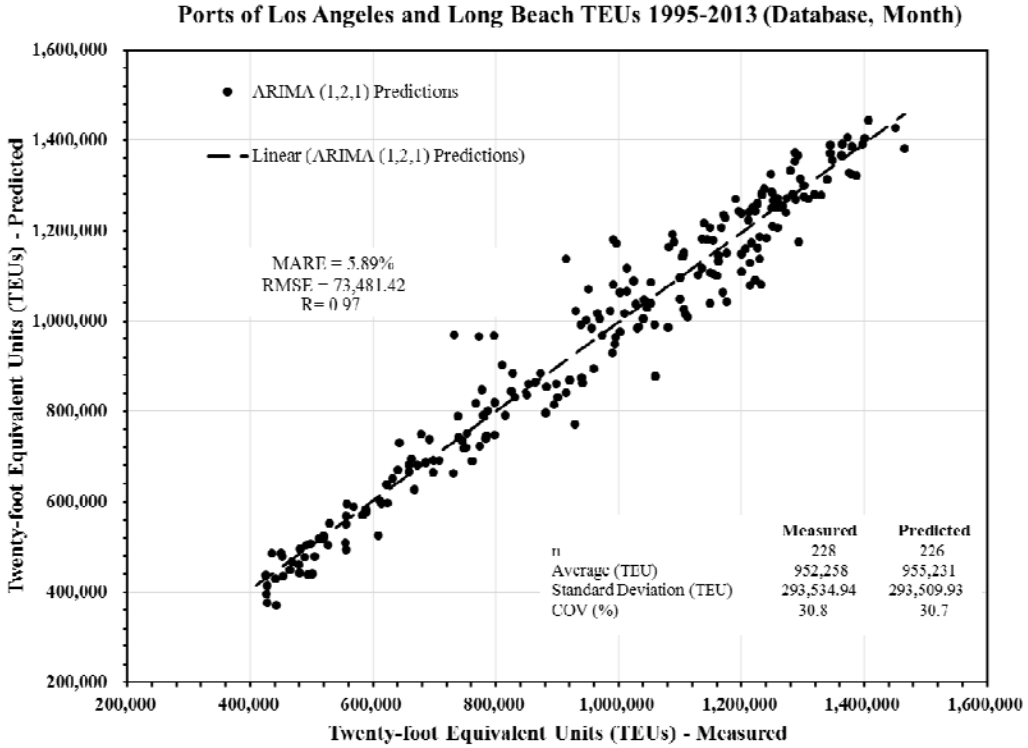

Figure 34. Measured vs. predicted TEUs 1995-2013 ARIMA (1,2,1) model equation

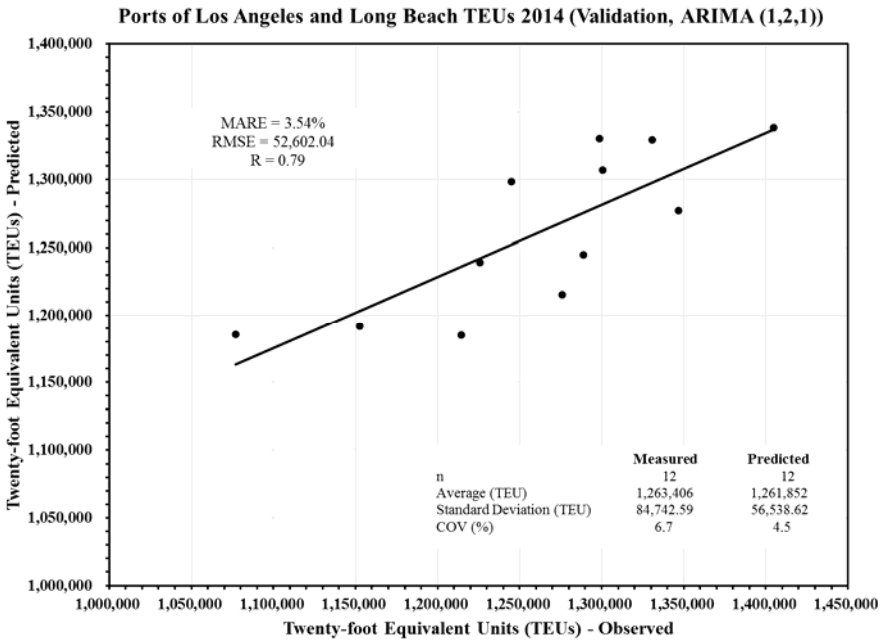

Figure 35. Validation of measured vs. predicted TEUs 2014 ARIMA (1,2,1) model equation

After comparing the ARIMA modeling, it was found that ARIMA (1,2,1) was best because it had the lowest MARE percentage. Based on this finding, an ARIMA (1,2,1) equation was developed. The ARIMA (1,2,1) equation can be represented by Equation 8, which was developed by Uddin, McCullough, and Crawford [22].

$$\blacktriangledown^2 * Y_t = C + (1 - \phi_1 B-) * (1 - \theta_1 B) * a_t \quad (8)$$

Y_t = Discrete time series
$\blacktriangledown^2$ = Regular Differencing operator of order one
C = Constant
$1 - \phi_1 B$ = Regular AutoRegressive process of order one
$1 - \theta_1 B$ = Regular Moving Average process of order three
a_t = random shock term; normally distributed, independent with zero mean, and variance equal to σ_a.

Figure 36 indicates that there was only a 0.13% difference of the predicted and measured data from 1995-2014 and a MARE of 5.77%. This provided further validation that ARIMA (1,2,1) is the best ARIMA model for the ports of Los Angeles and Long Beach TEU data.

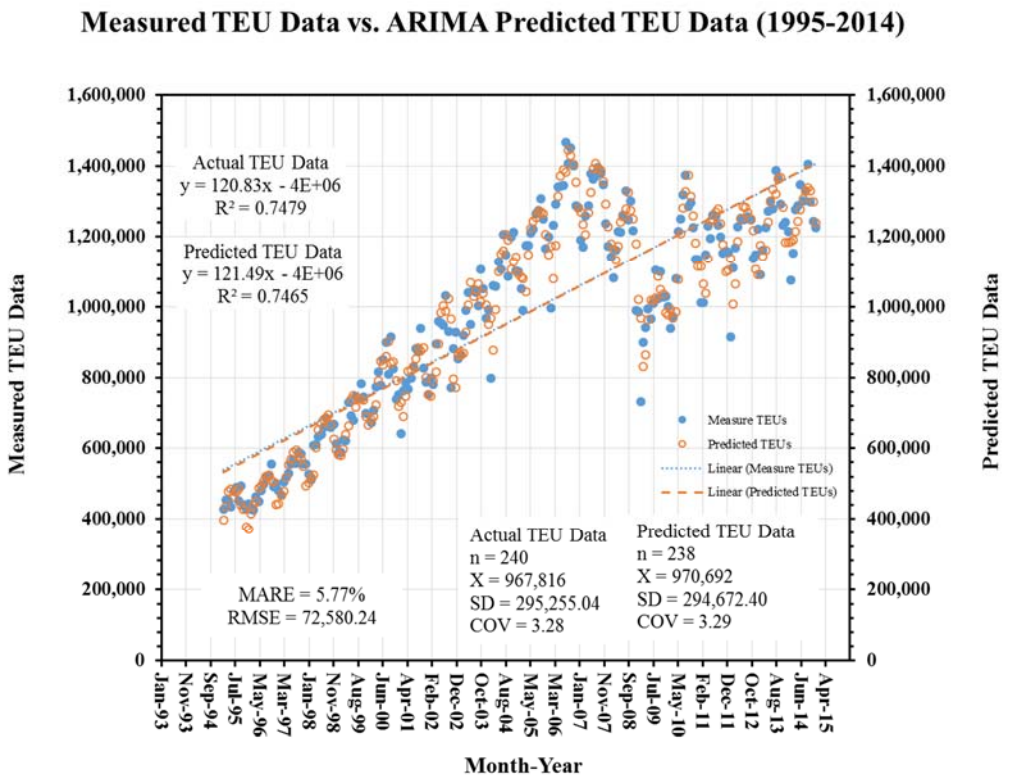

Figure 36. Measured vs. predicted TEU data for the ARIMA (1,2,1) model equation

3.1.4 Validation of ARIMA (1,2,1) and Regression Equations and Forecasting for TEU Demand of Selected Ports

Comparing the two data results shows whether regression equation or ARIMA (1,2,1) was a more accurate tool for data forecasting. Figure 25 is the regression model, and Figure 36 is for the ARIMA (1,2,1). The regression equation was found to have a MARE of 9.86% and a RMSE of 115,448.67. While the regression equation is reasonable, the ARIMA (1,2,1) showed only a 5.77% MARE value and a 72,580.24 RMSE value. Because the MARE and RMSE values are smaller for the ARIMA (1,2,1), it is more accurate than the regression equation in predicting and forecasting TEU demand. This shows that the ARIMA (1,2,1) should be selected and used for future forecasting testing.

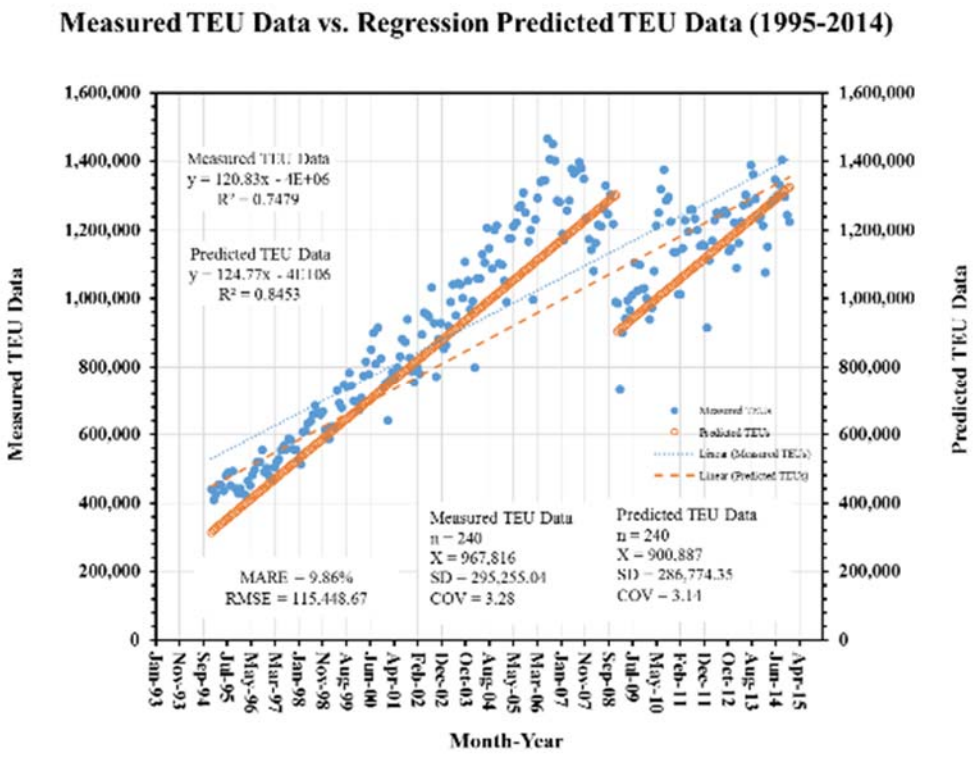

Figure 25. Measured vs. predicted TEU data for the regression equation

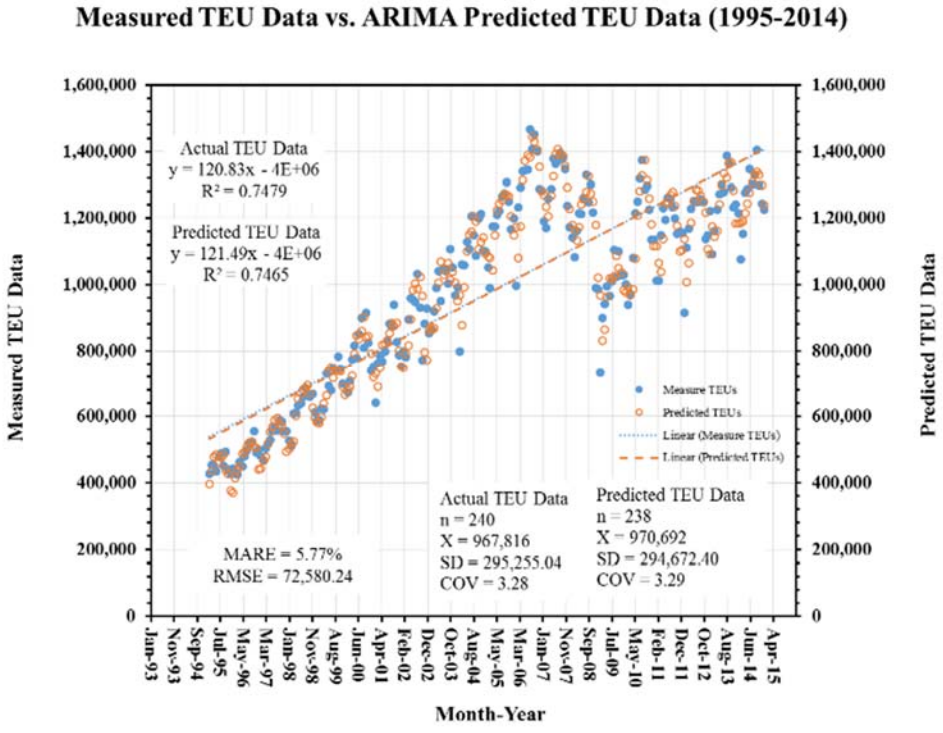

Figure 36. Measured vs. predicted TEU data for the ARIMA (1,2,1) model equation

3.2 Regression and ARIMA Analysis for TEU Demand Modeling Using California GDP as the Independent Variable

With a very high sequential R of 0.97, monthly time as an independent variable is not appropriate. Therefore, monthly GDP data for the state of California was found for the new independent variable [23]. Figure 37 shows the measured monthly TEU data for the ports of Los Angeles and Long Beach and the monthly GDP data for the state of California. As can be seen, this data was better for the TEU data than time because California GDP also took a dip during the economic recession. This might produce more accurate results when predicting future TEU values.

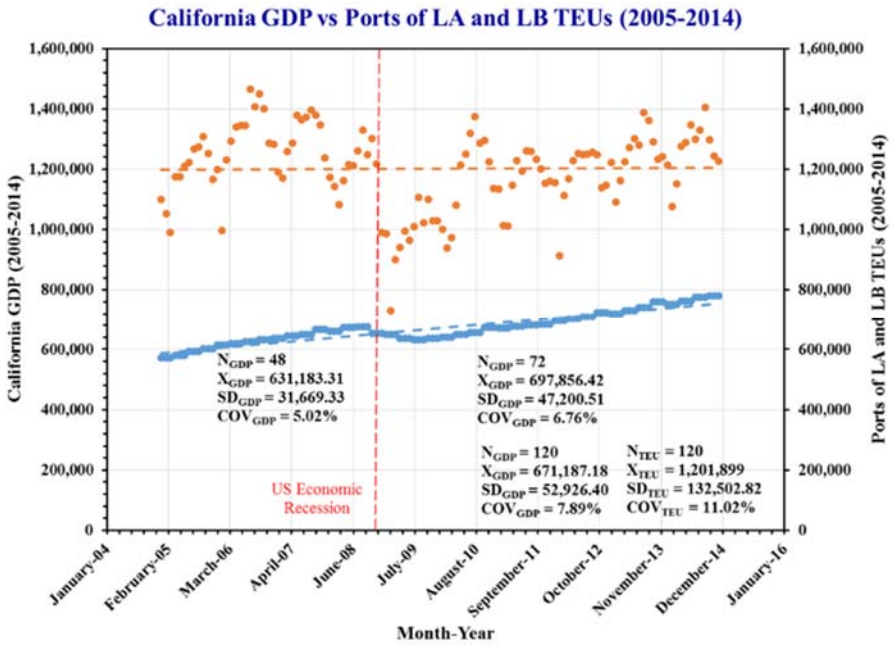

Figure 37. California GDP vs. ports of Los Angeles and Long Beach TEUs

3.2.1 Regression Equation and Validation for 2005-2014 TEU Data using California GDP as the Independent Variable

The regression equation was developed to determine the correlation of the 2005-2014 TEU data and California GDP data [14, 22]. Regression Equation 9 was developed. Figure 38

was made using Equation 4 on all the TEU data, from 2005 to 2013. Figure 38 shows the MARE value to be 9.22%. Figure 39 shows validation of Equation 9 using 2014 TEU data. The MARE value was found to be 5.54%, which is reasonable. Figure 40 shows further validation of Equation 9 using 2005-2014 TEU data. The MARE value was found to be 8.86%, which is reasonable.

$$TEU = 924{,}864.161 + (0.409 \times GDP) \quad (9)$$

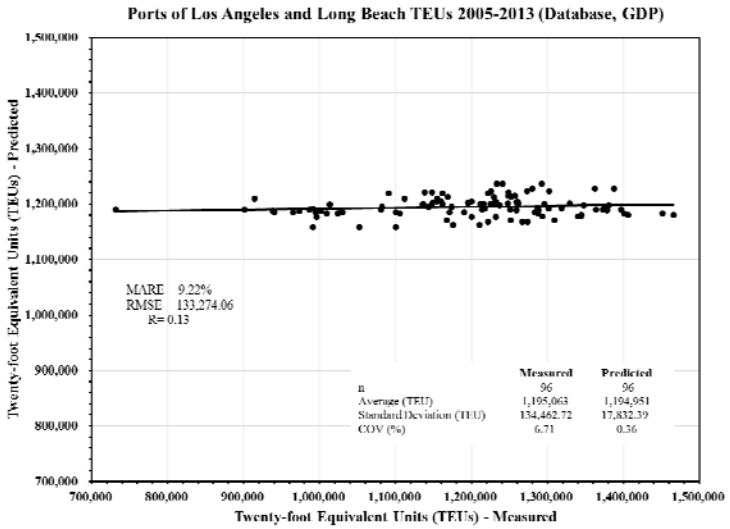

Figure 38. Measured vs. predicted TEUs 2005-2013 (Regression Equation)

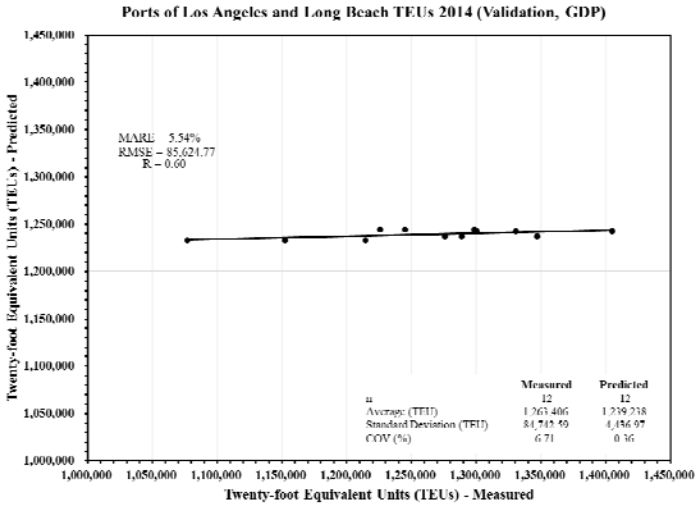

Figure 39. Validation of measured vs. predicted TEUs 2014 (Regression Equation)

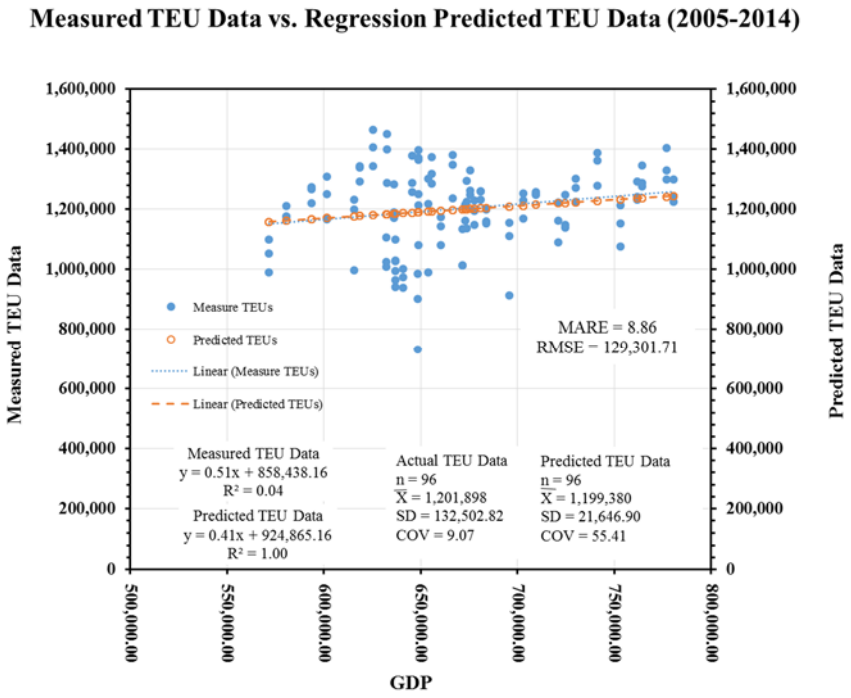

Figure 40. Measured vs. predicted TEU data for regression equation with GDP as the independent variable

3.3 Comparison of ARIMA (1,2,1) and Regression Equations for TEU Demand Modeling

Comparing the two data results shows whether Regression or ARIMA modeling is a more accurate tool to use for data forecasting. Table 9 shows the comparison of ARIMA (1,2,1), regression equation with time as the independent variable, and regression equation with California GDP as the independent variable. Table 9 shows the percent difference for all three of the cases. Table 9 indicates that the ARIMA (1,2,1) predicted values had a MARE value of 3.54%, the regression equation with time as the independent variable had a MARE value of 9.86%, and the regression equation with California GDP as the independent variable had a MARE value of 8.86%. In this case, the ARIMA (1,2,1) was the best of the three cases and was the best for predicting future values. However, unlike the regression equation, the ARIMA (1,2,1) did not take the economic recession into account with a dummy variable. For this reason, both methods will be used in the following section to see which is more accurate at showing

future values. Looking at just the regression equations, it is easily seen that the use of California GDP data as the independent variable yielded better results than did the regression equation that used time as the independent variable. This was because the economic recession had the same effect on California GDP and the ports of Los Angeles and Long Beach TEUs. Time is a constant measurement and did not take the recession into account.

Table 9. Comparing ARIMA (1,2,1) and regression equations

Cumulative Month	Month (Observed)	Total Loaded (TEUs)	ARIMA (1,2,1) Predictions	Regression Equation Predictions (Time)	Regression Equation Predictions (California GDP)
		(TEUs)	(TEUs)	(TEUs)	(TEUs)
229	Jan-14	1,214,434	1,184,840	1,332,281	1,232,861
230	Feb-14	1,076,959	1,185,659	1,338,198	1,232,861
231	Mar-14	1,152,483	1,191,770	1,344,116	1,232,861
232	Apr-14	1,275,880	1,215,255	1,350,034	1,237,411
233	May-14	1,288,651	1,244,670	1,355,952	1,237,411
234	Jun-14	1,346,954	1,277,252	1,361,870	1,237,411
235	Jul-14	1,300,467	1,307,033	1,367,788	1,242,630
236	Aug-14	1,330,785	1,329,227	1,373,706	1,242,630
237	Sep-14	1,404,904	1,338,614	1,379,624	1,242,630
238	Oct-14	1,298,692	1,330,134	1,385,542	1,244,054
239	Nov-14	1,244,860	1,298,667	1,391,460	1,244,054
240	Dec-14	1,225,804	1,239,114	1,397,378	1,244,054
	Total	15,160,873	15,142,234	16,377,949	14,870,869
	Average	1,263,406	1,261,853	1,364,829	1,239,239
	SD	88,510.8	59,052.7	21,337.3	4,633.2
	COV	7.0%	4.7%	1.6%	0.4%
	MARE		3.54%	9.86%	8.86%
	RMSE		52,602.04	115,448.67	129,301.71
R Value			0.79	0.48	0.60

3.4 Predicting TEU Demand for Future 5, 10, 15, and 20 Years Using Regression Equations

3.4.1 Predicting 5, 10, 15, and 20 Years in the Future Using Regression Equation

Regression Equation 10 will be used to predict the years of 2019, 2024, 2029, and 2034. Regression Equation 10 is again shown below. Table 10 shows the results of 5, 10, 15, and 20

years into the future, and Figure 41 shows a graph of the data for the predicted years using the regression Equation 10.

TEU = 308,935.109 + (5,917.916 x Month_R) + (-403,857.290 x ER_Dummy) (10)

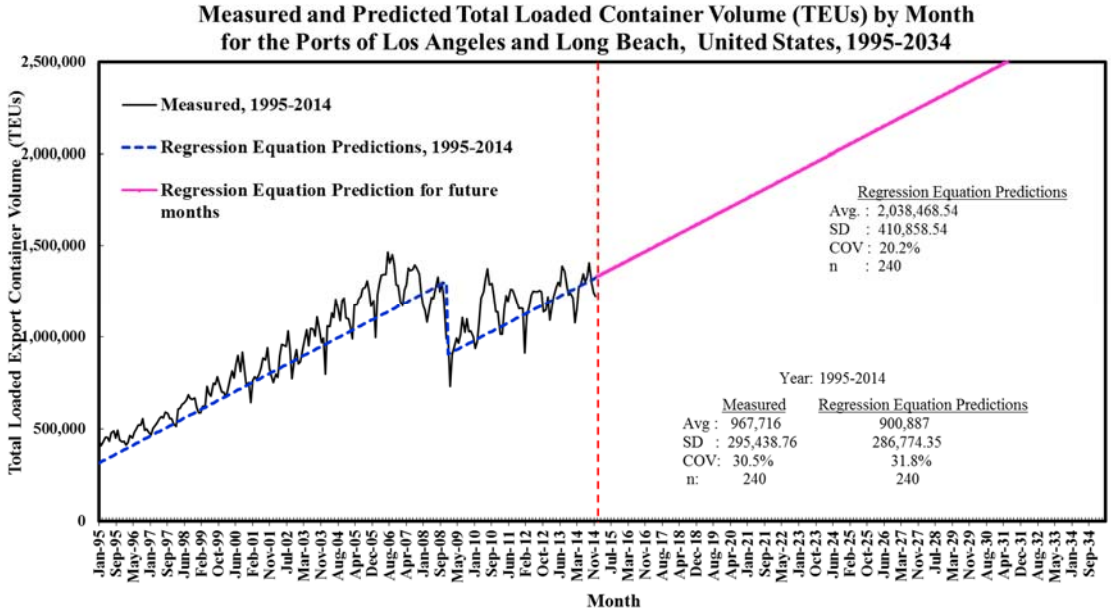

Figure 41. Predicting TEU values for 5, 10, 15 and 20 years in the future using regression equation with time as the independent variable

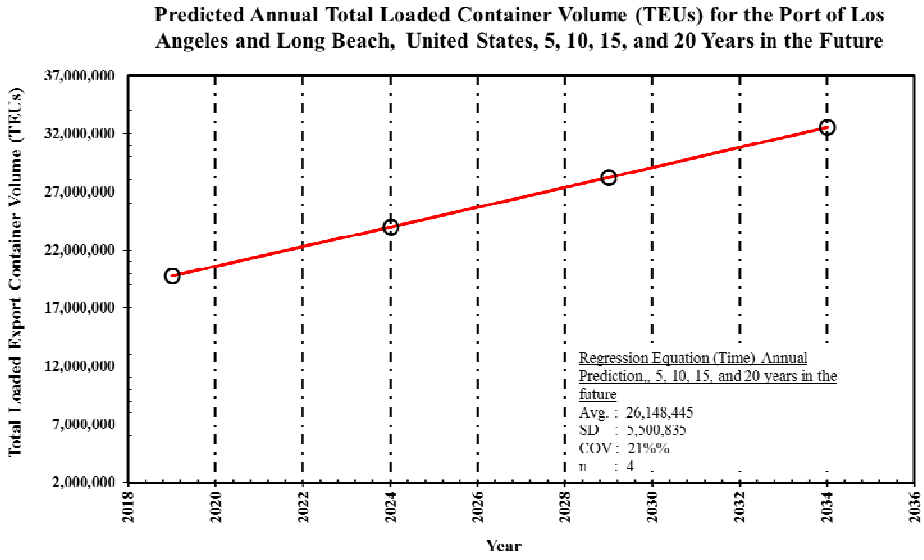

Figure 42. Total annual TEUs for 5, 10, 15, and 20 years in the future using regression equation with time as the independent variable

Figure 41 shows a steady increase for the years 2019, 2024, 2029, and 2034 from 2014. Table 10 shows the exact percent change from the 2014 yearly averages. The yearly total of 2014 was compared to the yearly predicted totals for 2019, 2024, 2029, and 2034. According to Table 10, the total yearly TEUs will increase by 23.3% in the first 5 years at the ports of Los Angeles and Long Beach, and by 2034, the yearly average TEUs will increase by 53.4%.

Table 10. Average and total TEUs for predicted 5, 10, 15, and 20 years in the future

Year	Average Monthly Total (TEUs)	Annual Total (TEUs)	% Increase from Annual Total in 2014
	(TEUs)	(TEUs)	(TEUs)
2019	1,647,904	19,774,849	23.3
2024	2,000,020	24,000,241	36.8
2029	2,355,095	28,261,141	46.4
2034	2,713,129	32,557,548	53.4
Average	2,179,037	26,148,445	40.0

3.4.2 Predicting 5, 10, 15, and 20 Years in the Future Using ARIMA (1,2,1)

As shown in Figure 43, ARIMA (1,2,1) was the most accurate of the three models tested. This model had only a 0.10 difference between measured and predicted data. Figure 43 indicates that the TEU data will increase the first few years before declining. The ARIMA (1,2,1) took the recession into account, which resulted in a dip in the TEU future data about 12-14 years after 2014. Figure 44 shows the annual total TEUs for 5, 10, 15, and 20 years in the future. According to Table 11, in the first 5 years after 2014 there will be a 3.8 total annual TEU increase, however, in 20 years by 2034 there will be a -13.3 decrease from 2014. According to Table 11, this will be an annual -2.0% TEU decline.

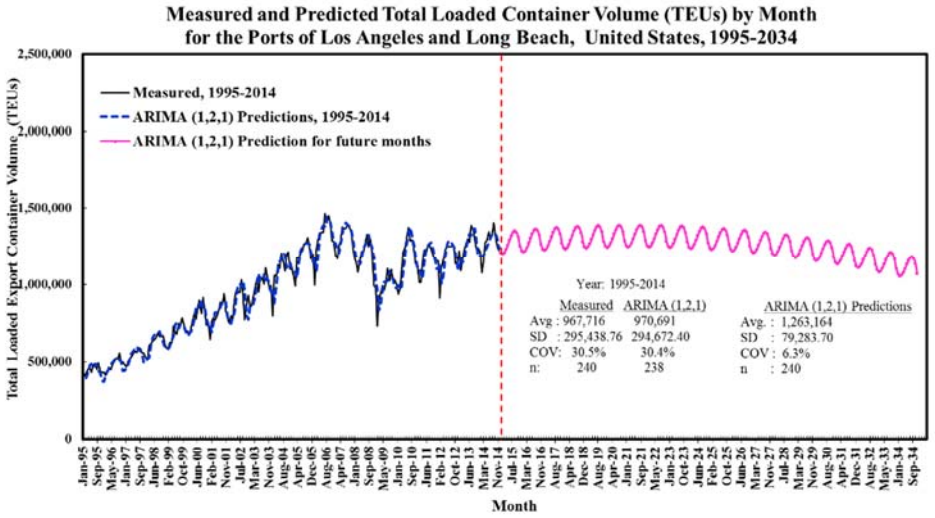

Figure 43. Predicting TEU values for 5, 10, 15 and 20 years in the future using ARIMA (1,2,1) modeling equation

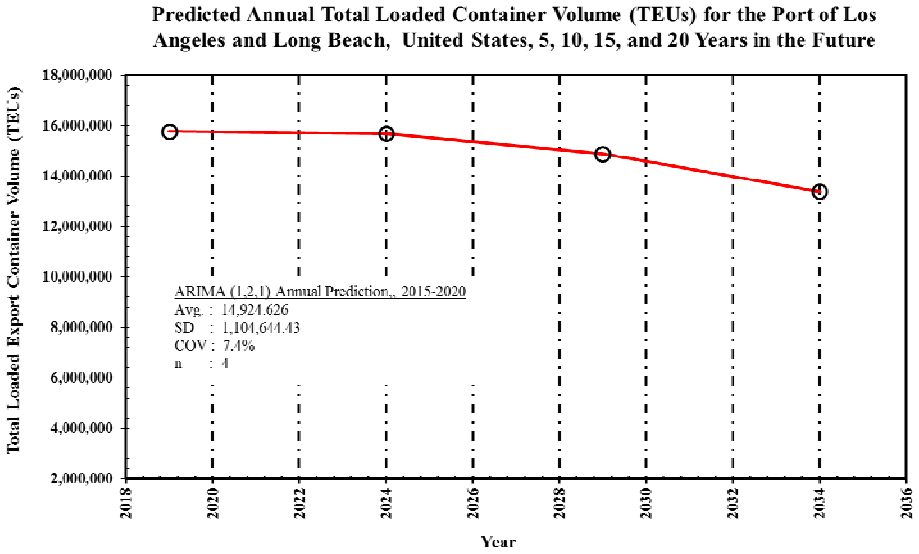

Figure 44. Total annual TEUs for 5, 10, 15, and 20 years in the future using ARIMA (1,2,1) model equation

Table 11. Average and total TEUs for predicted 5, 10, 15, and 20 years in the future

Year	Average Monthly Total (TEUs)	Annual Total (TEUs)	% Increase from Annual Total in 2014
	(TEUs)	(TEUs)	(TEUs)
2019	1,313,696	15,764,357	3.8
2024	1,306,280	15,675,356	3.3
2029	1,240,010	14,880,125	-1.9
2034	1,114,889	13,378,665	-13.3
Average	1,243,719	14,924,626	-2.0

3.5 Summary and Recommendations

In summary, the predicted vs. measured values for ARIMA (1,2,1) had a 6.32% less difference in MARE than the regression equation with time as the independent variable. Therefore, the ARIMA modeling was a more effective tool. In this study, monthly data did not work with the TEU data because there was an economic recession in 2008, causing the data to fall drastically from the preceding year. The regression equation was able to utilize a dummy variable to label each monthly value as either before or after the economic recession, but the regression equation violates the sequential R requirement. Based on this study, ARIMA (1,2,1) is the recommended method for predicting future TEU data values.

CHAPTER IV

SPATIAL MAPPING OF SELECTED PORT INFRASTRUCTURE AND LANDUSE OF SELECTED AREAS USING LANDSAT-8 IMAGERY

4.1 Landsat-8 Pan-sharpened Imagery Analysis for Port Infrastructure and Landuse of Selected Areas

According to Uddin [24], "GIS database is integral to effective decision support systems for airports, highways, roads, street networks, river resources, and other infrastructure assets which represent areas of massive infrastructure investments." Multispectral satellite imagery, such as Landsat-8 imagery, is the way of the future in identifying these port infrastructures. According to Uddin [25], "The availability of cost-competitive, high-resolution, multispectral satellite imagery provides tremendous opportunities for analyzing infrastructure inventory, land use/land cover and traffic volume, as well as assessing environmental and post-disaster conditions". Landsat-8 imagery will be used in this thesis to show port area infrastructure and land use.

Landsat-8 imagery is multispectral satellite imagery collected every 16 days. According to the United States Geological Survey (USGS), the satellite uses two instruments. "The Operational Land Imager (OLI) sensor includes refined heritage bands, along with three new bands: a deep blue band for coastal/aerosol studies, a shortwave infrared band for cirrus detection, and a Quality Assessment band. The Thermal Infrared Sensor (TIRS) provides two

thermal bands. These sensors both provide improved signal-to-noise radiometric (SNR) performance quantized over a 12-bit dynamic range" [26].

Section 4.1.1 through 4.1.7 are the steps necessary to create pan-sharpened imagery. These sections show imagery being created for the Oxford, MS area. These steps were repeated for the ports of Los Angeles, Long Beach, and Gulfport. Section 4.1.8 will show the final Landsat-8 pan-sharpened imagery for all of the selected areas.

4.1.1 Determining the Area of Interest (AOI) of the Oxford, MS area using Google Earth

a) Start Google Earth by double clicking on the Google Earth icon [27].

b) Under the Search box, type "Oxford, MS" as the search term, then click Search. The AOI will be displayed on the screen in Google Earth (Figure 45).

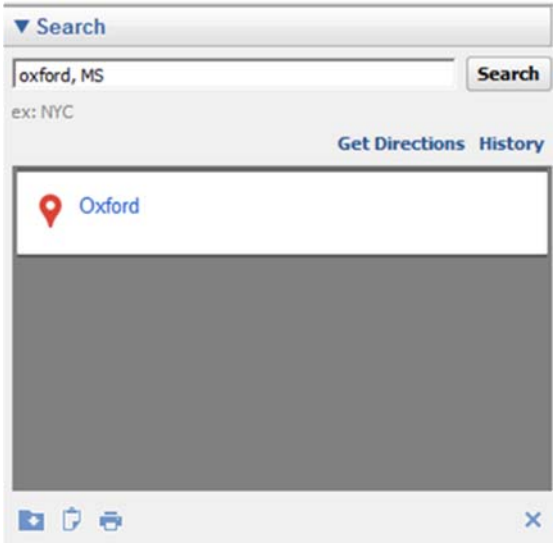

Figure 45. Searched by Google Earth

c) Next, on the main menu, click the Add Polygon symbol, and the New Polygon dialog box appears as shown in Figure 46.

d) Type "Oxford" as the name of the polygon, select red color and a width of 3 for lines, and then select Outlined under Area.

e) Draw a polygon that covers the entire Oxford area, as shown in Figure 47.

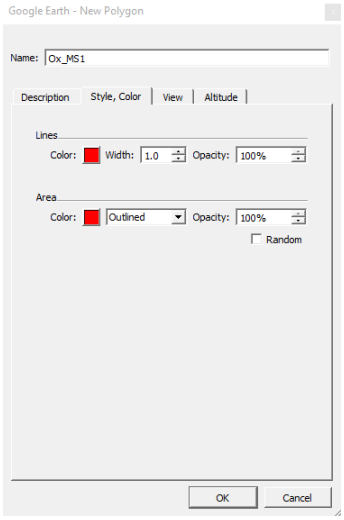

Figure 46. Defining the color and width for the AOI polygon line

f) Place the cursor to the left side of the selected area. Make four points around the selected area and make sure to get the entire desired area inside the polygon. The polygon made for the AOI of Oxford, MS can be seen in Figure 47. Also, show the dimensions for the polygon made.

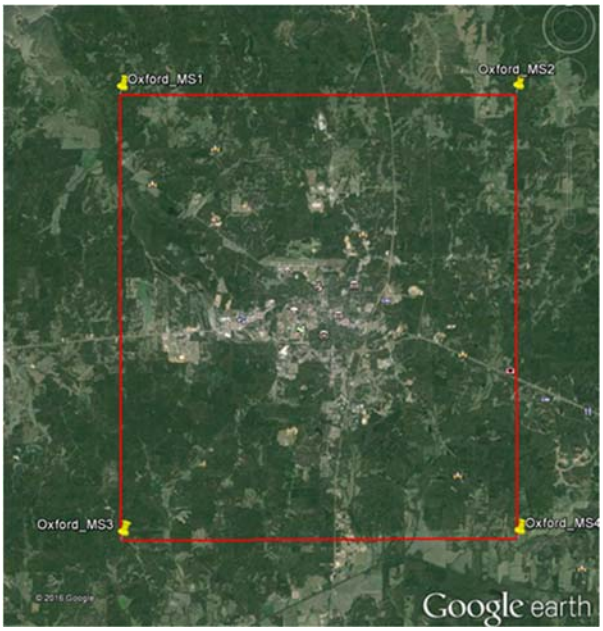

Figure 47. Defining color and box size of the AOI polygon

4.1.2 Creating a map of the AOI

a) On the menu in Google Earth, click Add Place Mark, then move the yellow place marker to one of the corners of the AOI. Then, enter the name of the corner and the latitude coordinate and longitude coordinate of the yellow corner place marker.

b) Repeat the same steps for the other corners of the AOI.

c) Press Print Screen on the keyboard and paste the imagery made in Google Earth into the Paint program**.**

d) Use the tools in the Paint program to type the coordinates for the latitude and longitude of each corner of the map (Figure 48). The Opaque text option yields the white background for the text.

e) Go to File>Save as>JPEG picture**;** then enter the name of the JPEG picture.

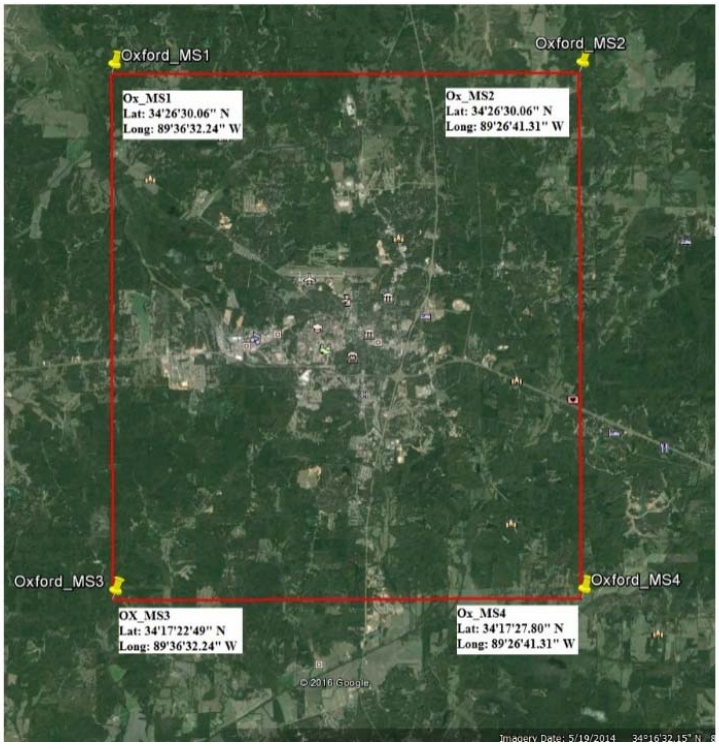

Figure 48. Map of the AOI-labeled polygon created in the Paint program

4.1.3 Account Registration

a) Open Earth Explorer at website http://earthexplorer.usgs.gov/ (Figure 49).

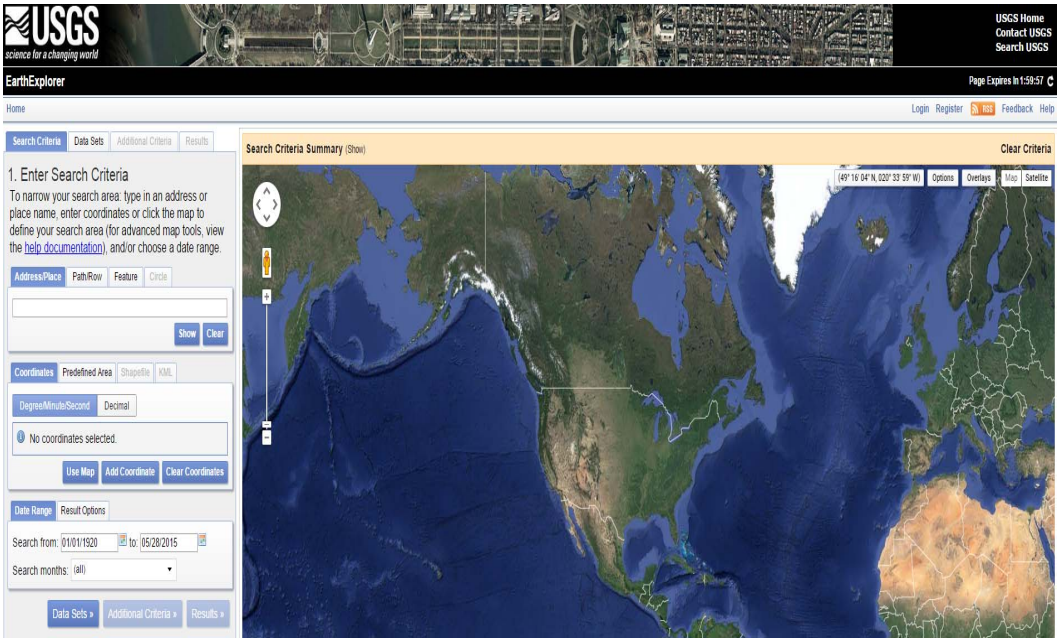

Figure 49. Earth Explorer website

b) Click on the Register in the top right corner of the Earth Explorer website [26].

c) Enter a Username, New Password and Confirm New Password, then Click Continue.

d) Continue to complete the other required steps (Contact Demographic, Contact Information, and Complete Registration).

e) Open the email that was used for registration, and an email from USGS will have been received.

f) Click on the link in the email to confirm and activate the account. Note that the user name must be remembered.

4.1.4 Searching and downloading Landsat-8 imagery of the Oxford, MS area from the USGS website using Earth Explorer

a) Login to USGS using your USGS registered username and password. (Figure 50)

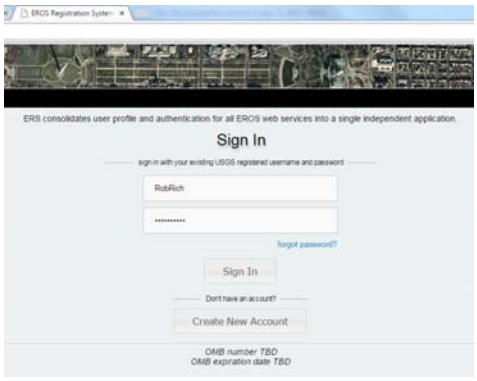

Figure 50. Sign in USGS

b) Under Search Criteria, type the place name for which you want to download the imagery. Type in “Oxford, MS” and then click Show.

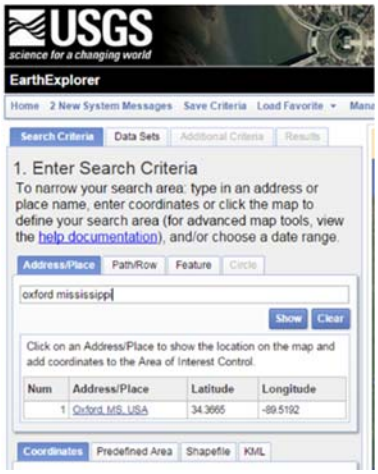

Figure 51. Looking up Oxford, MS

c) Click on the area found. The area will be shown on the map.

d) Zoom into the Oxford, MS area being sought.

e) Click Use Map, and the map used will turn red.

f) Next, zoom out of the Oxford, MS area. The size of the rectangular box can be changed by moving the points at the corners of the box (Figure 51).

g) Click on Data Sets, and a list of data sets will appear. Then, click on Landsat Archive.

h) Check only Landsat-8 as shown in Figure 52.

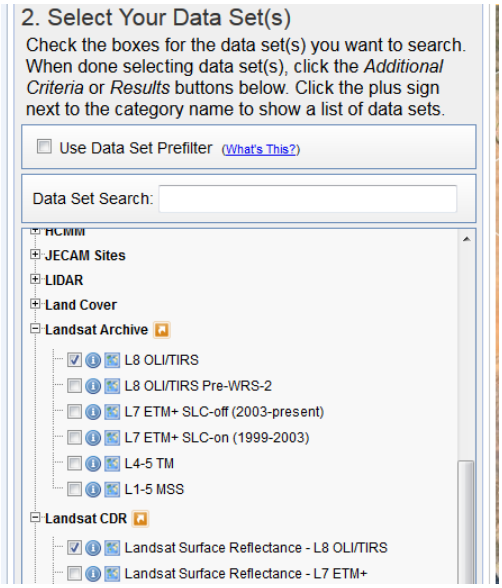

Figure 52. Select data set window

i) Click Additional Criteria. Under Cloud Cover, select "Less than 10%" as shown in Figure 53.

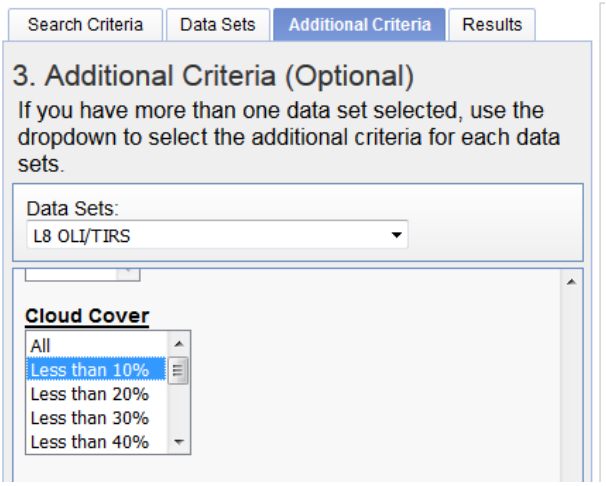

Figure 53. Additional criteria window

j) Click on Results, and note that the list of imageries covers the box made in Figure 48. Then, select the best imagery that covers the red box (Figure 54).

Figure 54. Search results window

k) Select the correct imagery as shown in Figure 55, then click on Metadata. This Metadata dialog window appears in Figure 56.

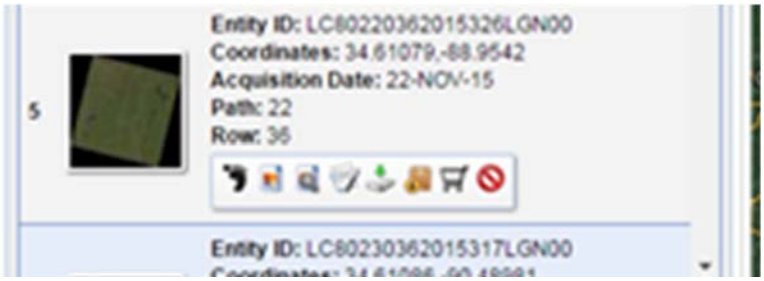

Figure 55. Imagery selected

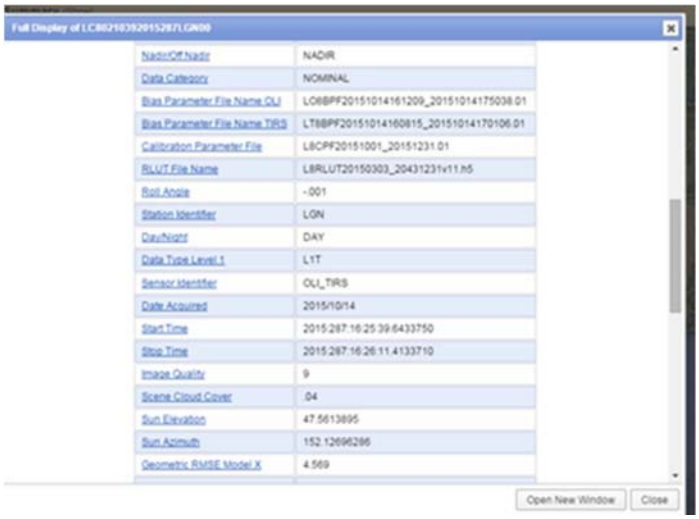

Figure 56. Metadata information window

l) Click on the Download option seen in Figure 57. The Download option window appears as shown in Figure 58.

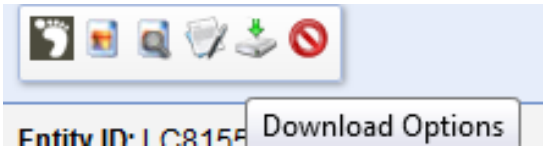

Figure 57. Download option

m) Choose the "Level 1 Geo TIFF Data Product" option. This option allows the downloading of all needed bands.

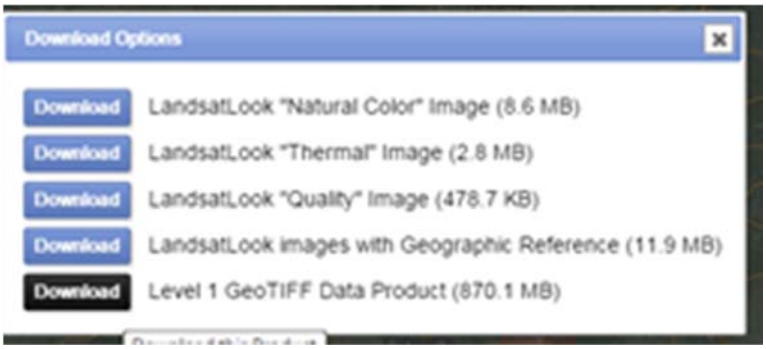

Figure 58. Download options for Landsat-8 satellite imagery

n) Finally, extract the downloaded file to obtain all bands, as shown in Figure 59.

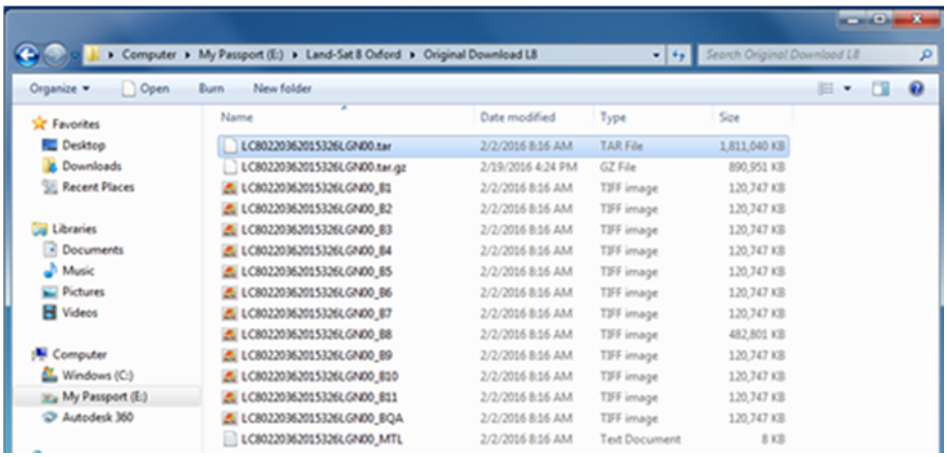

Figure 59. List of download bands files

4.1.5 Creating Landsat-8 multispectral imagery using ERDAS IMAGINE 2013

Landsat-8 has 11 bands, and each band has a different range of wavelength. Bands 1 through 7 and band 9 have 30m resolution. Band 8 has 15m resolution, and bands 10 and 11 have 100m resolution. The smaller the pixel size, the clearer the imagery will be.

a) Click on the symbol for ERDAS IMAGINE 2013 [28] on Desktop. The main interface of ERDAS IMAGINE appears in Figure 60.

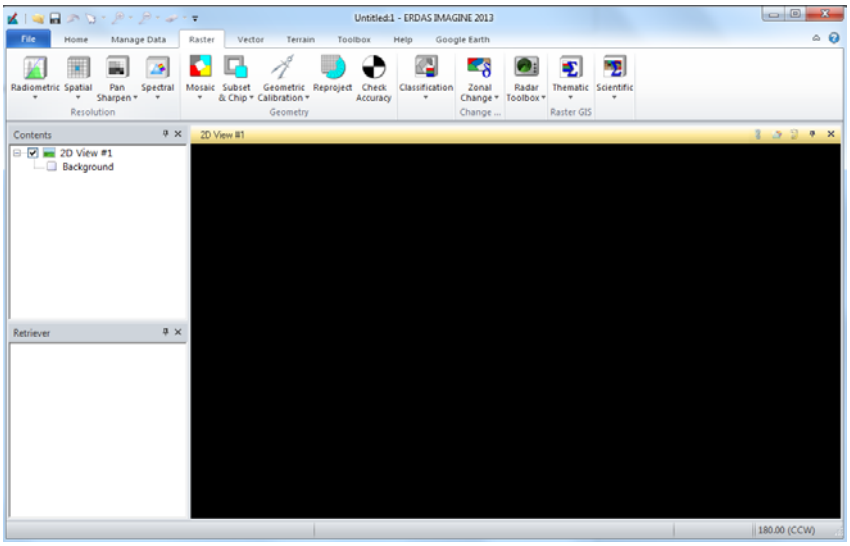

Figure 60. ERDAS beginning imagery

b) From the home screen, go to Raster>Spectral>Layer Stack. The screen shown in Figure 61 appears.

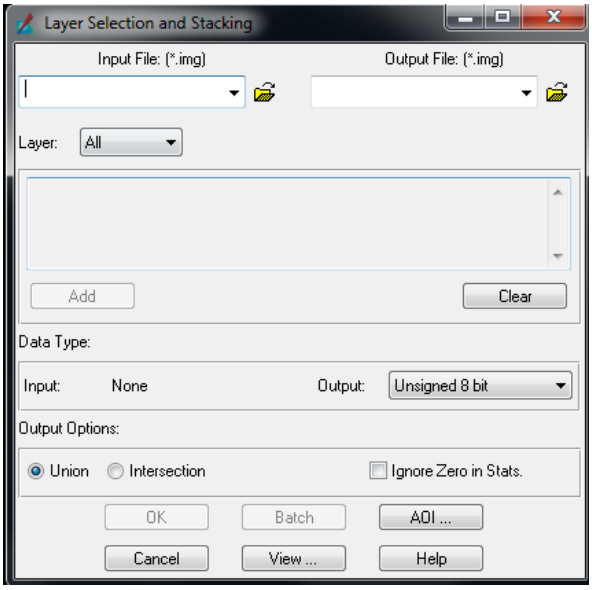

Figure 61. Open to stack and select layers

c) From the input box, as shown in Figure 61, use the selected tiff files for B1. B1 stands for band 1. Go to the location where all the bands were saved, as seen in Figure 62. The final input box for band 1 can be seen in Figure 63.

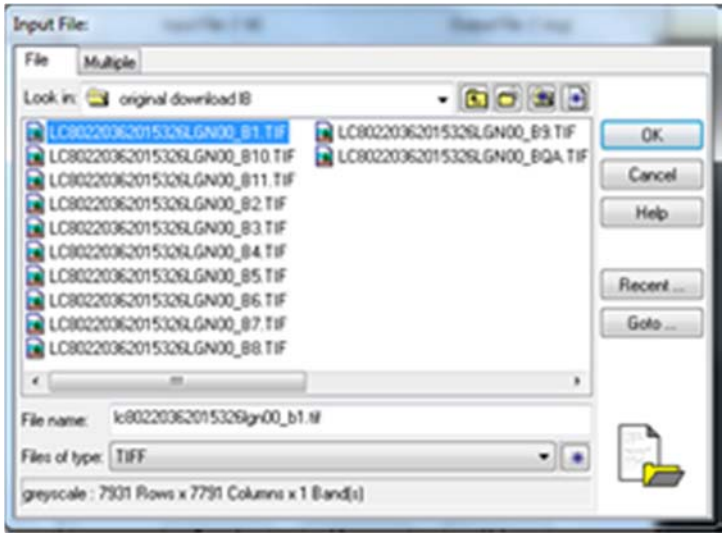

Figure 62. Folder location of all saved bands

Figure 63. Input for B1

d) Repeat step c for B2, B3, B4, B5, B6, B7, and B9. Name the output folder and save it to the folder in which the work is being performed. This is the multispectral imagery, which should be saved as ls8_multispectral_imagery_oxford.img. The final input can be seen in Figure 64.

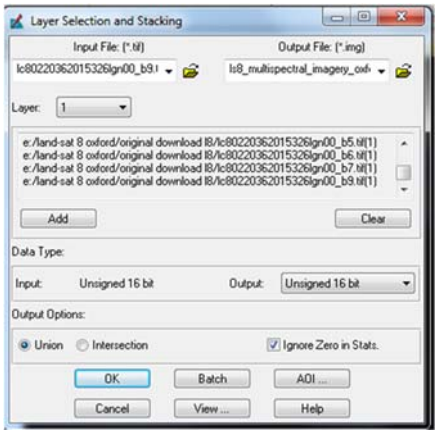

Figure 64. Final window with all bands

e) Next, open the output file just created. The final output file is shown in Figure 65. The output file takes time to create, as the bands are combined. In this case, the

multispectral imagery took over an hour to run before it could be opened. Figure 66 shows the final multispectral imagery created in the ERDAS software.

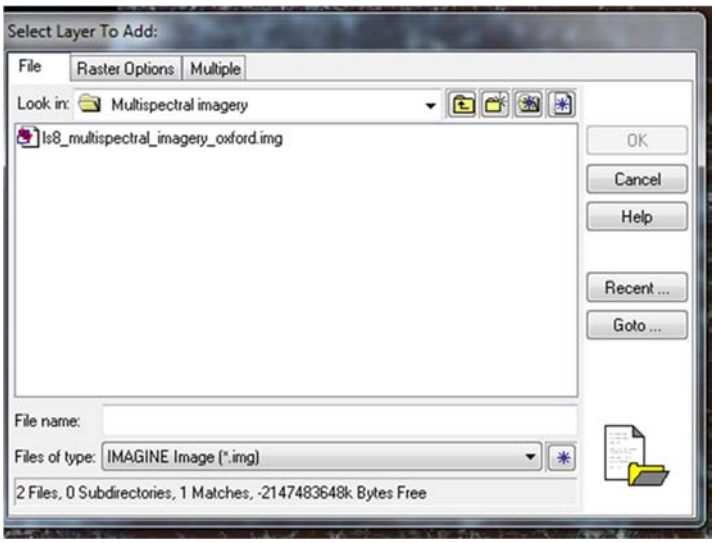

Figure 65. Final output of multispectral imagery

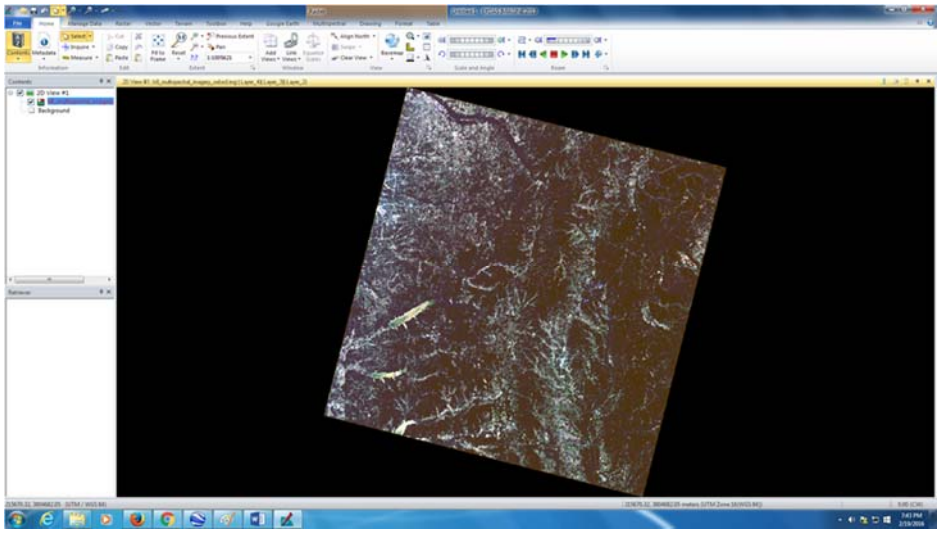

Figure 66. Final Landsat-8 multispectral imagery in ERDAS

4.1.6 Creating Landsat 8 Pan-Sharpened imagery using ERDAS IMAGINE 2013

In this section, the imagery is converted from a 30m x 30m imagery and made into a 15m x 15m imagery to give it more pixels and a higher resolution.

a) Go to Raster>Pan-Sharpened>HPF Resolution Merge in ERDAS [28]. Once this is completed, a window will appear. This window can be seen in Figure 67.

b) In the High Resolution box, select the B8 band from the folder containing all of the bands, and then select the multispectral imagery already created in the multispectral input file. The output file was named pansharpened_mul_imagery.img. This can also be seen in Figure 67. The box beside Ignore Zero should also be checked. After this, click OK.

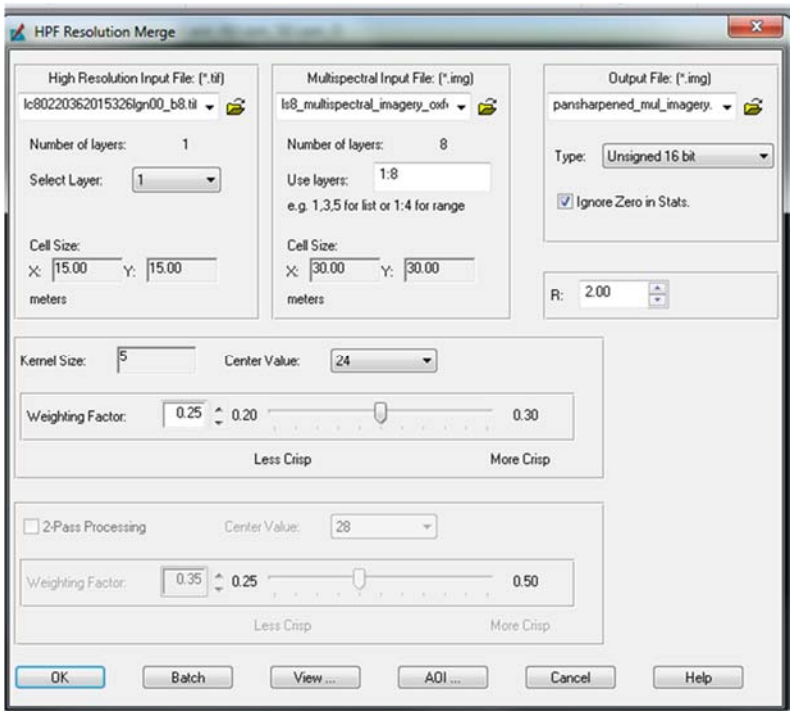

Figure 67. Pan-sharpened imagery window

c) The imagery will now run to create the pan-sharpened imagery. This step will take several hours for the computer to complete. In this case, about 4 hours was needed to create the pan-sharpened imagery. Figure 68 shows what the screen looks like when the imagery has been completed.

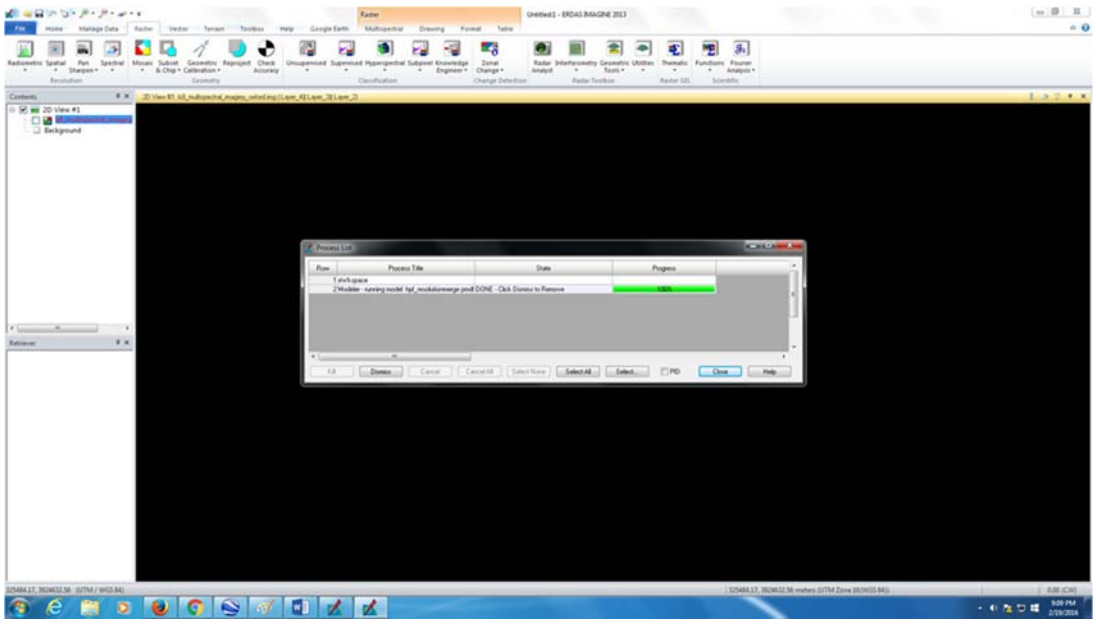

Figure 68. Screen indicating that pan-sharpened imagery is complete

d) Now, open the pan-sharpened imagery to verify that everything worked accurately and that there are no errors. The final pan-sharpened imagery can be seen in Figure 69.

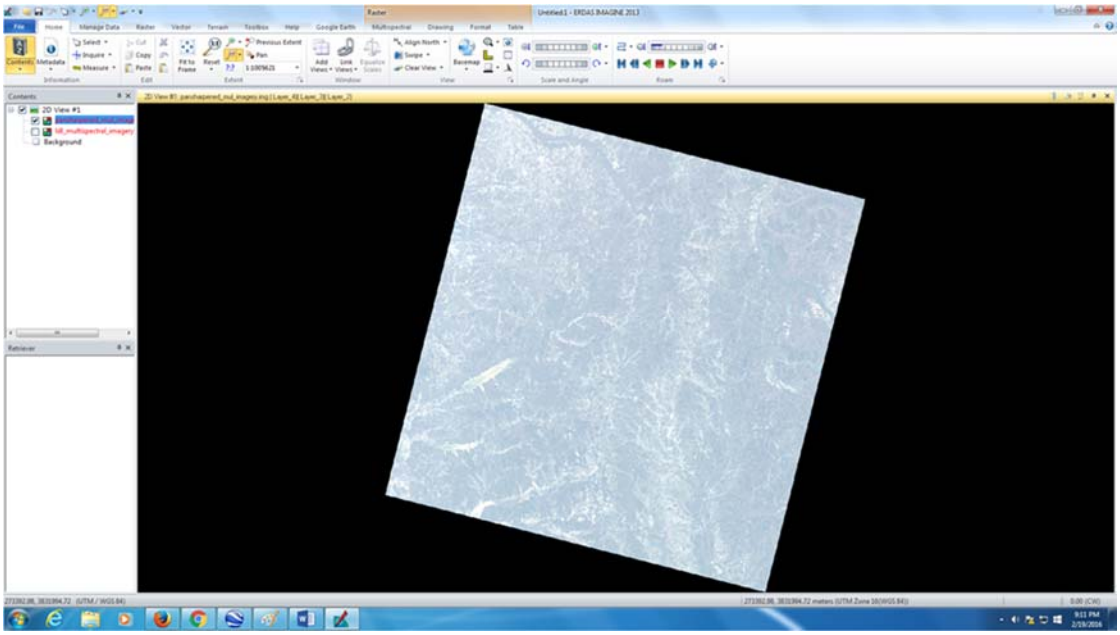

Figure 69. Final Landsat-8 pan-sharpened imagery

4.1.7 Creating Subset Landsat-8 pan-sharpened imagery using ERDAS IMAGINE 2013

In this section, the area from the pan-sharpened imagery for which the study is to be performed will be selected by using the subset tool in ERDAS [28].

a) Zoom in on the area on the pan-sharpened imagery for which the study is to be performed. The zoomed-in imagery of the Oxford, MS area can be seen in Figure 70.

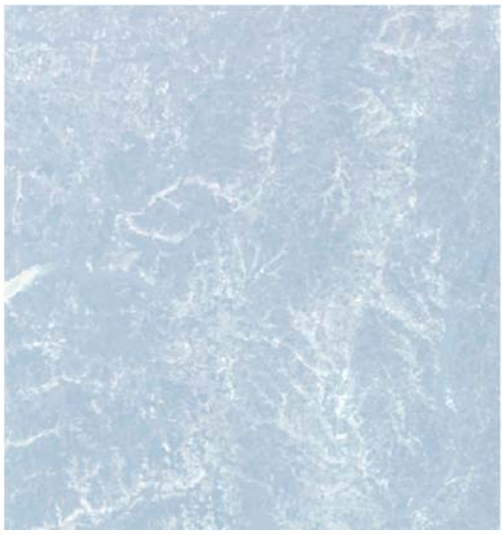

Figure 70. Zooming in on Oxford, MS

b) Go to Home>Inquire>Inquire Box on the ERDAS main screen. In the box, change the type to Lat/Lon and type in the coordinates found in Figure 48. The points box is shown in Figure 71.

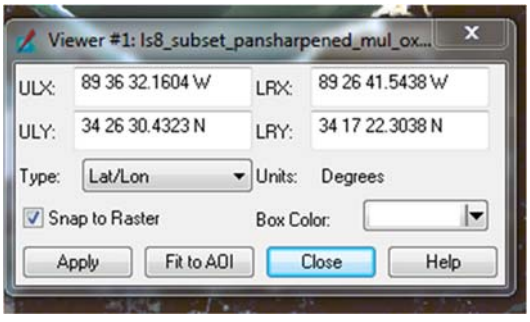

Figure 71. Inserting the Latitudes and Longitudes of Oxford, MS

c) Now, change Lat/Lon back to Map and go to Raster>Subset & Chip>Create Subset Imagery. The subset window appears, which is shown in Figure 72. In this window, enter the pan-sharpened imagery in the input file and name it, then click OK. In this case, the output file was named ls8_smaller_subset_oxford.img. Figure 73 shows the final subset imagery made in ERDAS.

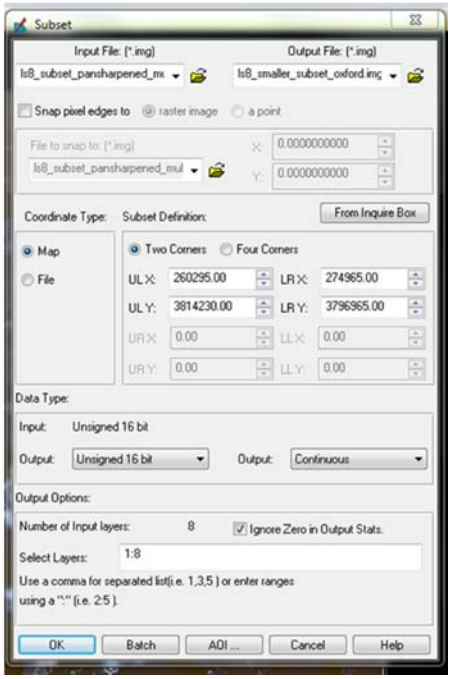

Figure 72. Subset window

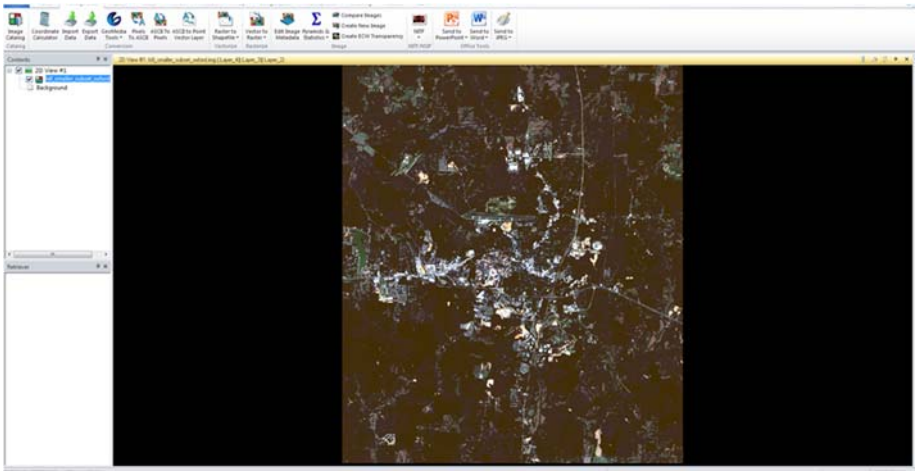

Figure 73. Final subset of the Landsat-8 pan-sharpened imagery

d) Next, be sure to export the imagery into a JPEG file. To accomplish this, go to Manage Data>Export Data. The window for this can be seen in Figure 74.

Figure 74. Making a JPEG of the subset pan-sharpened imagery

4.1.8 Final Landsat-8 pan-sharpened imagery of the ports of Los Angeles and Long Beach, the Port of Gulfport, and the Oxford, MS areas

This section discusses the final Landsat-8 subset pan-sharpened imageries for the selected areas. The same procedure as set forth above was used to obtain the final results for each study area, which is shown in Figures 75, 76, and 77. The differences between the Landsat-8 multispectral and pan-sharpened imageries were that the multispectral imageries had a pixel size of 30m x 30m and combined bands 1, 2, 3, 4, 5, 6, 7, and 9 to create the imagery, while the pan-sharpened imagery had a 15m x 15m pixel size and used only band 8 combined with the multispectral imagery to create the imagery. The Landsat-8 pan-sharpened imagery had more and smaller pixels than the multispectral imagery, making the imagery clearer and easier to use to identify the infrastructure and landuse.

Figure 75. Ports of Los Angeles and Long Beach Landsat-8 pan-sharpened imagery

Figure 76. Oxford, MS Landsat-8 pan-sharpened imagery

Figure 77. Port of Gulfport Landsat-8 pan-sharpened imagery

4.2 Infrastructure and Landuse Mapping of the Ports of Los Angeles and Long Beach, Port of Gulfport, and the Oxford, MS Areas

In this section of the thesis, the landuse was found for the selected research areas by the use of planimetrics in Geomedia pro [29]. The infrastructure of the area was also identified through the use of planimetrics. Section 4.2.1 explains how the planimetrics of the Oxford, MS area was performed using Landsat-8 imagery. This procedure was repeated for the other research areas. Section 4.2.2 shows the final layout window of each research area's planimetrics.

4.2.1 Use of Geomedia pro for manual planimetrics

To start, select the Landsat-8 pan-sharpened subset imagery made of the ports of Los Angeles and Long Beach, Port of Gulfport and Oxford, MS areas in Geomedia. In the imageries, identify the trees, water, asphalt, concrete, and other features that can be identified manually. The items needing to be identified can be seen in Uddin's ENGR 597 lecture notebook [8]. Figure 78 shows the water area of the Oxford, MS area. Next, create a new area feature in Geomedia. For water, create a new feature named "water," as seen in Figure 79, and outline the selected area. Now, repeat this step to identify other features within the imagery until all of the features in the entire imagery have been identified. The snap tools should be utilized to ensure that no space is left unidentified on the imagery. These steps will be performed for all of the subject areas in this thesis.

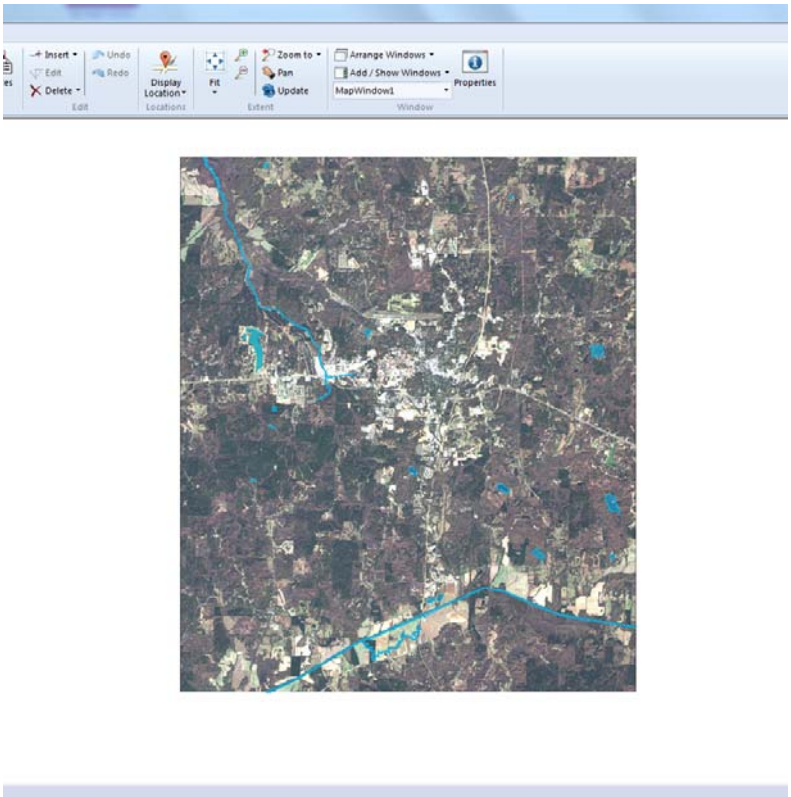

Figure 78. Manual water planimetrics of the Oxford, MS area with imagery in the background

Figure 79. Manual water planimetics without imagery in the background

4.2.2 Final infrastructure and landuse mapping of the ports of Los Angeles and Long Beach, Port of Gulfport, and Oxford, MS areas through the use of planimetrics

The use of planimetrics to locate the infrastructure and landuse of the research areas can be seen in Figures 80, 81, and 82. The final planimetrics of each area will be utilized in the next section of this thesis to compare to the calibrated BANS classification method.

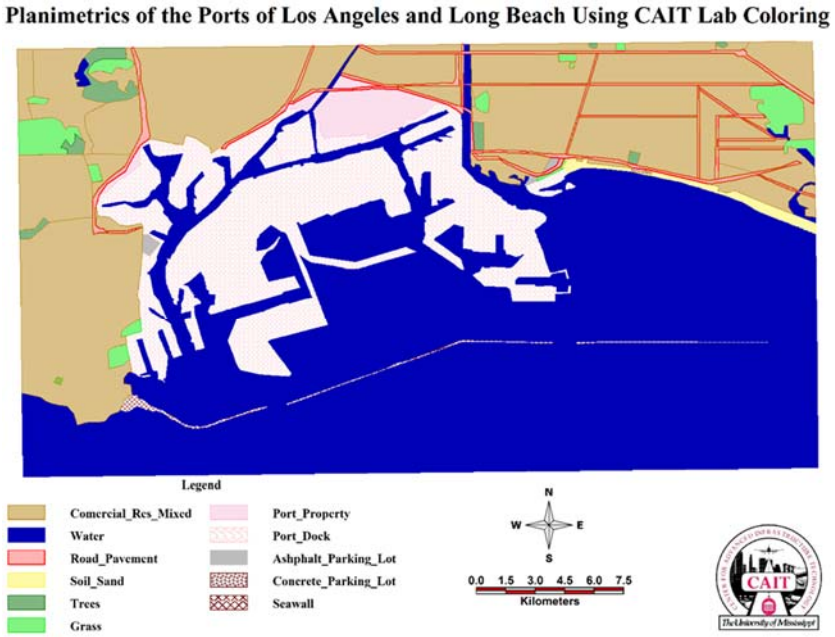

Figure 80. Final planimetrics of the ports of Los Angeles and Long Beach area

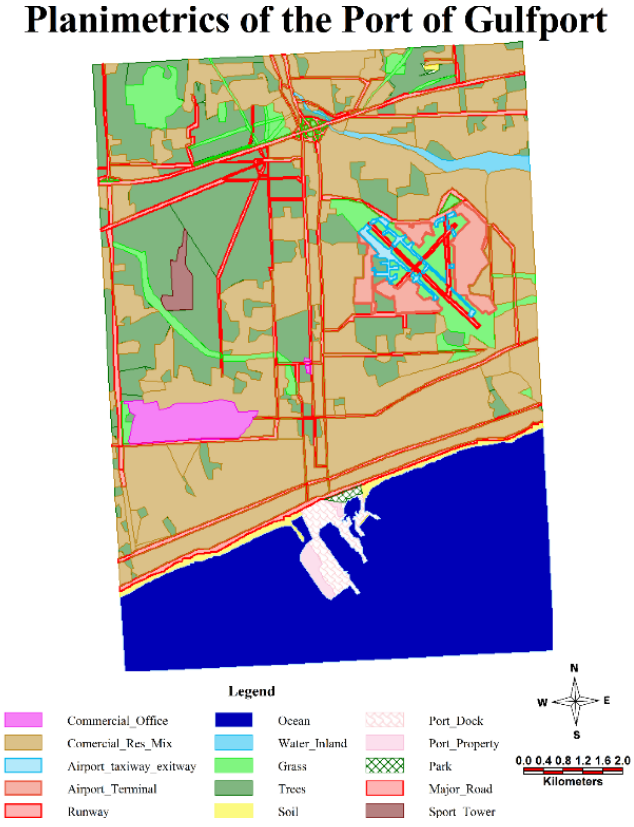

Figure 81. Final planimetrics of the port of Gulfport area

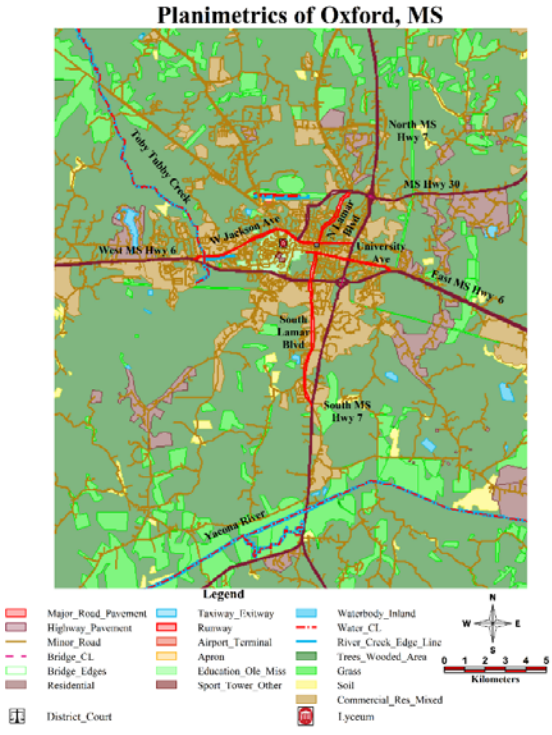

Figure 82. Final planimetrics of Oxford, MS

4.3 Calibrated BANS Classification of Ports of Los Angeles and Long Beach, Port of Gulfport, and Oxford, MS Areas and Comparison of Planimetrics and Calibrated BANS Classification of the Ports of Los Angeles and Long Beach, Port of Gulfport, and Oxford, MS Areas

4.3.1 Creating the calibrated BANS classification for the Ports of Los Angeles and Long Beach, Port of Gulfport, and Oxford, MS Areas

Because only IKONOS Landsat-8 imagery had been used to obtain the calibrated BANS classification by Wadajo [30], a modification to the specifications had to be made. Ratios were found, and each type of area had to be designated. Equation 11 shows the ratio equation used for each feature. Table 12 shows the final classifications.

Ratio for each=Landsat-8 imagery Color Band Mean / IKONOS imagery Color Band Mean (11)

Table 12. Calibrated BANS classification requirements for Geomedia

Steps	Decision Criteria	Polygon map	Surface class legend color
1	Vector map of built-up area pixels	Yes	Light Magenta
2	Asphalt: 4,018.50<= Green <= 7,301.70	No	Grey
3	Building/Concrete: Step 1-Step 2 Pixels	No	Light Magenta
4	Vector map of water area pixels	Yes	Blue
5	NonBuilt-up, NonWater pixels	No	
6	Soil: Red >= 14,254.50	No	Yellow
7	NonBuilt-up, NonWater, and NonSoil pixels	No	
8	Red<= 3,900.0	No	Dark Green
9	Grass: Step 7 – 8 pixels	No	Light Green

In Geomedia Pro, enter the classification for each surface. There are six different feature areas in which classifications were made. Figures 83, 84, and 85 show the steps for the asphalt and building/concrete features. To enter the classification for the asphalt and building/concrete, go to the Functional Attribute tab. The window that appears can be seen in Figure 83. In this window, input the classification. In this case, the classification reads IF[Input.B3>=4018.5 AND Input.B3<=7301.7,"Asphalt","Building/Concrete"]. (Note: This will change based on the surface that is being sought.)

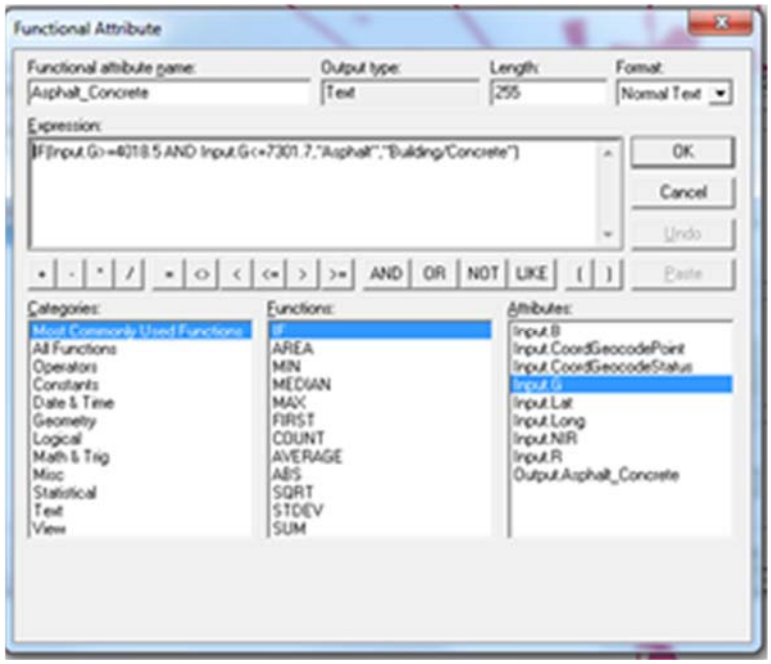

Figure 83. Functional attribute window

After this is performed, the geocoded points will appear on the Geomedia screen, although the points will not be the correct color. In this case, the asphalt needs to be changed to grey, and the building/concrete needs to be changed to color 23. To accomplish this, go to Thematic Maps and select Unique Value Thematic, which can be seen in Figure 84. In this window, change the color of each point in the style box, then click OK. Figure 85 shows the final results for the asphalt and building/concrete areas.

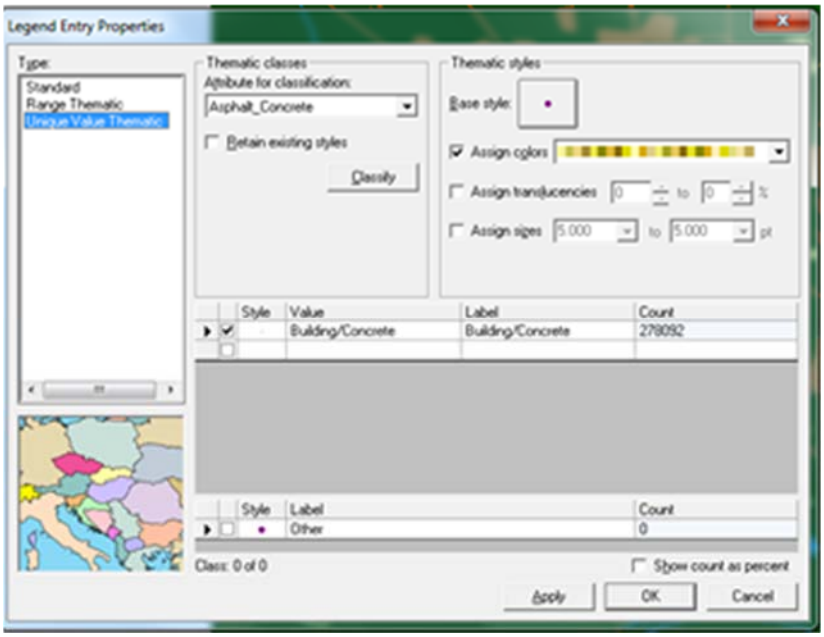

Figure 84. Select the unique value thematic map

Figure 85. Final asphalt and building/concrete areas

Repeat the steps at the beginning of section 4.3 of this thesis for the remaining features. The remaining features are water, soil, trees, and grass. The only difference will be to change the classification for each feature and to select the appropriate color. The final calibrated BANS classification map with all the features completed is shown in Figure 86. Repeat these steps to

obtain the calibrated BANS classification for all three of the research areas. The final calibrated BANS classifications made in Geomedia can be seen in Figures 86, 87, and 88.

Figure 86. Calibrated BANS classification for Oxford, MS

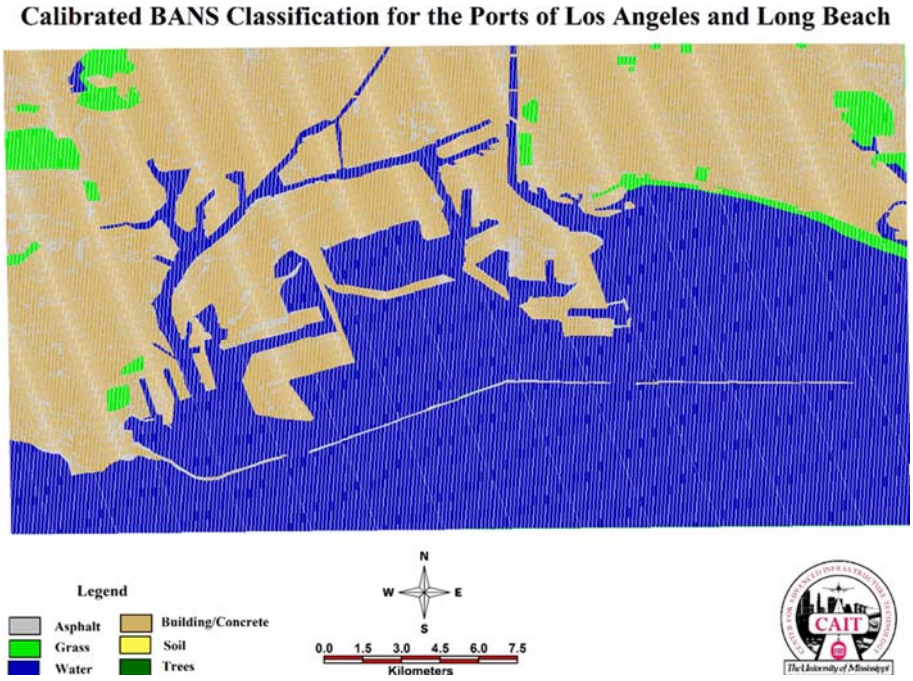

Figure 87. Calibrated BANS classification for the ports of Los Angeles and Long Beach

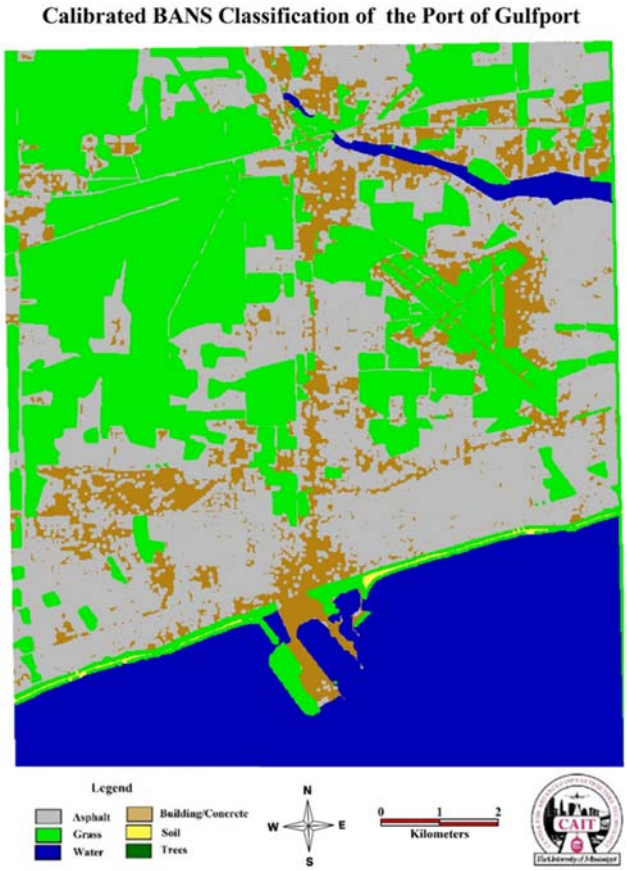

Figure 88. Calibrated BANS classification for the port of Gulfport

4.3.2 Comparing the planimetrics and calibrated BANS classifications of the selected research areas

After completing the calibrated BANS classification section for all the selected areas, a table was created for each area comparing the areas of the planimetrics and calibrated BANS classification that were made. The planimetrics features were combined into the six features as used by the calibrated BANS classification analysis so that the calibrated BANS classification and planimetrics results could be compared for identifying the selected area's landuse and infrastructure. Tables 13, 14, and 15 show the comparisons between the planimetrics and calibrated BANS classification for the ports of Los Angeles and Long Beach, Port of Gulfport, and Oxford, MS areas.

Table 13. Ports of Los Angeles and Long Beach landuse differences for planimetrics and calibrated BANS classification

Los Angeles/Long Beach Port Classification of Land Use					
Surface Class	Planimetrics (Groundtruth)		Calibrated BANS (LA/LB Site)		Difference
	m^2	%	m^2	%	%
	A1	A2	B1	B2	100((B1-A1)/A1)
BC Building/Concrete	97,501,547.10	44.01%	84,407,687.24	38.10%	-13.43%
A Asphalt	4,999,696.90	2.26%	17,944,941.38	8.10%	258.98%
W Water	112,371,888.40	50.72%	112,322,040.50	50.70%	-0.04%
S Soil	1,213,630.00	0.55%	0.00	0.00%	-100.00%
T Tree	1,617,382.00	0.73%	0.00	0.00%	-100.00%
G Grass	3,838,341.80	1.73%	6,867,817.07	3.10%	78.93%
N No Data	0.00	0.00%	0.00	0.00%	0.00%
SUM	221,542,486.20	100.00%	221,542,486.20	100.00%	0.00%
Total Built-up Area (Building/Concrete, Asphalt)	102,501,244.00	46.27%	102,352,628.62	46.20%	-0.14%
	(102.50 km^2)		(102.35 km^2)		
Total Natural Surface (Soil, Grass, Trees, Water)	119,041,242.00	53.73%	119,189,857.58	53.80%	0.12%
	(119.04 km^2)		(119.19 km^2)		
SUM	221,542,486.20	100.00%	221,542,486.20	100.00%	100.00%
	(221.54 km^2)		(221.54 km^2)		

Table 14. Port of Gulfport landuse differences for planimetrics and calibrated BANS classification

Gulfport Site Classification of Land Use					
Surface Class	Planimetrics (Groundtruth)		Calibrated BANS (Gulfport)		Difference
	m^2	%	m^2	%	%
	A1	A2	B1	B2	100 ((B1-A1)/A1)
BC Building/Concrete	45,039,330.80	42.21%	25,397,573.10	23.80%	-43.61%
A Asphalt	6,985,595.60	6.55%	26,416,014.28	24.76%	278.15%
W Water	26,656,204.30	24.98%	26,564,004.41	24.90%	-0.35%
S Soil	1,286,119.60	1.21%	566,847.05	0.53%	-55.93%
T Tree	21,194,938.30	19.86%	0.00	0.00%	-100.00%
G Grass	5,534,211.80	5.19%	27,751,961.56	26.01%	401.46%
N No Data	0.00	0.00%	0.00	0.00%	0.00%
SUM	106,696,400.40	100.00%	106,696,400.40	100.00%	0.00%
Total Built-up Area (Building/Concrete, Asphalt)	52,024,926.40	48.76%	51,813,587.38	48.56%	-0.41%
	(52.02 km^2)		(51.81 km^2)		
Total Natural Surface (Soil, Trees, Grass, Water)	54,671,474.00	51.24%	54,882,813.02	51.44%	0.39%
	(54.67 km^2)		(54.88 km^2)		
SUM	106,696,400.40	100.00%	106,696,400.40	100.00%	0.00%
	(106.70 km^2)		(106.70 km^2)		

Table 15. Oxford, MS landuse differences for planimetrics and calibrated BANS classification

Oxford, MS Classification of Land Use					
Surface Class	Planimetrics (Groundtruth)		Calibrated BANS (LA Site)		Difference
	A1	A2	B1	B2	100 ((B1-A1)/A1)
	m^2	%	m^2	%	%
BC Building/Concrete	57,133,953.00	13.78%	62,570,700.00	15.09%	9.52%
A Asphalt	5,480,469.20	1.32%	0.00	0.00%	-100.00%
W Water	3,574,967.30	0.86%	3,579,525.00	0.86%	0.13%
S Soil	5,672,408.50	1.37%	5,668,425.00	1.37%	-0.07%
T Tree	290,509,715.10	70.08%	342,705,579.00	82.67%	17.97%
G Grass	52,152,715.90	12.58%	0.00	0.00%	-100.00%
N No Data	0.00	0.00%	0.00	0.00%	0.00%
SUM	414,524,229.00	100.00%	414,524,229.00	100.00%	0.00%
Total Built-up Area (Building/Concrete, Asphalt)	62,614,422.20	15.11%	62,570,700.00	15.09%	-0.07%
	(62.61 km^2)		(62.57 km^2)		
Total Natural Surface (Soil, Trees, Grass, Water)	351,909,806.80	84.89%	351,953,529.00	84.91%	0.01%
	(351.91 km^2)		(351.95 km^2)		
SUM	414,524,229.00	100.00%	414,524,229.00	100.00%	0.00%
	(414.52 km^2)		(414.52 km^2)		

In comparing the manual planimetrics data of the three areas, it can be seen that only 15.11% of the total area of Oxford, MS was built-up area. The Gulfport area had a built-up area of 48.76%, and the Los Angeles/Long Beach area had a built-up area of 46.27%. The built-up areas of the Gulfport and Los Angeles/ Long Beach locations would have been even larger had the selected locations not contained a significant amount of water as part of their natural surface areas. The data also showed that Oxford had more natural area in the manual planimetrics than did Los Angeles/Long Beach and Gulfport. In the calibrated BANS classification for all three study areas, only trees or grass were identified, and none of the three studies identified both trees and grass. It appears that both the grass and tree features in each study were identified together as either all grass or all trees. Comparing the percent difference between manual planimetrics and calibrated BANS classification for each area was another key point. The Oxford area had only a -0.07% difference in total built-up area and a 0.01% difference in total natural area. The Los Angeles and Long Beach area had a -0.14% difference in total built-up area and a 0.12% difference in total natural area. The Gulfport area had a -0.41% difference in total built-up area and a 0.39% difference in total natural area. All three of the studies were under 1% difference in total built-up and total natural areas. This data indicates that the studies were accurate, as they were finding data similar to the planimetrics. The planimetrics for each of the three studies took, on average, 100 hours longer to perform than did the calibrated BANS classification. The calibrated BANS classification took approximately 3 hours on average for each area. This data indicates that the calibrated BANS classification method is a more efficient and practical method. Calibrated BANS classification is also a more efficient tool because the element of user error is greatly reduced, as the landuse is automatically determined without the need to draw any

polygons. The calibrated BANS results show large errors in the classifications of asphalt, grass, and trees. This requires revision in spectral criteria.

4.4 Surface Temperature of Three Selected Study Sites

After finding the areas' landuse by calibrated BANS classification, a weighted typical hot summer day temperature was analyzed for the following three study sites.

Site 1: Ports of Los Angeles and Long Beach, CA

Site 2: Port of Gulfport, MS

Site 3: Oxford, MS

According to Boriboonsomin and Uddin, "Increased surface temperature, due to built-up areas produces heat-island effect, which is known to influence O_3 [Ozone] level" [31]. The purpose of this analysis was to use the landuse data found by the calibrated BANS classification, including the built-up areas, to find the average weighted surface temperatures for the study sites.

First, the surface class temperatures on a typical summer day at air temperature, which can be observed in Figure 89, were reported by Boriboonsomin and Uddin [31]. This analysis was conducted for a typical summer day when the air temperature is 27.2 °C [31]. As shown in this figure, each of the six surface classes had a different value for surface temperature: asphalt is 64.9 degrees Celsius (°C), building/concrete is 57.2 °C, dry soil is 56.9 °C, wet soil is 47.7 °C, grass is 46.8 °C, tree/wooded area is 45.3 °C, and water is 34.4 °C. These surface temperatures were used to find an average weighted temperature for each surface area in the three study sites. Next, the calibrated BANS classification data was used for each of the three sites. This data can be found in Tables 13, 14, and 15 from earlier in this thesis. After this, the surface temperatures and calibrated BANS classification feature percentages were multiplied together for each site.

The final step was to sum up all of the temperatures found for each feature to determine the final average weighted temperature of the sites. Tables 16, 17, and 18 show the data which was used for these computations. Figure 90 shows the average weighted temperatures found for each of the three study sites. The ports of Los Angeles and Long Beach site had an average weighted temperature of 45.94 °C, the port of Gulfport site had an average weighted temperature of 50.72 °C, and the Oxford site had an average weighted temperature of 47.16 °C. The ports of Los Angeles and Long Beach site had the largest building/concrete area and the most water area. This water area caused the ports of Los Angeles and Long Beach site to have the lowest average weighted temperature. The port of Gulfport site had the highest average weighted temperature because it had the highest percentage of asphalt.

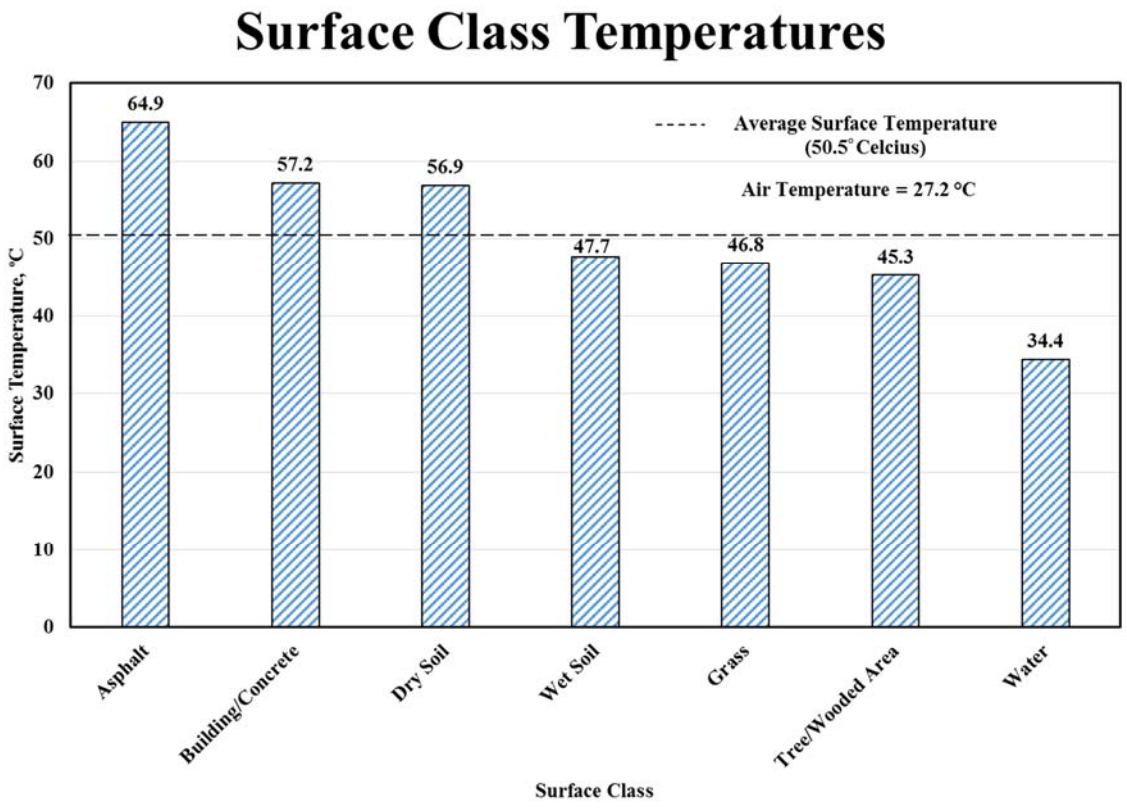

Figure 89. Surface temperatures by landuse feature

Table 16. Average weighted temperature of the ports of Los Angeles and Long Beach site

Ports of Los Angeles and Long Beach Site			
Surface Class	Surface Temperature (°C)	Calibrated BANS Classification Feature Percentage	Temperature (°C)
Building/Concrete	57.2	38.10%	21.79
Asphalt	64.9	8.10%	5.26
Water	34.4	50.70%	17.44
Soil	56.9	0.00%	0.00
Tree/Wooded Area	45.3	0.00%	0.00
Grass	46.8	3.10%	1.45
Average Weighted Temperature			45.94

Table 17. Average weighted temperature of the port of Gulfport site

Port of Gulfport Site			
Surface Class	Surface Temperature (°C)	Calibrated BANS Classification Feature Percentage	Temperature (°C)
Building/Concrete	57.2	23.80%	13.61
Asphalt	64.9	24.76%	16.07
Water	34.4	24.90%	8.57
Soil	56.9	0.53%	0.30
Tree/Wooded Area	45.3	0.00%	0.00
Grass	46.8	26.01%	12.17
Average Weighted Temperature			50.72

Table 18. Average weighted temperature of the Oxford, MS site

Oxford, MS Site			
Surface Class	Surface Temperature (°C)	Calibrated BANS Classification Feature Percentage	Temperature (°C)
Building/Concrete	57.2	15.09%	8.63
Asphalt	64.9	0.00%	0.00
Water	34.4	0.86%	0.30
Soil	56.9	1.37%	0.78
Tree/Wooded Area	45.3	82.67%	37.45
Grass	46.8	0.00%	0.00
Average Weighted Temperature			47.16

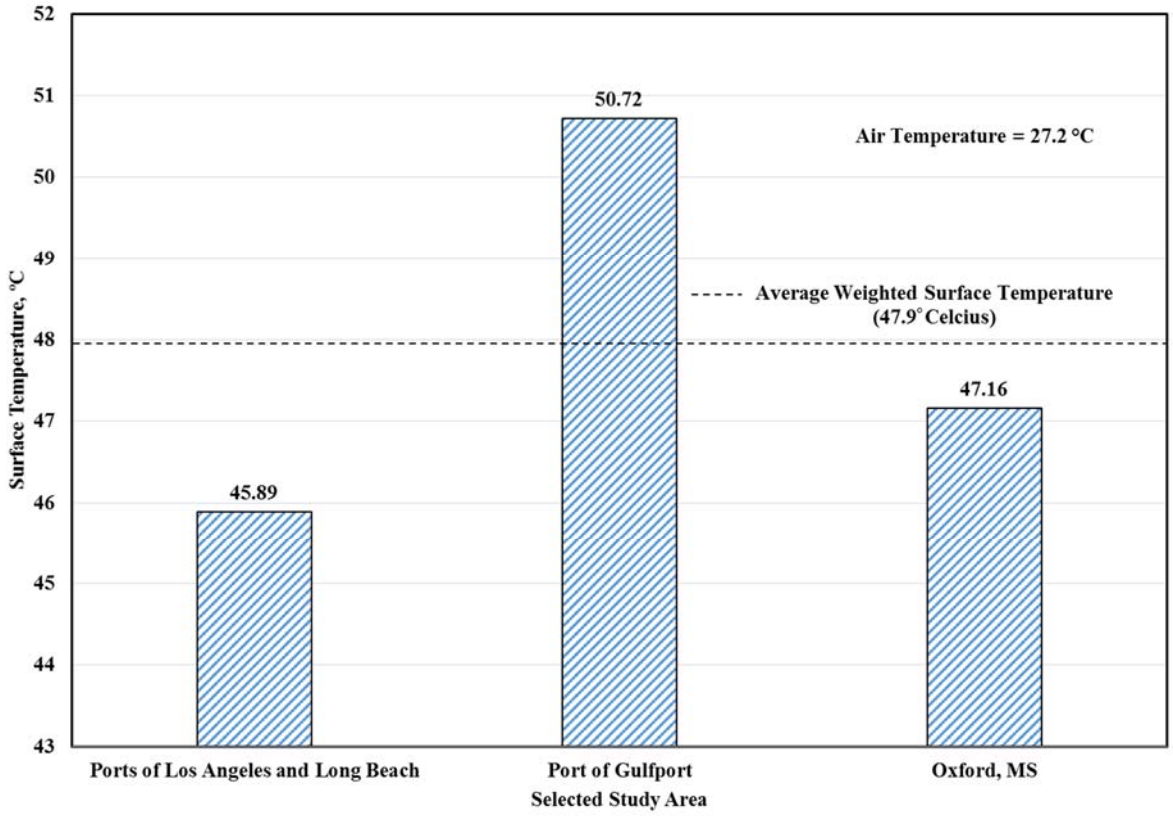

Figure 90. Average weighted surface temperature for selected study sites

4.5 Comparing the Population Density for the Cities of Oxford, MS, Los Angeles, CA, and Gulfport, MS Areas

This section of the thesis focuses on finding and comparing the population densities for the Cities of Oxford, MS, Los Angeles, CA, and Gulfport, MS. Unlike section 4.3.2, in which the cities and their surrounding areas were compared, this section will compare the population densities for the city areas only. This was done to make a comparison of the three city areas as a whole and to provide an understanding of why one area may be more built-up or less built-up than another. Figure 91 shows the Oxford, MS city boundary area. Figure 91 was created to find the square miles for the area. Next, the population for Oxford, MS was determined [32]. Then, Equation 12 was used to calculate the population density of the area. These steps were repeated for the cities of Gulfport, MS and Los Angeles, CA. Table 19 below shows the final results obtained for all three cities.

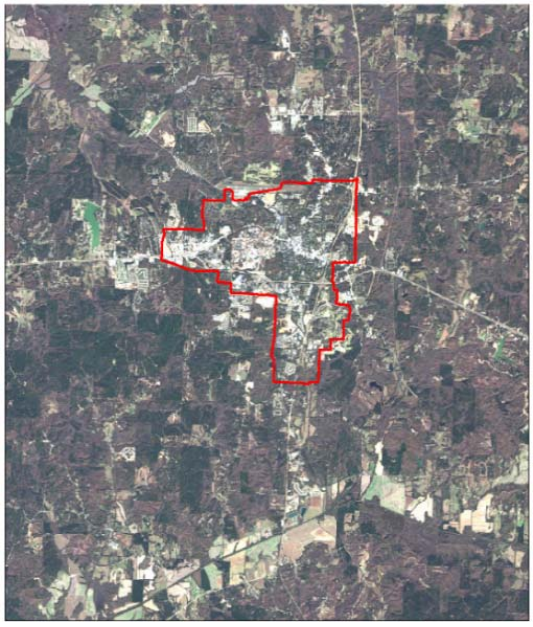

Figure 91. Oxford, MS city limits

$$\text{Population Density} = \text{City Population} / \text{City Land Area} \quad (12)$$

Table 19. Population density comparison of the three selected areas

	Population	Land Area (Square Miles)	Population Density (People/Square Mile)
City of Oxford, MS	20,865	10.75	1,941
City of Los Angeles, CA	3,884,000	503.00	7,722
City of Gulfport, MS	71,012	64.21	1,106

As shown in Table 19, the City of Los Angeles, CA had the highest population density with 7,722 people per square mile. Although the City of Gulfport had more than three times as many people as the City of Oxford, Oxford had over 800 more people per square mile than Gulfport.

4.6 Recommended Applications for Imagery Analysis

It is recommended that a revised BANS classification be developed using Landsat-8 imagery to improve accuracy. This revised L-BANS method should be used for mapping a port area's current infrastructure and landuse, to provide useful information for evaluating the present conditions of the area and to assist in planning for improvements.

CHAPTER V

SPATIAL MAPPING OF CARGO VESSELS AND ASSOCIATE EMISSION IMPACTS

This chapter will discuss case studies of spatial mapping of cargo vessels through vessel counts. CO_2 emissions data was also developed through a case study of a sample cargo vessel route across the Atlantic Ocean.

5.1 AIS Cargo Vessel Data Analysis of Spatial Mapping

In this section, five locations were studied around the U.S. and Europe to make analysis of the number of cargo vessels present in these locations hourly. A website was used to count the vessels within the selected areas [33]. Figure 92 shows the five selected locations in which the cargo vessels counts were taken. The five locations selected were West Pacific Alaska [W], Pacific Ocean [P], Gulf/Caribbean [G], U.S. East Coast Atlantic [EA], and Europe Atlantic [E]. Figure 93 is a screen shot of one of the five locations on the website and is an example of the number which were counted hourly [33]. The five different locations are spaced out to observe vessel data in different areas. Four of the areas are located in U.S. shipping area and the fifth area is of the European shipping area between Europe and the U.S. east coast. This will show most of the daily flow of cargo shipping vessels around the U.S. coast lines.

World Map With Shipping Buffer for US and Europe, 2015

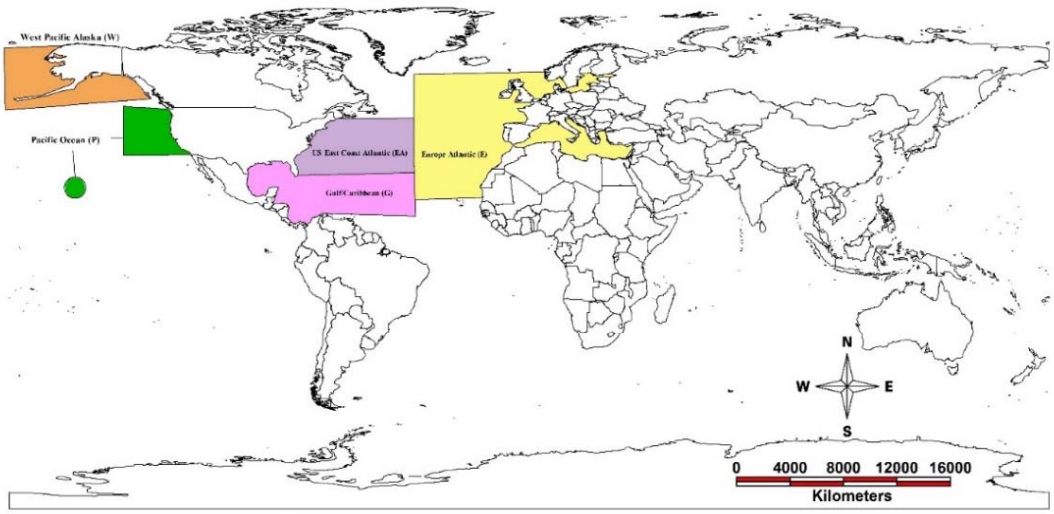

"Marine Traffic". 2015.Web. http://www.marinetraffic.com/en/ais/home/centrix:-20/centery:20/zoom:3. Accessed June 30, 2015.

G_RR_Ships_2015_World
M_RR_Ships_2015_World
Lay_RR_Ships_2015_World
L_RR_Ships_2015_World
D_RR_Ships_2015_World

Figure 92. Study locations selected

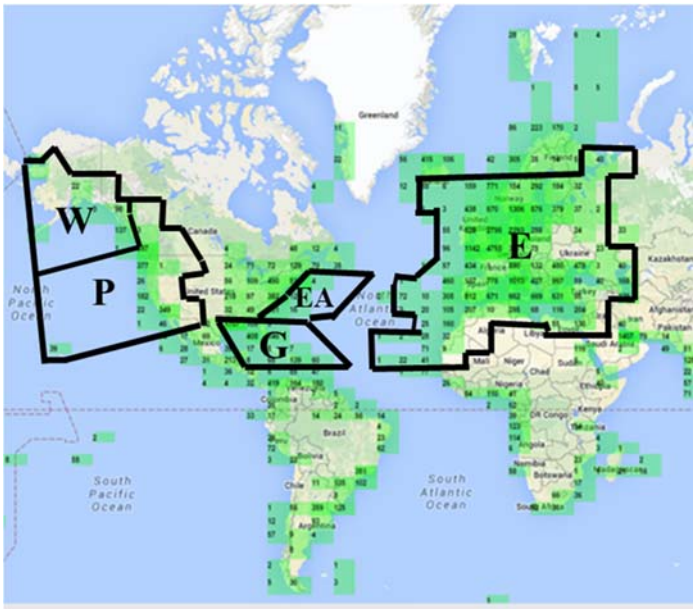

Figure 93. Locations of selected vessel counts on the website map [33]

An analysis of each of the five locations was performed in this thesis. To make these analyses, cargo vessels were counted on Monday, September 7, 2015, at 12:00 AM, 1:00 AM, 5:00 AM, 6:00 AM, 12:00 PM, 1:00 PM, 5:00 PM, and 6:00 PM CST. These times were selected to establish how the vessel count would change throughout the day. Interpolation and extrapolation were used to determine the number of vessels present between the hours the counts were made. This was done to determine the 24-hour daily average of the five locations. Figures 94, 95, 96, 97, and 98 and Tables 20, 21, 22, 23, and 24 show the vessel counts for each of the five locations. The figures also show the percentage of the maximum cargo vessel count for each individual hour count. Equation 13 was used to make these calculations. These calculations were necessary because every vessel did not leave the area prior to the next hour's count, and the numbers derived from these calculations assisted in establishing the number of cargo vessels leaving and entering the particular location each hour.

$$\text{Percentage of maximum cargo vessel count} = \left(\frac{hourly\ vessel\ total}{maximum\ hourly\ count}\right) x\ 100 \qquad (13)$$

Table 20. Data from the West Pacific Alaska [W] location

West Pacific Alaska [W]				
	1	2	3	3= 1 or 2/(largest value in 1)*100
	Orginal Vessel Count Data	Adjusted Data for Missing Cells by Interpolation/Extrapolation	Cargo Vessel Count Data Per Hour	Percent Change Normalized to Maximum Value Count
12:00 AM	103		103	100.0%
1:00 AM	102		102	99.0%
2:00 AM		99	99	96.1%
3:00 AM		96	96	93.2%
4:00 AM		93	93	90.3%
5:00 AM	90		90	87.4%
6:00 AM	92		92	89.3%
7:00 AM		93	93	90.3%
8:00 AM		94	94	91.3%
9:00 AM		95	95	92.2%
10:00 AM		96	96	93.2%
11:00 AM		97	97	94.2%
12:00 PM	98		98	95.1%
1:00 PM	100		100	97.1%
2:00 PM		99	99	96.3%
3:00 PM		98	98	95.5%
4:00 PM		98	98	94.8%
5:00 PM	97		97	94.2%
6:00 PM	96		96	93.2%
7:00 PM		94	94	91.3%
8:00 PM		82	92	89.3%
9:00 PM		90	90	87.4%
10:00 PM		88	88	85.4%
11:00 PM		86	86	83.5%
12:00 AM		84	84	81.6%
Average	97	93	95	

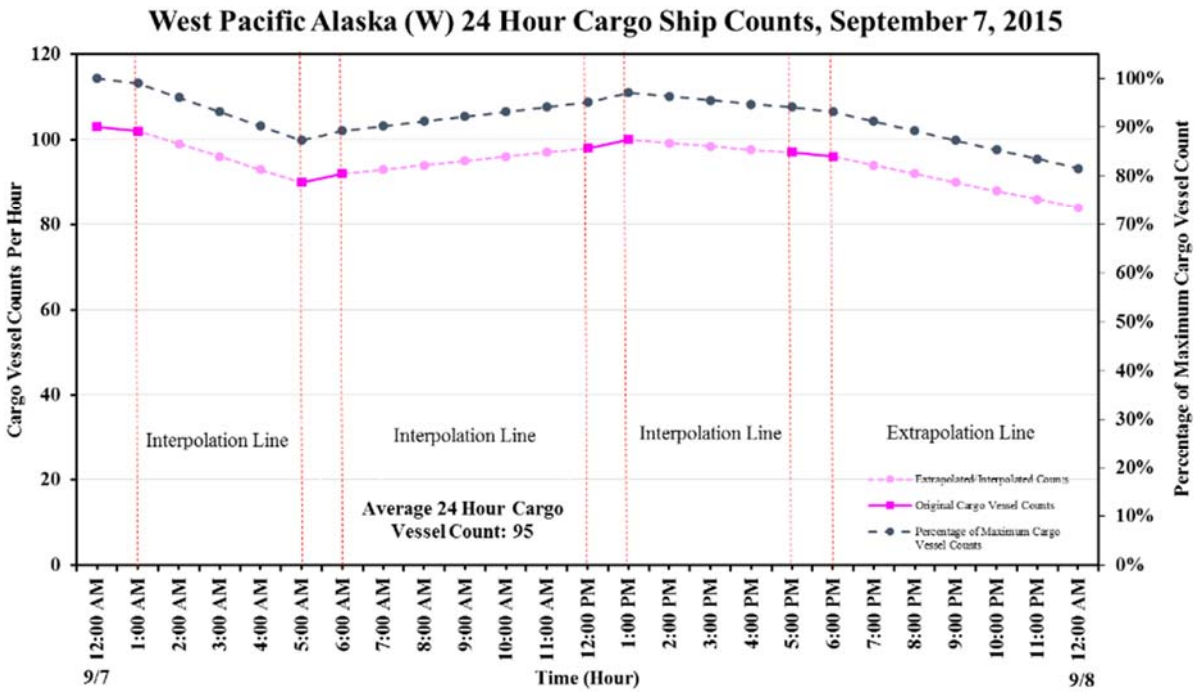

Figure 94. West Pacific Alaska [W] vessel counts and percentage of maximum vessel count

Figure 94 and Table 20 show the hourly cargo vessel counts for the West Pacific Alaska [W] location. This location had between 84-103 cargo vessels each hour during the 24-hour count period. The average 24-hour cargo vessel count for this location was 95 vessels. The low cargo vessel count of 84 occurred at 12:00 AM CST on September 8, 2015, and the maximum cargo vessel count of 103 occurred at 12:00 AM CST on September 7, 2015. The lowest percentage of the maximum vessel count value in this location was 81.6%. This represented a large percentage of the maximum value, which may indicate that few vessels entered and exited this location on this day.

Table 21. Data from the Pacific Ocean [P] location

Pacific Ocean [P]				
	1	2	3	3= 1 or 2/(largest value in 1)*100
	Orginal Vessel Count Data	Adjusted Data for Missing Cells by Interpolation/Extrapolation	Cargo Vessel Count Data Per Hour	Percent Change Normalized to Maximum Value Count
12:00 AM	194		194	92.4%
1:00 AM	189		189	90.0%
2:00 AM		191	191	90.7%
3:00 AM		192	192	91.4%
4:00 AM		194	194	92.1%
5:00 AM	195		195	92.9%
6:00 AM	194		194	92.4%
7:00 AM		195	195	92.7%
8:00 AM		195	195	93.0%
9:00 AM		196	196	93.3%
10:00 AM		197	197	93.6%
11:00 AM		197	197	94.0%
12:00 PM	198		198	94.3%
1:00 PM	203		203	96.7%
2:00 PM		205	205	97.5%
3:00 PM		207	207	98.3%
4:00 PM		208	208	99.2%
5:00 PM	210		210	100.0%
6:00 PM	208		208	99.0%
7:00 PM		206	206	98.1%
8:00 PM		204	204	97.1%
9:00 PM		202	202	96.2%
10:00 PM		200	200	95.2%
11:00 PM		198	198	94.3%
12:00 AM		196	196	93.3%
Average	199	199	199	

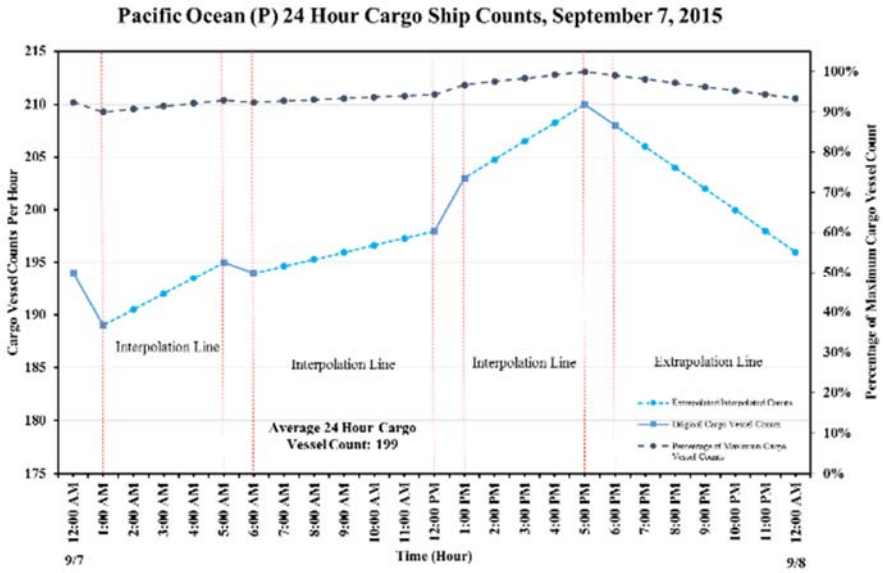

Figure 95. Pacific Ocean [P] vessel counts and percentage of maximum vessel count

Figure 95 and Table 21 show the hourly cargo vessel counts for the Pacific Ocean [P] location. This location had between 189-210 cargo vessels each hour during the 24-hour count period. The average 24-hour cargo vessel count for this location was 199 vessels. The low cargo vessel count of 189 occurred at 1:00 AM CST on September 7, 2015, and the maximum cargo vessel count of 210 occurred at 5:00 PM CST on September 7, 2015. The lowest percentage of the maximum vessel count value in this location was 90.0%. This represented a large percentage of the maximum value, which may indicate that few vessels entered and exited this location on this day.

Table 22. Data from the Gulf/Caribbean [G] location

Gulf/Caribbean [G]				
	1	2	3	3= 1 or 2/(largest value in 1)*100
	Orginal Vessel Count Data	Adjusted Data for Missing Cells by Interpolation/Extrapolation	Cargo Vessel Count Data Per Hour	Percent Change Normalized to Maximum Value Count
12:00 AM	405		405	78.8%
1:00 AM	404		404	78.6%
2:00 AM		410	410	79.7%
3:00 AM		416	416	80.8%
4:00 AM		421	421	82.0%
5:00 AM	427		427	83.1%
6:00 AM	431		431	83.9%
7:00 AM		438	438	85.2%
8:00 AM		445	445	86.5%
9:00 AM		452	452	87.8%
10:00 AM		458	458	89.2%
11:00 AM		465	465	90.5%
12:00 PM	472		472	91.8%
1:00 PM	465		465	90.5%
2:00 PM		467	467	90.8%
3:00 PM		469	469	91.1%
4:00 PM		470	470	91.4%
5:00 PM	472		472	91.8%
6:00 PM	478		478	93.0%
7:00 PM		484	484	94.2%
8:00 PM		490	490	95.3%
9:00 PM		496	496	96.5%
10:00 PM		502	502	97.7%
11:00 PM		508	508	98.8%
12:00 AM		514	514	100.0%
Average	444	465	458	

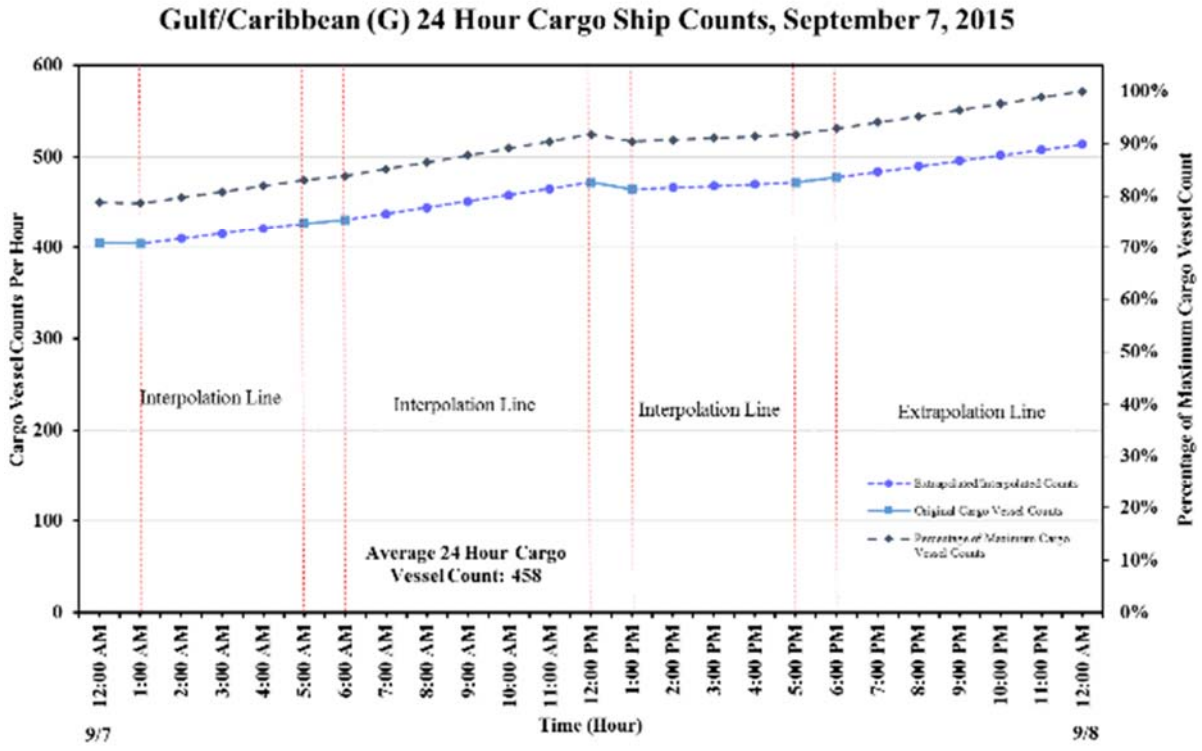

Figure 96. Gulf/Caribbean [G] vessel counts and percentage of maximum vessel count

Figure 96 and Table 22 show the hourly cargo vessel counts for the Gulf/Caribbean [G] location. This location had between 404-514 cargo vessels each hour during the 24-hour count period. The average 24-hour cargo vessel count for this location was 458 vessels. The low cargo vessel count of 404 occurred at 1:00 AM CST on September 7, 2015 , and the maximum cargo vessel count of 514 occurred at 12:00 AM CST on September 8, 2015. The reason for these cargo vessel count results may have been that September 7, 2015, was Memorial Day, and businesses may have been closed until September 8, 2015. The lowest percentage of the maximum vessel count value in this location was 78.8%. Over 20% of the maximum value had exited the location at 1:00 AM, indicating that the vessels were active on this day at this location.

Table 23. Data from the East Coast Atlantic [EA] location

East Coast Atlantic [EA]				
	1	2	3	3= 1 or 2/(largest value in 1)*100
	Orginal Vessel Count Data	Adjusted Data for Missing Cells by Interpolation/Extrapolation	Cargo Vessel Count Data Per Hour	Percent Change Normalized to Maximum Value Count
12:00 AM	230		230	94.3%
1:00 AM	229		229	93.9%
2:00 AM		230	230	94.2%
3:00 AM		231	231	94.5%
4:00 AM		231	231	94.8%
5:00 AM	232		232	95.1%
6:00 AM	229		229	93.9%
7:00 AM		227	227	92.8%
8:00 AM		224	224	91.8%
9:00 AM		222	222	90.8%
10:00 AM		219	219	89.8%
11:00 AM		217	217	88.7%
12:00 PM	214		214	87.7%
1:00 PM	209		209	85.7%
2:00 PM		210	210	86.2%
3:00 PM		212	212	86.7%
4:00 PM		213	213	87.2%
5:00 PM	215		215	88.1%
6:00 PM	220		220	90.2%
7:00 PM		224	224	91.8%
8:00 PM		228	228	93.4%
9:00 PM		232	232	95.1%
10:00 PM		236	236	96.7%
11:00 PM		240	240	98.4%
12:00 AM		244	244	100.0%
Average	222	226	225	

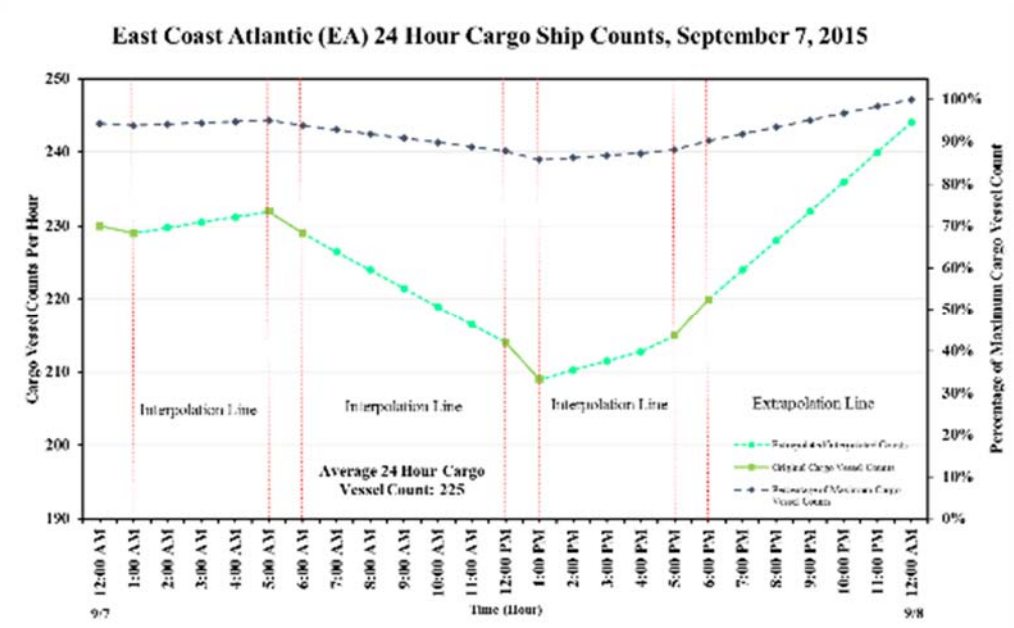

Figure 97. East Coast Atlantic [EA] vessel counts and percentage of maximum vessel count

Figure 97 and Table 23 show the hourly cargo vessel counts for the East Coast Atlantic [EA] location. The average 24-hour cargo vessel count for this location was 225 vessels. The low cargo vessel count of 209 occurred at 1:00 PM CST on September 7, 2015, and the maximum cargo vessel count of 244 occurred at 12:00 AM CST on September 8, 2015. The reason for these cargo vessel count results may have been that September 7, 2015, was Memorial Day, and businesses may have been closed until September 8, 2015. The lowest percentage of the maximum vessel count value in this location was 85.7%.

Table 24 shows the results of hourly vessel counts for a 24-hour period for E route. The average hourly vessels count is 5,847 per day.

Table 24. Data from the Europe Atlantic [E] location

Europe Atlantic [E]				
	1	2	3	3= 1 or 2/(largest value in 1)*100
	Orginal Vessel Count Data	Adjusted Data for Missing Cells by Interpolation/Extrapolation	Cargo Vessel Count Data Per Hour	Percent Change Normalized to Maximum Value Count
12:00 AM	5,741		5,741	94.5%
1:00 AM	5,803		5,803	95.5%
2:00 AM		5,870	5,870	96.6%
3:00 AM		5,937	5,937	97.7%
4:00 AM		6,004	6,004	98.8%
5:00 AM	6,071		6,071	99.9%
6:00 AM	6,077		6,077	100.0%
7:00 AM		6,070	6,070	99.9%
8:00 AM		6,064	6,064	99.8%
9:00 AM		6,057	6,057	99.7%
10:00 AM		6,050	6,050	99.6%
11:00 AM		6,044	6,044	99.5%
12:00 PM	6,037		6,037	99.3%
1:00 PM	6,029		6,029	99.2%
2:00 PM		5,954	5,954	98.0%
3:00 PM		5,879	5,879	96.7%
4:00 PM		5,804	5,804	95.5%
5:00 PM	5,729		5,729	94.3%
6:00 PM	5,703		5,703	93.8%
7:00 PM		5,657	5,657	93.1%
8:00 PM		5,611	5,611	92.3%
9:00 PM		5,565	5,565	91.6%
10:00 PM		5,519	5,519	90.8%
11:00 PM		5,473	5,473	90.1%
12:00 AM		5,427	5,427	89.3%
Average	5,899	5,823	5,847	

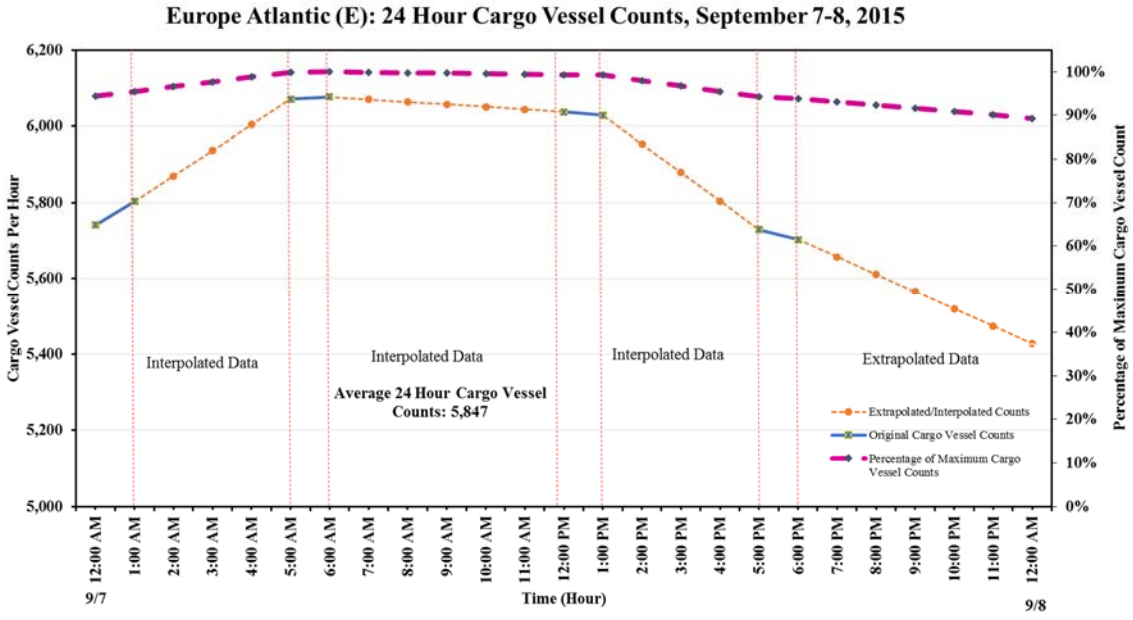

Figure 98. Europe Atlantic [E] vessel counts and percentage of maximum vessel count

Figure 98 and Table 24 show the hourly cargo vessel counts for the Europe Atlantic [E] location. This location had between 5,427-6,077 cargo vessels each hour during the 24-hour count period. The average 24-hour cargo vessel count for this location was 95 vessels. The low cargo vessel count of 5,427 occurred at 12:00 AM CST on September 8, 2015, and the maximum cargo vessel count of 6,077 occurred at 6:00 AM CST on September 7, 2015. The lowest percentage of the maximum vessel count value in this location was 89.3%. With only 11.7% of the maximum value exiting the location, this location retained a large number of vessels throughout the day.

The data showed that the Pacific Ocean location had 90% of the maximum count in the location for the entire 24 hours, the highest percentage among the study locations. The Europe location had an average of 5,427 cargo vessels per hour in this location, the highest among the study locations. The Gulf/Caribbean location had the second highest per hour average, with an average of 458 cargo vessels per hour. Figure 99 provides a comparison between the 5 regions.

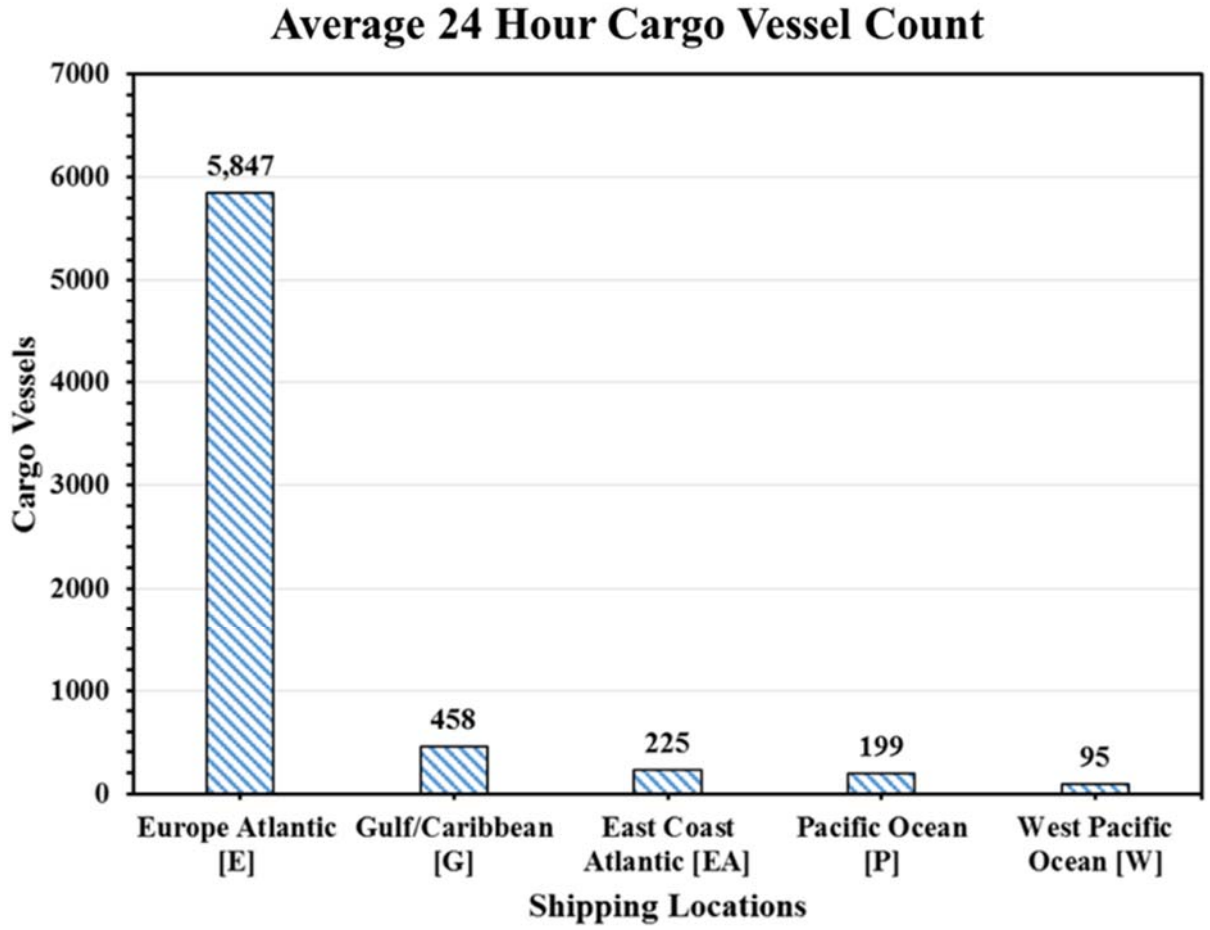

Figure 99. Comparison of the five selected shipping locations

5.2 Shipping Emissions Analysis and Impacts

A study on CO_2 emissions data was calculated using a sample cargo vessel trip. The study was made for a 12,000 TEU cargo vessel for an assumed trip from the Port of New York to the Port de Honfleur in France. This shipping route and distance may be seen in Figure 100.

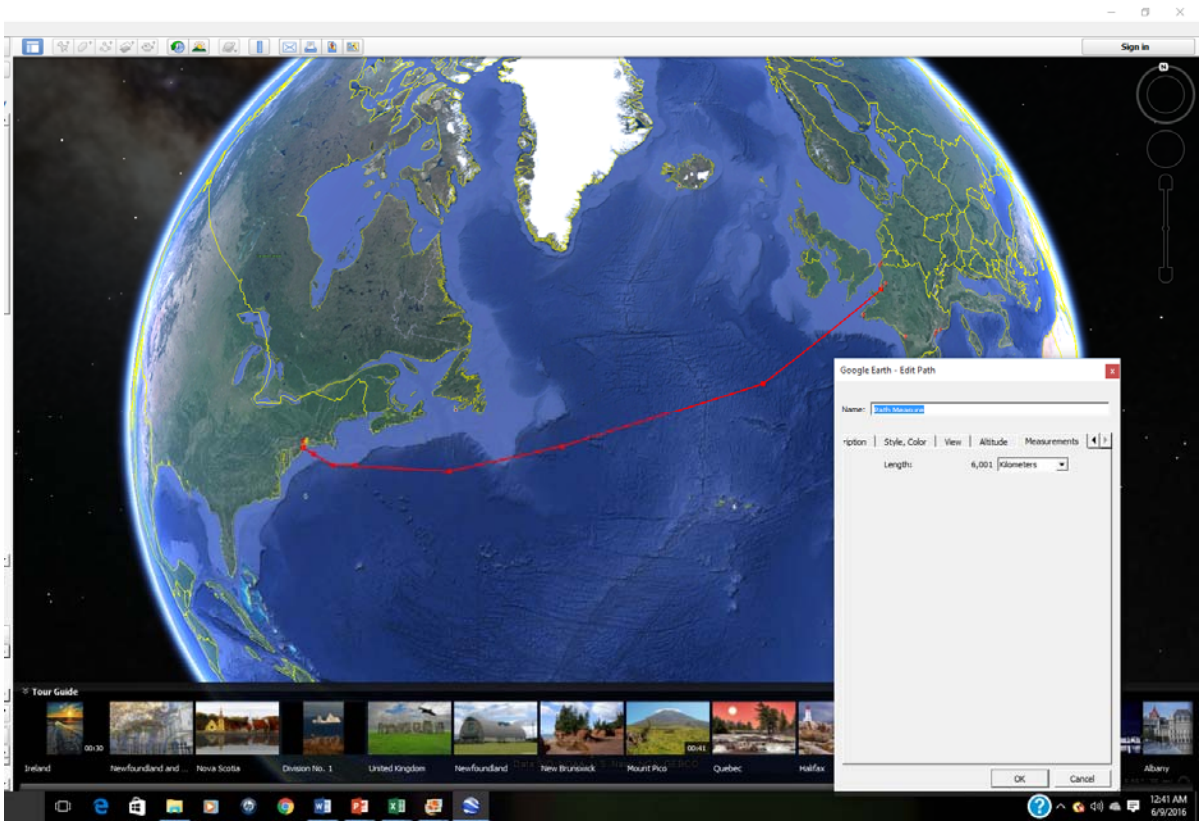

Figure 100. Shipping route between Port of New York and Port de Honfleur in France

The distance of the trip was 6,001 kilometers [27]. It was known that a cargo vessel emits 22.2 lbs. of CO_2 per gallon when traveling [34]. It was also known that a 12,000 TEU cargo vessel consumes 125 gallons of gas per mile [35]. Equation 14 was used to calculate the number of miles per gallon (MPG) a 12,000 TEU cargo vessel achieves [35]. Equation 15 was used to convert kilometers to miles [36]. Equation 16 was created by Uddin [37]. This equation was used to calculate the CO_2 emissions for the trip.

MPG of a 12,000 TEU cargo vessel = 1 mile / 125 gallons = .008 mpg (14)

Trip Distance = 6001 km x .621371 miles/km = 3,728.85 miles (15)

CO_2 Emissions = (miles / vehicle fuel efficiency) x pounds of CO_2 emitted per gallon (16)

CO_2 Emissions = (3,728.85 miles / 0.008 mpg) x 22.2 pounds of CO_2 = 10,347,559 lbs. of CO_2

As shown by this example, a trip from the Port of New York to the Port de Honfleur in France may result in the release of 10,347,559 lbs. or 5,174 short tons of CO_2 per trip. This is only for one single trip. With this in mind, steps need to be taken now to reduce CO_2 emissions, such as bigger sized ships.

5.3 Emission Impacts of Port Infrastructure and Inland Cargo Distribution

The impacts of the emission of pollutants may be divided into three categories: direct impacts, which include "the immediate consequence of transport activities" from emissions; indirect impacts, which include "the secondary (or tertiary) effects of transport activities on environmental systems," such as respiratory and cardiovascual problems; and cumulative impacts, which include "the additive, multiplicative or synergetic consequences of transport activities," [38].

The mode of transportation used to ship cargo can have an effect on emissions. As shown in Figure 1, shipping one ton of cargo one kilometer by container ships and rail produce the lowest number of grams of CO_2 [6].

5.4 Recommended Applications

The AIS data on commercial websites are already being used to monitor shipping traffic and to help enhance safety. The use of AIS data in this research showed that a reasonable estimate of global shipping traffic can be made for selected navigation routes. This shipping traffic analysis can be further used to estimate CO_2 emissions.

CHAPTER VI

SUMMARY, CONCLUSIONS, AND RECOMMENDATIONS

6.1 Summary of Research Accomplished

The import and export of goods is a major part of the U.S. economy, and the volume of cargo handled by U.S. ports is expected to increase in the future as population increases. U.S. ports must make plans now to accommodate this expected growth in volume, as every U.S. state would be adversely affected if improvements are not made to the capacity, infrastructure, and efficiency of U.S. ports. Due to this expected growth in volume and increase in shipping, ports must also address the need for alternative, more efficient shipping routes for cargo vessels and take steps to alleviate the expected increase in CO_2 emissions.

A major West Coast port area, the adjoining ports of Los Angeles and Long Beach, California, was selected for case study. An initial study was made to determine where the goods from the study area were distributed throughout the U.S. A statistical demand prediction model for the study area was developed based on TEU data, and TEU data predictions were made for 5, 10, 15, and 20 years into the future using ARIMA (1,2,1) and the regression equation with year and dummy variable as the independent variables. Spatial maps of infrastructure and landuse were developed using pan-sharpened Landsat-8 imagery for the study area and for two other selected areas. The accuracy and efficiency of the BANS classification of infrastructure and landuse was evaluated by comparing with the manual planimetrics. AIS data was developed through ship counts. CO_2 emissions data was calculated using a sample cargo vessel trip.

6.2 Conclusions

Key findings for the cargo demand portion of this thesis are as follows:

- Of the three major port regions in the U.S., container liner service ports in the East Coast region handled the most tons annually at 39.83% of the total 2010 U.S. freight.
- The state that handled the most freight in the West Coast region in 2010 was California, which was only one of three states with container liner service ports that handled over 90 million tons of freight in 2010.
- The ports of Los Angeles and Long Beach distribute 89.0% of their total imports to destinations in California. The top five U.S. states to which the ports of Los Angeles and Long Beach distributed their goods were California, Arizona, Nevada, Texas, and Washington.
- Linear optimization analysis was performed on import freight of 66.76 million tons shipped from the ports of Los Angeles and Long Beach to destinations in California, Arizona, Nevada, Texas, and Washington. This analysis showed that shipping costs were reduced by 27.4% by diverting 30% of the freight from road to rail.

Key findings for TEU prediction modeling are as follows:

- Regression equations with time as the independent variable and with California GDP as the independent variables were compared to ARIMA (1,2,1) to determine which of these was the better method to predict future TEU values. ARIMA (1,2,1) was determined to be the better method with a lower MARE value of 5.34% and a lower RMSE value of 52,602.04.

- Using a dummy regression equation with year and dummy variable for the 2008 economic recession as the independent variables, the ports will have 36.8% more TEUs coming through the ports in 10 years. However, because the original data included an economic recession about 13 years into the measured TEU data, the ARIMA (1,2,1) found an increase of 3.3% in the next 10 years and a decrease of 13.3% in the next 20 years. The 2015 TEU data showed a 0.01% increase from the 2014 TEU data. This is supportive of ARIMA (1,2,1) because it predicted a 3.3% increase in the next 10 years and a 13.3% decrease in 20 years.

Key findings for the spatial mapping portion of this thesis are as follows:

- Landsat-8 pan-sharpened imagery was analyzed for the selected study sites. For the ports of Los Angeles and Long Beach, the planimetrics analysis revealed that this area had little in the way of trees, grass, and soil and much larger areas of water and building/concrete in its imagery. The calibrated BANS classification generally yielded the same results as the planimetrics. The most notable difference was that the calibrated BANS classification did not identify any trees or soil. The difference between the planimetrics and calibrated BANS classification for the built-up area was -0.14% and for the natural area was 0.12%.
- For the Port of Gulfport, the planimetrics analysis revealed that the area had a larger portion of trees and grass than the ports of Los Angeles and Long Beach, although Gulfport still had a fair amount of building/concrete. The calibrated BANS classification yielded nearly the same results as the planimetrics. The most notable difference was that the calibrated BANS classification did not identify any trees. The

difference between the planimetrics and calibrated BANS classification for the built-up area was -0.41% and for the natural area was 0.39%.

- For the Oxford, MS area, the planimetrics analysis revealed that the area had a large proportion of trees and grass. The calibrated BANS classification yielded generally the same results as the planimetrics. The most notable difference was the calibrated BANS classification did not identify any trees or asphalt. The difference between the planimetrics and calibrated BANS classification for the built-up area was -0.07% and for the natural area was 0.01%.
- In each study, not all results of the calibrated BANS classification were similar to those obtained through the use of manual planimetrics, but the calibrated BANS classification analysis took much less time to perform than planimetrics. The calibrated BANS classification is not subjective nor manual. It is an efficient method for mapping infrastructure and landuse. It is not reasonably accurate at classifying asphalt, grass, and trees. It is recommended to develop a new L-BANS surface classification using Landsat-8 spectral data.

Key findings for the spatial mapping of cargo vessels and associate emissions impacts portion of this thesis are as follows:

- Based on a 24-hour vessel count performed on five selected navigation routes, the West of Europe's coast had the most vessels at an average of 5,847 cargo vessels per hour in the 24-hour period. The top region in the U.S. was the Gulf/Caribbean with an average of 458 cargo vessels per hour in the 24-hour period.

- Based on an analysis of a sample cargo vessel route from the Port of New York to the Port de Honfleur in France, it was found that one 12,000 TEU vessel could emit 10,347,559 lbs. or 5,174 short tons of CO_2 during this trip.

6.3 Recommendations

- It is recommended that more studies be performed on the distribution of commodities from U.S. ports to destinations in the U.S. in order to improve the efficiency of the overall shipping process and to optimize shipping costs.
- It is recommended that individual ports develop demand prediction models for future years using ARIMA modeling, so that they may plan for and make infrastructure and other improvements as needed to accommodate the expected increases in future cargo volume.
- It is recommended that a new L-BANS classification method be developed using Landsat-8 spectral data that can be used for mapping a port area's current infrastructure and landuse to provide useful information for evaluating the present conditions of the area and to assist in planning for improvements.
- It is recommended that data obtained by AIS be used as a tool for shipping flow analysis to assist in estimating shipping demand and to improve shipping efficiency and routing.
- It is recommended that steps be taken to reduce CO_2 emissions in shipping, especially in light of the expected increase in the volume of shipping in the future.

LIST OF REFERENCES

LIST OF REFERENCES

[1] "U.S. Public Port Facts." American Association of Port Authorities. 2008. http://www.aapa-ports.org/files/PDFs/facts.pdf. Accessed May 15, 2016.

[2] Martin Associates. 2008. http://martinassoc.co/latest-news/. Accessed April 1, 2016.

[3] "2007 States and Country Data." U.S. Census Bureau. 2007. https://www.census.gov/did/www/saipe/data/statecounty/data/2007.html. Accessed April 1, 2016.

[4] "Missions." U.S. Army Corps of Engineers. 2006. http://www.usace.army.mil/Missions/. Accessed April 1, 2016.

[5] "General Notes." U.S. Customs Border Protection. 2007. https://www.cbp.gov/bulletins/42genno1.pdf. Accessed April 1, 2016.

[6] "Industry Issues." World Shipping Council. 2016. http://www.worldshipping.org/industry-issues/environment/air-emissions/faqs-answers/a1-why-is-the-liner-shipping-industry-so-important-economically. Accessed May 15, 2016.

[7] Uddin, W., Sherry, P., Eksioglu, B., and Mitchell, K. "Economically Viable Intermodal Integration of Surface and Waterway Freight Transport for Sustainable Supply Chain." 2015. http://www.olemiss.edu/projects/cait/ncitec/Uddin-NCITEC-Freight-Surface-Waterway-Project-26March2015.pdf. Accessed May 21, 2015.

[8] Uddin, W. *CE 495: Geospatial Analysis for Visualization Applications*. Course Lecture Notebook, University of Mississippi, 2013.

[9] Uddin, W., Hudson, W., Haas, R. "Geographical Information Systems (GIS)." *Public Infrastructure Asset Management*. McGraw-Hill. 2013. Pp. 481-488.

[10] "Ports with Container Liner Service." World Port Source. 2010. http://worldportsource.com/shipping/country/ports/USA.php. Accessed May 6, 2015.

[11] "Origin-Destination Files." Bureau of Transportation Statistics. 2007. http://www.rita.dot.gov/bts/sites/rita.dot.gov.bts/files/publications/commodity_flow_survey/index.html. Accessed May 6, 2015.

[12] "United States Census 2010." U.S. Census Bureau. 2010. http://www.census.gov/2010census/popmap/ipmtext.php?fl=01. Accessed May 7, 2015.

[13] "2008 U.S. Average Cost of Freight (Cents) Per Ton-Mile". The Effects of Rising Fuel Costs on Goods Movement Mode Choice and Infrastructure Needs. http://tampabay freight.com/wp-content/uploads/The-Effectof-Rising-Fuel-Costs-on-Goods-Movement-Mode-Choice-and-Infrastructure-Needs.pdf. Accessed October 28, 2016.

[14] Ports of Los Angeles and Long Beach. "Historical TEUs Statistics." http://www.portoflosangeles.org/maritime/stats.asp. Accessed February 17, 2015.

[15] Wilcox, R. *Applying Contemporary Statistical Techniques*. Elsevier Science. 2003.

[16] Rohatgi, V. *Statistical Inference*. Wiley and Sons. 1984.

[17] IBM. "IBM SPSS Software." http://www.ibm.com/analytics/us/en/technology/spss/. Accessed March 1, 2015.

[18] Riad, S., Mania, J., Bouchaou, L., Najjar, Y. "Predicting Catchment Flow in a Semi-arid Region via an Artificial Neural Network Technique". Hydrological Processes, Vol. 18, No. 13, September 2004, pp. 2387-2393.

[19] Dý´az-Robles, L., Ortega, J, Fu, J., Reed, G., Chow, J., Watson, J, Moncada-Herrera, J.. "A Hybrid ARIMA and Artificial Neural Networks Model to Forecast Particulate Matter in Urban Areas: The Case of Temuco, Chile". Atmospheric Environment, Vol. 42, No. 35, November 2008, pp. 8331- 8340.

[20] McCleary, R. and Hay, R. *Applied Time Series Analysis for the Social Sciences*. Sage Publications. 1980.

[21] Nguyen, Q. Extreme Weather Disaster Resilient Port and Waterway Infrastructure for Sustainable Global Supply Chain. *PhD Dissertation (In Progress).* University of Mississippi.

[22] Uddin, W., McCullough, B., and Crawford, M. "Methodology of Forecasting Air Travel Demand and Airport Expansion Needs." Transportation Research Record 1025, Journal of Transportation Research Board, Washington DC, 1985, pp. 7-14.

[23] "Quarterly Gross Domestic Product (GDP) by State." U.S. Department of Commerce. 2005-2014. http://www.bea.gov/iTable/iTable.cfm?reqid=70&step=1&isuri=1&acrdn=1#reqid=70&step=1&isuri=1&7003=200&7004=naics&7005=1&7006=06000&7001=5200&7002=5&7090=70&7093=levels. Accessed January 21, 2016.

[24] Uddin, W. "Remote Sensing Laser and Imagery Data for Inventory and Condition Assessment of Road and Airport Infrastructure and GIS Visualization." International Journal of Roads and Airports (IJRA), Vol. 1, No. 1, January 2011, pp. 53-67.

[25] Uddin, W. "Transportation Management: LiDAR, Satellite Imagery Expedite Infrastructure Planning." Earth Imaging Journal, January/February 2011, pp.24-27.

[26] USGS. Landsat-8. http://earthexplorer.usgs.gov/. Accessed 12/4/15.

[27] "Google Earth." Google. https://www.google.com/earth/. Accessed 11/25/15.

[28] "ERDAS IMAGINE." Intergraph. http://www.intergraph.com/assets/pressreleases/2012/10-09-2012c.aspx. Accessed 12/5/15.

[29] "Geomedia Pro." Intergraph. http://www.hexagongeospatial.com/products/producer-suite/geomedia. Accessed December 6, 2015.

[30] Wodajo, B. Geospatial Analysis of Spaceborne Remote Sensing Data for Assessing Disaster Impacts and Modeling Surface Runoff in the Building-Environment. *PhD Dissertation.* University of Mississippi. May 2009.

[31] Uddin, W. and Boriboonsomsin, K. "A Consideration of Heat-Island Effect in Ground-Level Ozone Forecasting Model and Its Application in Rural Areas of Northern Mississippi." January 2006, Annual Meeting of the Transportation Research Board, National Academy; Washington, D.C. https://trid.trb.org/view.aspx?id=777182. Accessed August 10, 2016.

[32] "Census Data." U.S. Census Bureau. 2013. http://www.census.gov/search-results.html?page=1&stateGeo=none&searchtype=web&cssp=SERP&q=2013+oxford+ms&search.x=0&search.y=0&search=submit. Accessed May 7, 2016.

[33] "Marine Traffic." Marine Traffic. 2015. http://www.marinetraffic.com/en/ais/home/centerx:-20/centery:20/zoom:3. Accessed June 30, 2015.

[34] "Why is Ship Efficiency Important?" Maritime. http://maritime.about.com/od/Pollution/a/Why-Is-Ship-Efficiency-Important.htm. Accessed November 16, 2015.

[35] "Standard Containers." Ready to Launch. http://www.r2launch.nl/index.php/packaging/container. Accessed November 16, 2015.

[36] "Metric Conversions." http://www.metric-conversions.org/length/kilometers-to-miles.htm. Accessed on April 28, 2016.

[37] Uddin, W. *CE 481. "Transportation Engineering I*. Course Lecture Notebook, Mississippi, 2013.

[38] Rodrigue, J. "The Environmental Impacts of Transportation." Hofstra University. https://people.hofstra.edu/geotrans/eng/ch8en/conc8en/ch8c1en.html. Accessed on April 23, 2016.

[39] Cobb, S. Economic Viability and Societal Benefits of Integrated Multimodal Freight Corridors and Sustainable Passenger Transportation. *Masters Thesis.* University of Mississippi. August 2015.

[40] Durmas, A. Geospatial Assessment of Sustainable Built Infrastructure Assets and Flood Disaster Protection. *Masters Thesis*. University of Mississippi. 2012.

[41] "Linear Programming: Introduction". Purplemath. http://www.purplemath.com/modules/lingprog.htm. Accessed October 27, 2016.

APPENDIXES

APPENDIX A

Optimization Analysis of Cargo Shipping Distribution and Results

Optimization Analysis of Cargo Shipping Distribution and Results

Linear optimization was performed for the ports of Los Angeles and Long Beach distribution data. The linear optimization was chosen because the process takes "various linear inequalities and finds the 'best' value obtainable under those conditions" [41]. In this case, the value sought will be the minimum value. Two different scenarios were analyzed. The first scenario involved shipping 100% of the freight from the ports of Los Angeles and Long Beach to selected state markets by truck. The second scenario involved shipping 70% of the freight by truck and shipping 30% of the freight by rail.

The following Equation 1 is used to calculate b_{ij}.

$$b_{ij} = (\text{Distance from port to state market x (unit cost/100)}) \quad (1)$$

b_{ij}= Unit cost per ton-mile of shipping one unit of freight from port (i) to state (j)

The first step in solving the linear optimization problem is creating an objective function. The objective function is as follows (Equation 2):

$$\text{Minimize: } Z = \sum_{i=1}^{I} \sum_{j=1}^{J} (y_{ij} \; x \; b_{ij}) \quad (2)$$

Z= Total cost (U.S.$) to ship from port (i) to each state market (j), where i=1,…I and j=1,2,3,…J

y_{ij}= Quantity of the freight tonnage shipped from port (i) to state market (j)

b_{ij}= Unit cost per ton-mile for freight shipping from port (i) to state market (j)
(This basic unit cost for freight truck is 42.38 cents per ton-mile and the freight rail unit cost is 3.70 cents per ton-mile.)

d_{ij}= distance from port to market = 364.0 miles to California market (j), 355.9 miles to Arizona market (j), 243.6 miles to Nevada market (j), 1,241.7 miles to Texas market (j), and 981.3 miles to Washington market (j)

The first constraint deals with the summing of all commodity freight shipped from the port location to all selected state markets, which cannot exceed the total commodity freight available at the port (Equation 3).

$$\sum_{j=1}^{J} y_{ij} \geq -T \quad (3)$$

T= Total freight available at port, where i=1,…I and j=1,2,3,…J

The second constraint deals with the total amount sent to a state market, which cannot be less than the amount of the commodity required in that state market as shown in Equation 4. Additionally, the amount of freight from port to state market must be a positive value as shown in Equation 5. The input data for the unit ton cost for both scenarios is shown in Tables A1 and A2.

$$\sum_{i=1}^{I} y_{ij} \geq r_j \quad (4)$$

r_j= Freight required at each port (i) for the state market (j), where i=1,…I and j=1,2,3,…J

$$y_{ij} \geq 0 \quad (5)$$

y_{ij}= Quantity of the freight tonnage shipped from port (i) to state market (j),

where i=1,..I and j=1,2,3,..J

Table A1. Unit cost per ton (Base Scenario 100% Road)

Linear Distance from the Ports to Each State Market and Unit Cost per Ton			
Ports (i)	State Markets (j)	Distance (Miles)	U.S. Dollars Per Ton Distances x (42.38/100)
Ports of Los Angeles and Long Beach	California, CA	364.0	$154.24
	Arizona, AZ	355.9	$150.81
	Nevada, NV	243.6	$103.22
	Texas, TX	1,241.7	$526.24
	Washington, WA	981.3	$415.87

Table A2. Unit cost per ton (Alternative Scenario 70% Road, 30% Rail)

Linear Distance from the Ports to Each State Market and Unit Cost Per Ton			
Ports (i)	State Markets (j)	Distance (Miles)	U.S. Dollars Per Ton Distances x (30.78/100)
Ports of Los Angeles and Long Beach	California, CA	364.0	$112.02
	Arizona, AZ	355.9	$109.53
	Nevada, NV	243.6	$74.97
	Texas, TX	1,241.7	$382.20
	Washington, WA	981.3	$302.04

Step by Step Excel Solver Procedure

1) The first step is to set up Solver in Excel. To accomplish this, click on File in the top left corner, and click on Options. Figure A1 will appear.

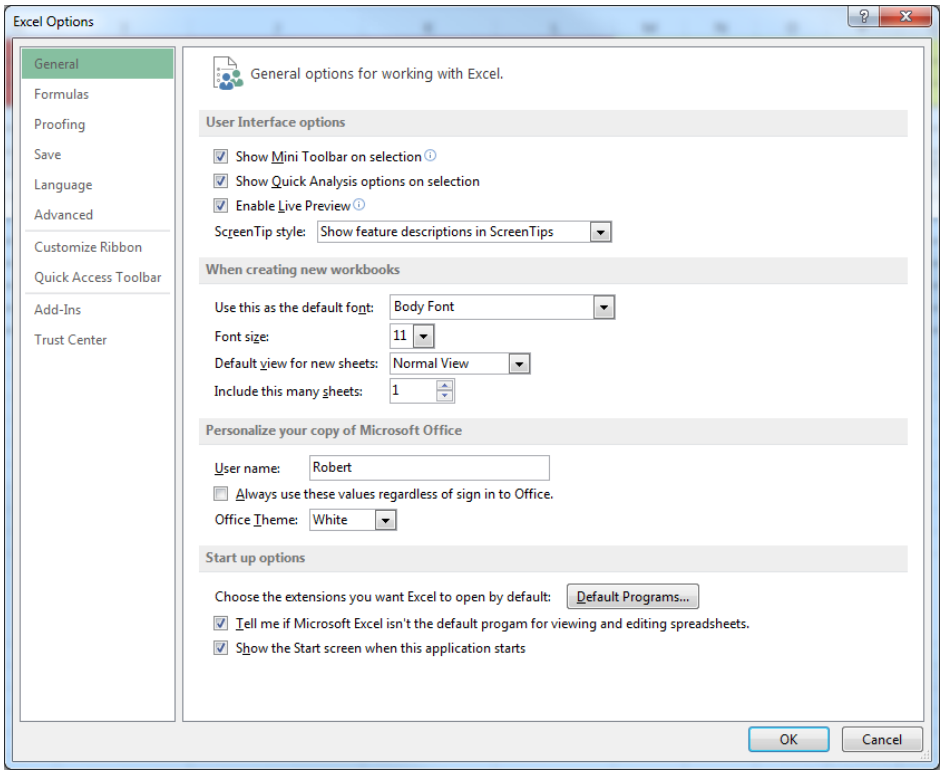

Figure A1. Excel Options menu

2) Next, go to the Customize Ribbon tab. Once there, select Developer under the main tabs. This can be seen in Figure A2. After clicking Developer, click OK.

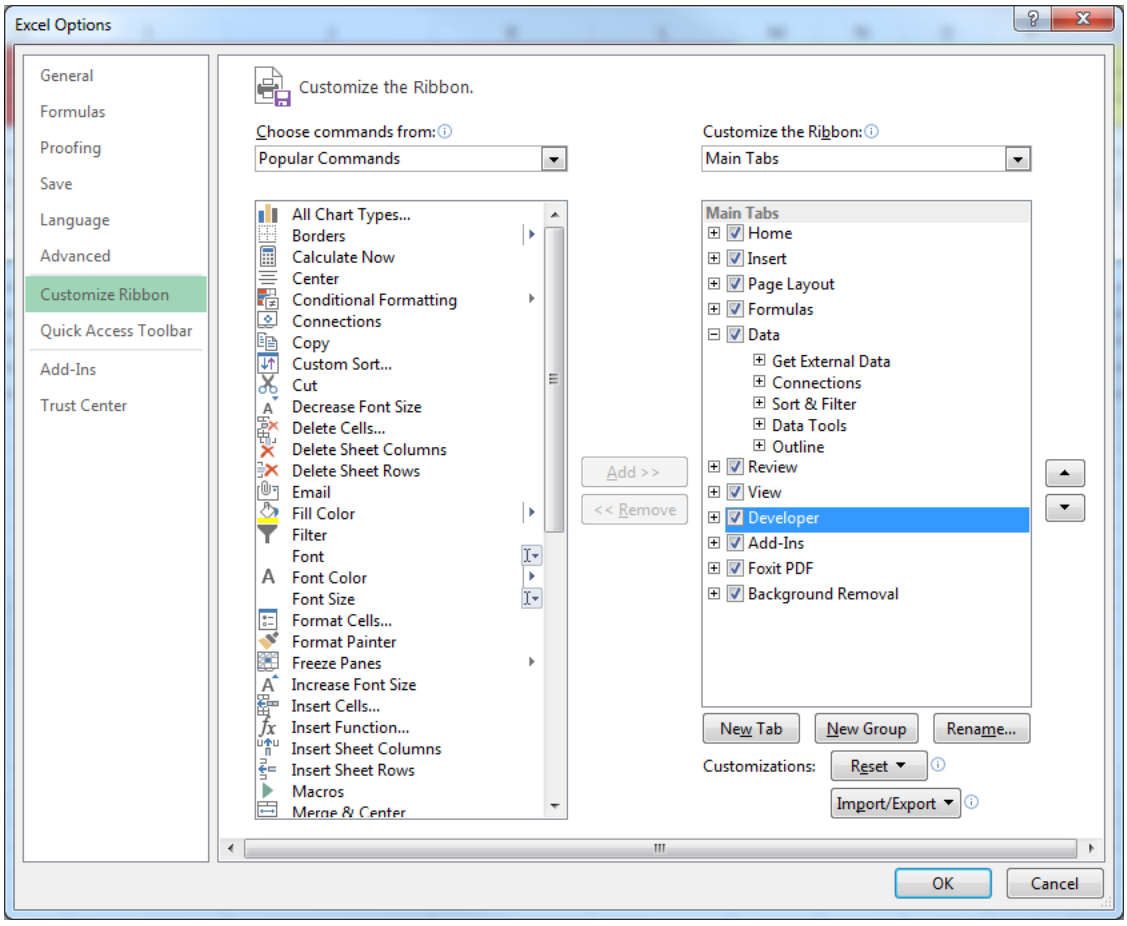

Figure A2. Selecting Developer under Customized Ribbon option

3) After selecting Developer, go to the top of the page and select Developer and click on the Add-Ins tab, and the page shown in Figure A3 will appear. Select Solver Add-In as shown in Figure A3. The Solver tab will be added in the Data tab as shown in Figure A4.

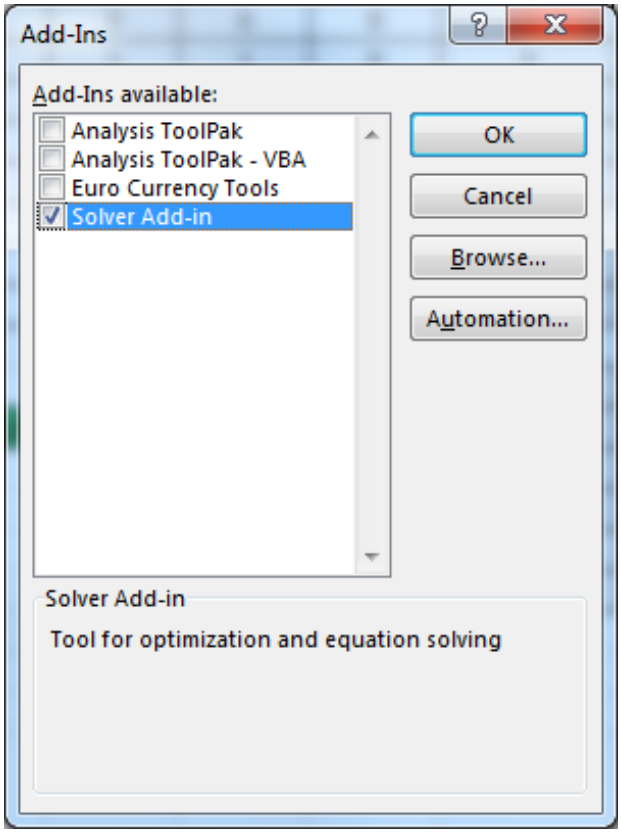

Figure A3. Selecting Solver Add-In tool for optimization

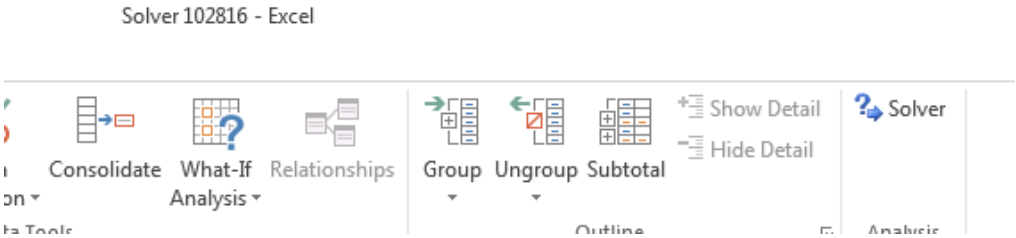

Figure A4. Solver tab in Microsoft Excel

4) The next step is to input the data, which in this case is the unit price and freight tons for each selected market. Constraints are also set up to be read in Excel Solver. Table A3 and Table A4 show how it appears before using Solver. The objective function can be seen in Table A5 and Equation 6. The freight million ton numbers 62.51, 1.44, 1.42, 0.83, and 0.56 were found from a commodity flow data analysis study [11].

Table A3. Setting up data to run Excel Solver (Base Scenario of 100% Truck)

	A	B	C	D	E	F	G	H
1			Ports of Los Angeles and Long Beach					
2			$Y_{1\text{-}A}$ (to California)	$Y_{1\text{-}B}$ (to Arizona)	$Y_{1\text{-}C}$ (to Nevada)	$Y_{1\text{-}D}$ (to Texas)	$Y_{1\text{-}E}$ (to Washington)	Z
3	y_{ij} (Freight in million tons)		0	0	0	0	0	0.0
4	b_{ij} (Unit cost per ton-mile in US$)		$154.24	$150.81	$103.22	$526.24	$415.87	
5	d_{ij} (Distance in miles)		364.0	355.9	243.6	1241.7	981.3	
6	Constraint 1: $y_{ij} \geq -T$	62.51	1	0	0	0	0	0.000
7		1.44	0	1	0	0	0	0.000
8		1.42	0	0	1	0	0	0.000
9		0.83	0	0	0	1	0	0.000
10		0.56	0	0	0	0	1	0.000
11	Constraint 2: $y_{ij} \geq r_j$	62.51	1	0	0	0	0	0.000
12		1.44	0	1	0	0	0	0.000
13		1.42	0	0	1	0	0	0.000
14		0.83	0	0	0	1	0	0.000
15		0.56	0	0	0	0	1	0.000

Table A4. Setting up data to run Excel Solver (Alternative Scenario 70% Truck and 30% Rail)

	A	B	C	D	E	F	G	H
1			Ports of Los Angeles and Long Beach					
2			$Y_{1\text{-}A}$ (to California)	$Y_{1\text{-}B}$ (to Arizona)	$Y_{1\text{-}C}$ (to Nevada)	$Y_{1\text{-}D}$ (to Texas)	$Y_{1\text{-}E}$ (to Washington)	Z
3	y_{ij} (Freight in million tons)		0	0	0	0	0	0.0
4	b_{ij} (Unit cost per ton-mile in US$)		$154.24	$150.81	$103.22	$526.24	$415.87	
5	d_{ij} (Distance in miles)		364.0	355.9	243.6	1241.7	981.3	
6	Constraint 1: $y_{ij} \geq -T$	62.51	1	0	0	0	0	0.000
7		1.44	0	1	0	0	0	0.000
8		1.42	0	0	1	0	0	0.000
9		0.83	0	0	0	1	0	0.000
10		0.56	0	0	0	0	1	0.000
11	Constraint 2: $y_{ij} \geq r_j$	62.51	1	0	0	0	0	0.000
12		1.44	0	1	0	0	0	0.000
13		1.42	0	0	1	0	0	0.000
14		0.83	0	0	0	1	0	0.000
15		0.56	0	0	0	0	1	0.000

Table A5. Objective function being used in Excel

	A	B	C	D	E	F	G	H	I	J
1			Ports of Los Angeles and Long Beach							
2			$Y_{1\text{-}A}$ (to California)	$Y_{1\text{-}B}$ (to Arizona)	$Y_{1\text{-}C}$ (to Nevada)	$Y_{1\text{-}D}$ (to Texas)	$Y_{1\text{-}E}$ (to Washington)	Z		
3	y_{ij} (Freight in million tons)		0	0	0	0				
4	b_{ij} (Unit cost per ton-mile in US$)		$112.02	$109.53	$74.97	$382.20		=C3*C4+D3*D4+E3*E4+F3*F4+G3*G4		
5	d_{ij} (Distance in miles)		364.0	355.9	243.6	1241.7				

$$= C3*C4 + D3*D4 + E3*E4 + F3*F4 + G3*G4 \quad (6)$$

Equation 6 is the objective function needed to run Solver. C3, D3, E3, F3, and G3 are the y_{ij} values from each port (i) to state market (j), and C4, D4, E4, F4, and G4 are the b_{ij} values or unit cost per ton-mile in US$ from each port (i) to state market (j).

5) Next, enter the data and constraints into Excel Solver. Click on Solver, and the image shown in Figure A4 will appear. Then click Add to add the constraints. Figure A5 shows the box that appears when Add is selected. Next, insert all constraints, clicking the Add button each time one is completed. In the By Changing Variable Cells field, insert the freight tons shipped to each market. The next step is to input the set objective number and to change the Select a Solving Method to Simplex LP. The final data in Solver before solving can be seen in Figure A6.

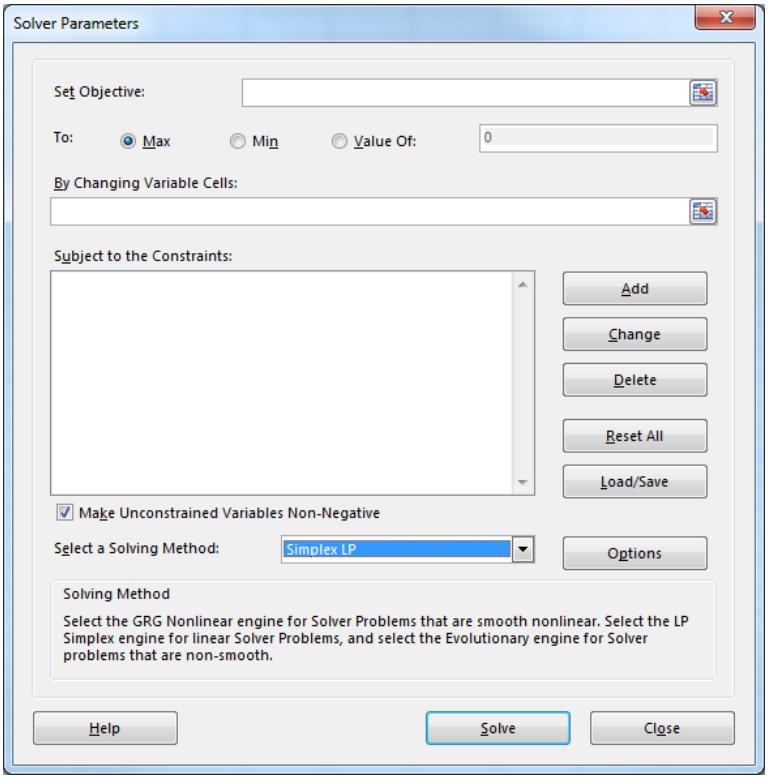

Figure A4. Solver parameters

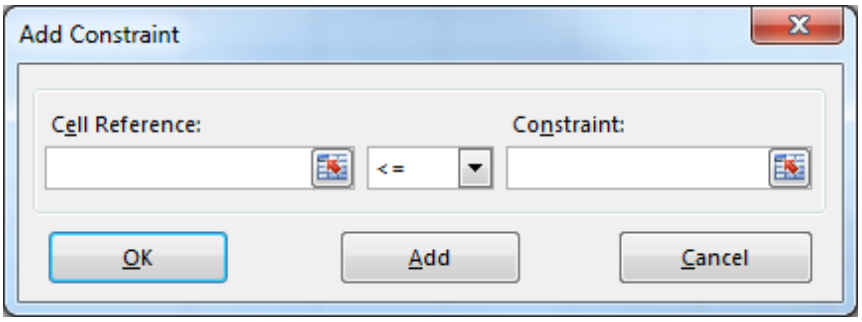

Figure A5. Adding Constraints

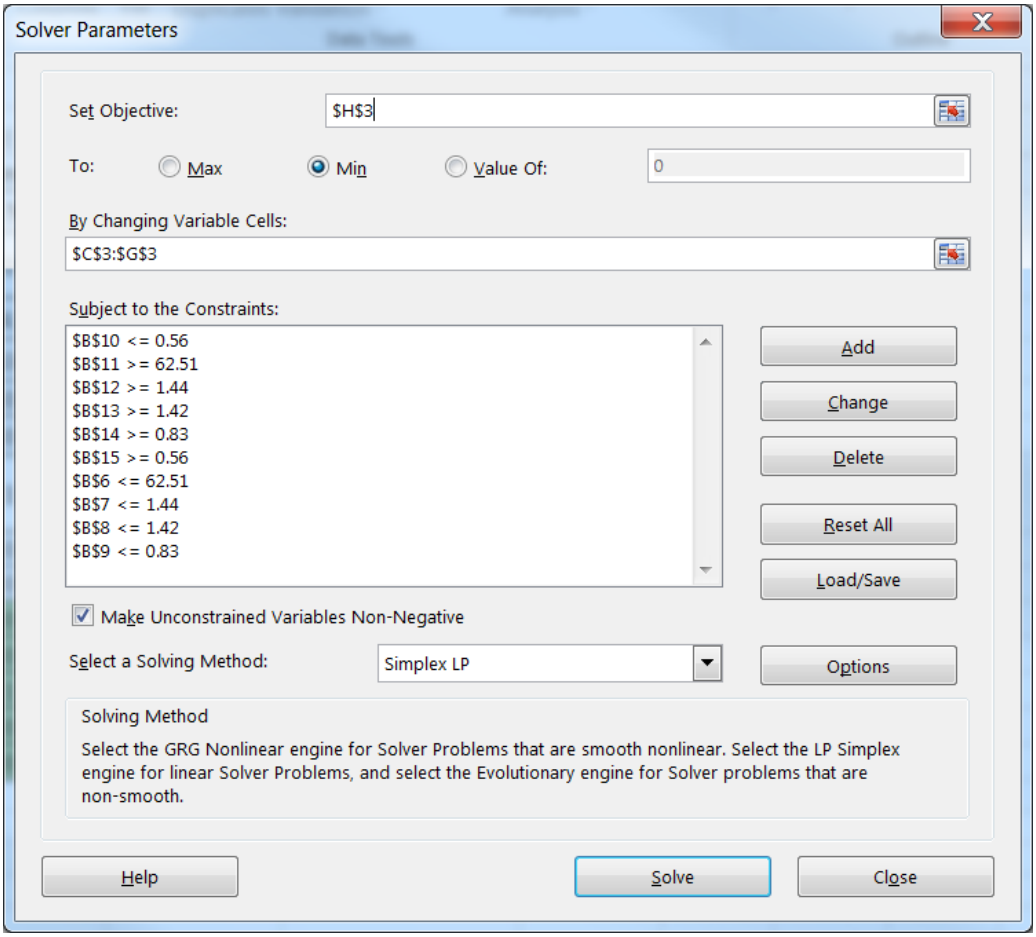

Figure A6. Final Solver parameters before solving the linear optimization problem

The freight million ton numbers 62.51, 1.44, 1.42, 0.83, and 0.56 were found from a commodity flow data analysis study [11].

6) The next step is to click Solve, and Figure A7 will appear. Click on Answer, Sensitivity, and Limits to obtain the results. After selecting these, click OK.

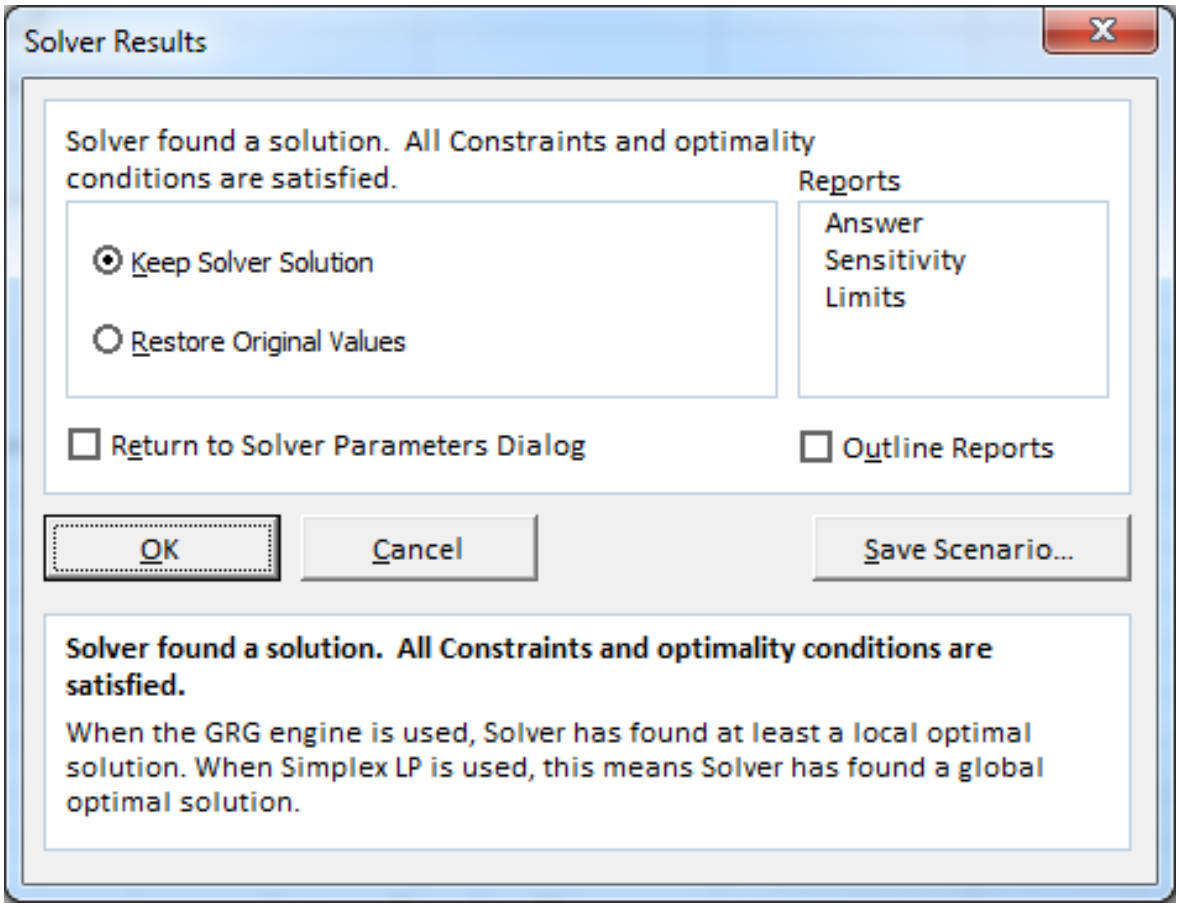

Figure A7. Solver results options

7) Finally, analyze the results from Solver. The Answer Report sheet tab will show the final minimum value results, as shown in Table A6. As shown in Table A6, the final minimum cost for 100% freight shipped by truck is $10,675 million U.S. dollars or $10.7 billion U.S. dollars.

Table A6. Final answer for optimized minimum cost value for base scenario

Objective Cell (Min)

Cell	Name	Original Value	Final Value
H3	yij (Freight in million tons) Z	$10,675.09	$10,675.09

Variable Cells

Cell	Name	Original Value	Final Value	Integer
C3	yij (Freight in million tons) Y1-A (to California)	62.51	62.51	Continuous
D3	yij (Freight in million tons) Y1-B (to Arizona)	1.44	1.44	Continuous
E3	yij (Freight in million tons) Y1-C (to Nevada)	1.42	1.42	Continuous
F3	yij (Freight in million tons) Y1-D (to Texas)	0.83	0.83	Continuous
G3	yij (Freight in million tons) Y1-E (to Washington)	0.56	0.56	Continuous

Constraints

Cell	Name	Cell Value	Formula	Status	Slack
B11	Constraint 2: yij ≥ rj	62.51	B11>=62.51	Binding	0
B12		1.44	B12>=1.44	Binding	0
B13		1.42	B13>=1.42	Binding	0
B14		0.83	B14>=0.83	Binding	0
B15		0.56	B15>=0.56	Binding	0
B6	Constraint 1: yij ≥ -T	62.51	B6<=62.51	Binding	0
B7		1.44	B7<=1.44	Binding	0
B8		1.42	B8<=1.42	Binding	0
B10		0.56	B10<=0.56	Binding	0
B9		0.83	B9<=0.83	Binding	0

In conclusion, linear optimization found the lowest minimum value to ship freight by 100% truck, and by 70% truck and 30% rail. This process showed that shifting some of the freight to rail would substantially lower the cost of shipping.

The final results for the two scenarios are shown in Tables A7 and A8. It was observed that a 27.4% decrease in minimum cost occurred when 30% of the truck freight was diverted to rail.

Table A7. Optimized minimum transportation costs for freight shipping 100% by road (base scenario)

Base Scenario (100% Truck)	Ports of Los Angeles and Long Beach Freight Available: 66.76 million tons					Z
	a	b	c	d	e	(Millions U.S. Dollars)
	CA	AZ	NV	TX	WA	
Unit Cost Per Ton	$154.24	$150.81	$103.22	$526.24	$415.87	
Freight Million Tons (Distributed)	62.51	1.44	1.42	0.83	0.56	$10,675.09

Table A8. Optimized minimum transportation costs for freight shipping 70% by road and 30% by rail (alternative scenario)

Alternative Scenario (70 % Truck and 30% Rail)	Ports of Los Angeles and Long Beach Freight Available: 66.76 million tons					Z
	a	b	c	d	e	(Millions U.S. Dollars)
	CA	AZ	NV	TX	WA	
Unit Cost Per Ton	$112.02	$109.53	$74.97	$382.20	$302.04	
Freight Million Tons (Distributed)	62.51	1.44	1.42	0.83	0.56	$7,753.16

VITA

Robert Richardson was born on September 10, 1993, in Memphis, Tennessee. In 1999, he moved with his family to Madison, Mississippi, where he attended elementary, middle, and high school. He received his bachelor's degree in civil engineering from The University of Mississippi in 2014. After completing his bachelor's degree, he pursued his master's degree in civil engineering under the supervision of Dr. Waheed Uddin, Professor and Director of the Center for Advanced Infrastructure Technology (CAIT), in the area of waterway transportation and sustainability. His master's thesis is entitled, "Cargo Shipping Demand Modeling, Infrastructure Mapping, and Emission Impacts of Selected U.S. Ports."